CANADIAN THESES

THÈSES CANADIENNES

NOTICE

The quality of this microfiche is heavily dependent upon the quality of the original thesis submitted for microfilming. Every effort has been made to ensure the highest quality of reproduction possible.

If pages are missing, contact the university which granted the degree.

Some pages may have indistinct print especially if the original pages were typed with a poor typewriter ribbon or if the university sent us an inferior photocopy.

Previously copyrighted materials (journal articles, published tests, etc.) are not filmed.

Reproduction in full or in part of this film is governed by the Canadian Copyright Act, R.S.C. 1970, c. C-30.

AVIS

La qualité de cette microfiche dépend grandement de la qualité de la thèse soumise au microfilmage. Nous avons tout fait pour assurer une qualité supérieure de reproduction.

S'il manque des pages, veuillez communiquer avec l'université qui a conféré le grade.

La qualité d'impression de certaines pages peut laisser à désirer, surtout si les pages originales ont été dactylographiées à l'aide d'un ruban usé ou si l'université nous a fait parvenir une photocopie de qualité inférieure.

Les documents qui font déjà l'objet d'un droit d'auteur (articles de revue, examens publiés, etc.) ne sont pas microfilmés.

La reproduction, même partielle, de ce microfilm est soumise à la Loi canadienne sur le droit d'auteur, SRC 1970, c. C-30.

THIS DISSERTATION HAS BEEN MICROFILMED EXACTLY AS RECEIVED

LA THÈSE A ÉTÉ MICROFILMÉE TELLE QUE NOUS L'AVONS REÇUE

NL-339 (r. 86/06)

Canada

THE UNIVERSITY OF ALBERTA

MODELLING AND ANALYSIS OF AN ACTIVE AIR SOLAR HEATING SYSTEM: APPLICATION OF TRNSYS SIMULATION

by

Ewen Yui Wang Leung

A THESIS

SUBMITTED TO THE FACULTY OF GRADUATE STUDIES AND RESEARCH

IN PARTIAL FULFILMENT OF THE REQUIREMENTS FOR THE DEGREE

OF Master of Science

Department of Mechanical Engineering

EDMONTON, ALBERTA

SPRING 1986

ISBN 0-315-30272-0

THE UNIVERSITY OF ALBERTA

RELEASE FORM

NAME OF AUTHOR Ewen Yui Wang Leung

TITLE OF THESIS MODELLING AND ANALYSIS OF AN ACTIVE AIR SOLAR HEATING SYSTEM: APPLICATION OF TRNSYS SIMULATION

DEGREE FOR WHICH THESIS WAS PRESENTED Master of Science

YEAR THIS DEGREE GRANTED SPRING 1986

Permission is hereby granted to THE UNIVERSITY OF ALBERTA LIBRARY to reproduce single copies of this thesis and to lend or sell such copies for private, scholarly or scientific research purposes only.

The author reserves other publication rights, and neither the thesis nor extensive extracts from it may be printed or otherwise reproduced without the author's written permission.

(SIGNED) .....

ADDRESS: 4807 - 115 Avenue
Edmonton, Alberta
Canada
T5W 0W3

DATED March 26, 1986

THE UNIVERSITY OF ALBERTA

FACULTY OF GRADUATE STUDIES AND RESEARCH

The undersigned certify that they have read, and recommend to the Faculty of Graduate Studies and Research, for acceptance, a thesis entitled MODELLING AND ANALYSIS OF AN ACTIVE AIR SOLAR HEATING SYSTEM: APPLICATION OF TRNSYS SIMULATION submitted by Ewen Yui Wang Leung in partial fulfilment of the requirements for the degree of Master of Science.

Gerald W. Sadler

Supervisor

Date 26 March 1986

To My Parents

Abstract

The basic thrust of the present work is to simulate the active air solar heating system installed on module six at the Alberta Home Heating Research Facility so that the thermal performance of the system can be analyzed in detail without tedious experimental work. This involved the development of a simulation model using an existing computer program, **TRNSYS**. The model was tested and verified by available experimental measurements.

The simulation model predicts the necessary energy quantities and system temperatures required for analysis of system energy flows, component energy losses and calculation of the solar contribution. Application to monthly performance analyses for 81-82, 82-83 and 83-84 heating seasons was done. For a heating season from September to March, the solar heating system was able to supply approximately 15% of the heating load, with the monthly solar contribution ranging from a low of about 4% in December or January to a high of about 50% in September. Energy saving can be achieved by reducing the lengths of the ducts connecting the collector to the module and by isolating the collector with dampers having low leakage.

Simulations are useful in studies of system dynamics and search for optimum design. Economic studies were not included in this thesis, but results of simulations can be used for economic analysis to find the lowest cost system.

Acknowledgements

The author would like to express his graditude to Professor G.W. Sadler, the thesis advisor, for his guidance, support and assistance in all stages of this investigation and in the preparation of this thesis.

Thanks are extended to Mr. M.Y. Ackerman for his helpful assistance with data acquisition and for his suggestions regarding treatment of the data.

Funding for this research was supported by the National Science and Engineering Research Council of Canada Grant A6532 and G1004.

Table of Contents

Chapter		Page
1.	INTRODUCTION	1
2.	TRNSYS	5
	2.1 Concepts and Definitions	5
3.	THE SOLAR HEATING SYSTEM	9
	3.1 The System	9
	3.2 Control Criteria for Operation Modes	14
4.	SIMULATION MODEL	19
	4.1 The Modelling System	19
	4.2 Data Processor	24
	4.3 Solar Collector Model	27
	4.4 Rockbed Model	29
	4.5 Space Heating Model	32
	4.6 Control System	35
	4.7 System Analyzer	42
	4.7.1 Information Flow Diagram	44
	4.7.2 Mathematical Description	46
	4.8 Information Flow of System	49
5.	METHODS OF SYSTEM PERFORMANCE ANALYSIS	60
	5.1 Solar Contribution	60
	5.2 Component Energy Losses	61
	5.2.1 Collector Loss	62
	5.2.2 Bin Loss	63
	5.2.3 Damper Leakage Loss	63
	5.2.4 Outside Module Duct Loss	64
6.	RESULTS AND DISCUSSION	65

6.1 Model Testing 66
6.1.1 Clear Day Test 66
6.1.2 Cloudy Day Test 82
6.1.3 Cold and Warm Month Test 87
6.2 Monthly Performance Analysis 96
6.2.1 Solar Contribution 98
6.2.2 Solar Distribution 98
6.2.3 Rockbed Storage 107
6.2.4 Damper Leakage Loss 109
6.2.5 Summary of System Energy Flows 114
6.2.6 Justification Of The Simulation Model 118
6.3 Parametric Study 125
7. CONCLUSIONS AND RECOMMENDATIONS 135
7.1 Conclusions 135
7.1.1 Modelling 135
7.1.2 Analysis 136
7.2 Recommendations 139
REFERENCES 141
BIBLIOGRAPHY 143
APPENDIX A: Parameters of Component Models 145
APPENDIX B: Subroutine Program of The System Analyzer ...149
Appendix C: Recommended System of Units for TRNSYS Simulation 151
Appendix D: Sample of Simulation Control Program with Results 152
Appendix E: Estimations of Component Properties 174
E-1: Overall Heat Loss Coefficient - Area Product of The Module 175

E-2: Lumped Thermal Capacitance of The Module 177

E-3: Overall Heat Loss Coefficient and Ntu of The Rockbed 180

E-4: Overall Heat Loss Coefficient of The Duct Outside The Module 189

List of Tables

Table		Page
3.1	Design Details of Module Six	11
3.2	$F_r U_L$ and $F_r(\tau\alpha)$ of The Solar Collector	13
4.1	Summary of Control Strategy	36
4.2	Outputs of Each Component of The System Controller	43
6.1	Comparison of Measured and Simulated Energy Quantities for 0, 2, 4 and 6% Leakage	73
6.2	Comparison of The Hourly, Monthly and Standard Test of The Collector Thermal Efficiency Curves	75
6.3	Comparison of Measured and Simulated Energy Quantities for 4% and 15% Leakage for The 2 Cloudy Days	88
6.4	Number of Hourly Records Available per Month	97
6.5	Monthly Solar Contribution for 81-82 Heating Season	99
6.6	Monthly Solar Contribution for 82-83 Heating Season	100
6.7	Monthly Solar Contribution for 83-84 Heating Season	101
6.8	Distribution of Solar Energy for 81-82 Heating Season	103
6.9	Distribution of Solar Energy for 82-83 Heating Season	104
6.10	Distribution of Solar Energy for 83-84 Heating Season	105
6.11	Simulated Energy Flows of The Storage Unit for 81-82 Heating Season	110
6.12	Simulated Energy Flows of The Storage Unit for 82-83 Heating Season	110

Table Page

6.13 Simulated Energy Flows of The Storage Unit for 83-84 Heating Season 111

6.14 Damper Leakage Loss for 81-82 Heating Season 112

6.15 Damper Leakage Loss for 82-83 Heating Season 112

6.16 Damper Leakage Loss for 83-84 Heating Season 113

6.17 Averages of Monthly Energy Quantities 122

6.18 Summary of Energy Quantities for Different Collector Areas and Storage Volumes for 82-83 Heating Season 131

6.19 Energy Quantities for Different Collector Areas and Storage Volumes for September and December 1982 132

List of Figures

Figure		Page
3.1	Schematic Solar Air System	10
3.2	Control Criteria of The Solar Air System	15
3.3	Schematic Air Flow Loop for Each Mode	16
4.1	Solar Heating System Model	20
4.2	Data Processor	25
4.3	System Controller	40
4.4	Information Flow Diagram of Components Outside The House	50
4.5	Information Flow Diagram of Components Within The House	51
4.6	Overall Configuration of The Active Air Solar Heating System	57
6.1	Measured and Simulated Collector Temperatures for 0% Leakage	67
6.2	Measured and Simulated Collector Temperatures for 2% Leakage	68
6.3	Measured and Simulated Collector Temperatures for 4% Leakage	69
6.4	Measured and Simulated Collector Temperatures for 6% Leakage	70
6.5	Comparison of The Collector Outlet Air Temperatures Predicted by Different Methods	77
6.6	Measured System Temperatures for 2 Consecutive Sunny Days, February 20th and 21st, 1982	80
6.7	Predicted System Temperatures for 2 Consecutive Sunny Days, February 20th and 21st, 1982	81
6.8	Measured System Temperatures for 2 Consecutive Cloudy Days, January 1st and 2nd, 1982	83

Figure Page

6.9 Predicted System Temperatures for 4% Leakage for The 2 Cloudy Days 84

6.10 Predicted System Temperatures for 15% Leakage for The 2 Cloudy Days 85

6.11 Daily Variations of Collected Solar Energy and Total Energy Supplied to The System for January 1982 89

6.12 Daily Variations of Collected Solar Energy and Total Energy Supplied to The System for March 1982 90

6.13 Daily Variations of Collected Solar Energy and Total Energy Supplied to The System for December 1982 91

6.14 Daily Variations of Collected Solar Energy and Total Energy Supplied to The System for October 1983 92

6.15 Daily Variations of Collected Solar Energy and Total Energy Supplied to The System for December 1983 93

6.16 Energy Flows for 81-82 Heating Season 115

6.17 Energy Flows for 82-83 Heating Season 116

6.18 Energy Flows for 83-84 Heating Season 117

6.19 Percent Error of Collected Solar Energy 119

6.20 Percent Error of Collector Loss 119

6.21 Percent Error of Auxiliary Energy 120

6.22 Percent Error of Total System Energy Supply 120

6.23 Percent Error of The Average Monthly Quantities 123

6.24 Effects of Changes of Collector Area and Storage Capacity for 82-83 Heating Season 126

6.25 Comparison of The Effect of Collector Area for September 1982, December 1982 and 82-83 Heating Season 129

Figure Page

6.26 Comparison of The Effect of Storage Capacity for September 1982, December 1982 and 82-83 Heating Season 129

6.27 Corrections for Non-optimum Collector Tilt for A Typical Installation at 35 Degree North Latitude 134

Nomenclature

A	area, m^2
A_c	collector area, m^2
b_o	incidence angle modifier coefficient
C_b	heat capacity of bed material, $J/kg \cdot °C$
C_f	heat capacity of fluid, $J/kg \cdot °C$
CAP	lumped thermal capacitance of house, $J/°C$
F_r	solar collector heat removal factor
$F_r U_L$	collector heat loss factor, $W/m^2 \cdot °C$
$F_r(\tau\alpha)$	transmittance–absorptance product factor
$F_r(\tau\alpha)_n$	normal incidence value of transmittance–absorptance product factor
h_v	volumetric heat transfer coefficient between the bed and the fluid, $W/m^3 \cdot °C$
I	total horizontal radiation, W/m^2
I_b	horizontal beam radiation, W/m^2
I_d	horizontal diffuse radiation, W/m^2
I_{dn}	direct normal beam radiation, W/m^2
I_T	total radiation on collector, W/m^2
I_{TC}	total radiation on collector during collector operation mode, W/m^2
$K_{(\tau\alpha)}$	incidence angle modifier
$K_{(\tau\alpha)_b}$	incidence angle modifier for beam radiation
k	thermal conductivity of rockbed in the axial direction, $W/m \cdot °C$
L	length, m
L_f	ratio of latent load to total cooling load

$\dot{m}$	mass flow rate, kg/s
$\dot{m}_b$	mass flow rate of air entering the rockbed from the bottom, kg/s
$\dot{m}_c$	collector fluid mass flow rate, kg/s
$\dot{m}_f$	heat exchanger cold side fluid mass flow rate, kg/s
$\dot{m}_i$	inlet mass flow rate, kg/s
$\dot{m}_o$	outlet mass flow rate, kg/s
$\dot{m}_t$	mass flow rate of air entering the rockbed from the top, kg/s
Ntu	number of heat transfer units
P	perimeter of rockbed wall, m
P_1	electric power supply for first stage heating, W
P_2	electric power supply for two stage heating, W
P_{min}	minimum power supply to keep the fan on, W
Q	energy quantity, J
$\dot{Q}$	energy rate, W
$\dot{Q}_{aux}$	instantaneous auxiliary energy, W
$\dot{Q}_c$	rate at which solar energy is gained by the collector during collector operation mode, W
$\dot{Q}_{CL}$	rate of energy lost from collector, W
$\dot{Q}_{cool}$	rate of cooling by air conditioner, W
$\dot{Q}_{DLL}$	rate of energy loss due to leakage of dampers during storage bed operation mode, W
$\dot{Q}_E$	rate of energy lost from rockbed, W
$\dot{Q}_{gain}$	all time variant heat gains, W

$\dot{Q}_H$	rate of energy supplied from the thermal system to meet the load, W
$\dot{Q}_{in}$	rate of energy gained or lost for each duct section, W
$\dot{Q}_L$	instantaneous heating load, W
$\dot{Q}_{lat}$	rate of latent cooling, W
$\dot{Q}_{loss}$	rate at which energy is lost from or gained by ducts outside of the house, W
$\dot{Q}_{OMBL}$	rate of energy lost through ducts outside the house during collector operation mode, W
$\dot{Q}_s$	rate at which energy is removed from the rockbed to meet the load, W
$\dot{Q}_{sens}$	rate of sensible cooling, W
$\dot{Q}_{store}$	rate of energy delivered to rockbed for storage, W
$\dot{Q}_{sys}$	rate of energy supplied to the thermal system, W
$\dot{Q}_T$	rate of energy transferred across the load heat exchanger, W
$\dot{Q}_u$	rate of energy gain of collector, W
T	temperature, °C
$\bar{T}$	average temperature, °C
T_a	ambient temperature, °C
T_b	temperature of bed material, °C
T_{ci}	inlet temperature of air to collector, °C
T_{co}	outlet temperature of air from collector, °C
T_{co_2}	air set temperature at collector outlet for heating from collector operation mode with electric coil off, °C

T_{env}	temperature of the surroundings of rockbed, °C
T_f	temperature of fluid, °C
T_H	upper input temperature of controller, °C
T_i	inlet temperature, °C
T_{inb}	temperature of air entering the rockbed from the bottom, °C
T_{int}	temperature of air entering the rockbed from the top, °C
T_L	lower input temperature of controller, °C
T_o	outlet temperature, °C
T_r	room temperature, °C
T_{s1}	set temperature of top storage bed for heating from storage operation mode with half electric coil on, °C
T_{s2}	set temperature of top storage bed for heating from storage operation mode with electric coil off, °C
T_{sb}	temperature at the bottom of the rockbed, °C
T_{st}	temperature at the top of the rockbed, °C
t	time, s
t_{d1}	time of last data reading, hr
t_{d2}	time of next data reading, hr
UA	overall heat loss coefficient – area product of a structure, W/°C
X_i	ith input value
x	position, m
Y_i	ith output value

β	collector tilt angle, degree
γ	control function
γ_1	control function of Damper No.1 and 3
γ_2	control function of Damper No.2 and 4
γ_F	main fan control function
γ_I	input control function
γ_O	output control function
ΔT_H	upper dead band temperature difference, °C
ΔT_L	lower dead band temperature difference, °C
ΔU	change in internal energy of the rockbed, J
ϵC_{min}	product of the effectiveness and minimum capacitance rate of load heat exchanger, W/°C
ζ	void fraction of rockbed
η	overall collector efficiency
θ	angle of incidence for collector surface, degree or dimensionless time
ρ_b	bed material density, kg/m^3
ρ_f	fluid density, kg/m^3
ρ_g	ground reflectance
ρ_r	apparent rock density, kg/m^3
$(\tau\alpha)$	transmittance-absorptance product
$(\tau\alpha)_b$	transmittance-absorptance product for beam radiation
$(\tau\alpha)_n$	normal incidence value of transmittance-absorptance product
ψ	collector surface azimuth angle, degree

1. INTRODUCTION

The rate of energy consumption by the world is growing rapidly due to increase in population, improvement of standard of living and industrial development. Robertson(1981) indicated that the amount of energy used per person in Canada today is twice what it was in the early 1960s, and the combined effect of population growth and the increase in energy consumption per person resulted in an average annual increase in demand of about 5% from 1960 to 1973. Rapp(1981) predicted that for a 3% energy growth per year, energy consumption in the United States in 2000 will be triple the energy consumption in 1960. Meanwhile, production rate of all fossil fuels predicted by Elliott and Turner(1972), on the contrary, appears to decrease in the foreseeable future. To ensure a continous supply of energy to meet the future demand, development of alternative energy sources are essential. Among all the alternative energy resources (nuclear, solar, wind, tide, etc.), Kreith and Kreider(1978) mentioned that "only nuclear and solar energy have the potential of supplying large amounts of power within the available time frame." There appears that in planning for future energy supply a choice between solar and nuclear energy should be made, and some believe solar radiation' is the most significant renewable energy source because it is free although the taking is not (Halacy 1973). Renewed interest in solar energy has developed since 1970.

'Immediately available energy directly from the sun.

It is currently being used for a wide range of applications to buildings such as domestic water heating, space heating and cooling. Solar energy is also used in industrial process heat, thermal conversion to electric energy generation, and evaporative processes. Although solar energy is regarded as an inexhaustible source potentially capable of supplying a significant portion of energy in the future, large-scale utilization of solar energy is a problem today because of technological and economic limitations. Thus, much research is needed to make solar energy competitive.

Residential energy consumption is a very topical subject in recent years since it consumes about 20% of Canada's total energy use. Usage of solar energy to reduce fossil-fuel consumption in residential heating has also gained an enormous surge of interest since 1970. To investigate energy conservation and solar heating strategies for residential construction in Alberta, six uninhabited single story modules at the Alberta Home Heating Research Facility were constructed. The modules are positioned in a single east-west row on the University of Alberta farm at Ellerslie, Alberta, and a small active air solar heating system was installed on one of the modules. The Canada Mortgage and Housing Corporation construction specifications were used to make the solar heating module representative of residential housing during the 1975-80 period. Although the high cost of active solar heating systems is difficult to

justify, except for special applications, even with increasing natural gas prices in Alberta, knowledge of the energy availability and the characteristic behavior of solar heating systems will provide the tools to utilize efficiently the sun's energy and remove the economic constraint, and this is the main purpose of this study.

The performance of the active air solar heating system on the university farm has been studied experimentally by Fung(1983) and Sadler and Leung(1985). Experimental determination of dynamic system behavior is usually time consuming and involves tedious data preparation and manipulation. Recently, simulation methods in the analysis of solar processes have been developed. These methods are powerful tools in understanding of transient solar heating systems and in their design. Close(1967) developed a method to determine which water heater system design factors are most important. Gupta(1971) used a response factor method for simulation of short term process operation. The f-chart method described by Beckman et al.(1977) is used for estimation of long term average performance and design of active solar and heat pump heating systems. **TRNSYS**, a modular solar process simulation program, developed by Klein et al.(1983), is designed for detailed analysis of systems whose behavior is dependent on the passage of time. **TRNSYS** is well suited for simulating transient solar heating systems with a minimum of programming effort.

In the present study, a model is developed to simulate the existing active air solar heating system by using the **TRNSYS** computer program. The thermal performance of the system expressed in terms of solar contribution, component energy losses and system energy flows using the simulation model will be presented and compared with the available experimental measurements. Chapter 2 introduces **TRNSYS** and provides the concepts and definitions for using the program. Chapter 3 describes the solar heating system and its operation. The simulation model of the system is established in Chapter 4 in which variation of the existing system and application of **TRNSYS** component models will be discussed. Chapter 5 develops the methods for analysis of system performance. In Chapter 6, the system model is tested by selecting specific test days and months. Application to monthly calculations for three heating seasons is presented. Simulation results for the effects of changes of component parameters will also be shown. This is followed by conclusion drawn from the study.

A number of thermal properties of the system components is required by **TRNSYS** as the parameters of the component models. The calculations of the thermal properties are given in Appendix E.

2. TRNSYS

TRNSYS is a modular solar process simulation program developed at the University of Wisconsin by Klein et al.(1983). The program contains a large number of component subroutines that represent the physical pieces of equipment commonly used in solar energy systems. If component models are not available from the library, the program allows the addition of user-formulated component subroutines. **TRNSYS** has the capability of interconnecting components in any desired manner. It solves algebraic and differential equations which describe the components, and facilitates information output. The program is widely used and well suited for simulating transient solar energy systems. In order to see how to prepare a system for simulation by **TRNSYS**, a brief description of the concepts and definitions is presented in this chapter.

2.1 Concepts and Definitions

A system is formed by connecting a set of components in such a way that a specified task can be accomplished by transmitting information into and out of each of the system components. This can be achieved by first identifying all of the components whose collective performance describes the performance of the system, and formulating a general mathematical description of each. Once this is done, it is necessary to construct an information flow diagram to show the interconnection of all of the components in the system.

An information diagram is a schematic representation of the information flow, and each component is represented as a box. Those pieces of information required by the component are represented as inward arrows to the box and those calculated by equations describing the component are represented as outward arrows from the box.

TRNSYS identifies a component by associating a TYPE number with it that indicates the types of component used in the system. For example, the solar collector model provided with **TRNSYS** is designated a TYPE 1 component and the fan model provided is designated a TYPE 3 component. These numbers have been assigned in **TRNSYS** as the names of the FORTRAN subroutines.

Since a system may contain two or more components of the same type, **TRNSYS** uses a UNIT number to distinguish each component. The UNIT number uniquely identifies the component and provides a reference number for each system component. Unlike the TYPE number, no two system components can have the same UNIT number, and this number is assigned by the user.

There are several types of information flow in **TRNSYS**. The set of information represented by outward arrows, flowing out of a component, is defined to be the OUTPUT variable set for that component. The set of information represented by inward arrows directed to a component from any other component in the system is defined to be the INPUT variable set. In general, an information INPUT to a

component must be an OUTPUT variable from one of the components of the system, and both variables may vary with time during the simulation. Those pieces of inflow information which are always constant throughout the simulation are known as PARAMETERS. TIME is a special kind of inflow information which is neither an INPUT nor a PARAMETER. **TRNSYS** contains a special component (Data Reader) which reads the values of the time dependent conditions such as ambient temperature and solar radiation at successive increments of time. It is important to distinguish among these four types of information flow (OUTPUT, INPUT, PARAMETER and TIME) because they are treated differently in **TRNSYS**.

A component may require a number of PARAMETERS and INPUTS, and produces a set of OUTPUTS. In order to convey the information flow diagram to **TRNSYS**, each piece of the different types of information flow for each component is numbered sequentially beginning with number one. The ordering of PARAMETERS, INPUTS and OUTPUTS for each component supplied by **TRNSYS** has been defined in the FORTRAN subroutine programs. For example, the TYPE 2 controller discussed in Chapter 4 has 3 PARAMETERS, 3 INPUTS and 1 OUTPUT. The first and second INPUTS are defined to be the upper and lower input temperatures respectively, and the third INPUT is the input control function. These INPUTS must be numbered in the same order as INPUT 1, INPUT 2 and INPUT 3 in the information flow diagram and so are the

PARAMETERS and OUTPUTS.

For transient simulation, the mathematical description of a component usually involves time-dependent differential equations. The number of differential equations and the initial values of the dependent variables must be specified. **TRNSYS** solves the differential equations by using Modified Euler Method. It is a first-order predictor-corrector algorithm using Euler's method for the predictor step and the derivative at the midpoint of the interval for the corrector step. However, if the differential equations can be expressed in a form which can be solved analytically, the numerical solutions would be replaced with analytical solutions for improving computational efficiency.

After constructing a system flow diagram with all the components defined, it is necessary to convey all of the information contained in the information flow diagram to **TRNSYS** so that the system can be simulated. **TRNSYS** simulation is defined and controlled by a set of control statements and data records. A detailed description of the control statements and their functions is given in Chapter 2 of Klein et al.(1983).

3. THE SOLAR HEATING SYSTEM

3.1 The System

The active air solar heating system is installed on module six at the Alberta Home Heating Research Facility. The system consists of a house module, a south facing solar collector, a rockbed storage unit, one air handling unit, motorized dampers, a two stage electric heater and a system controller. A schematic diagram of the system is shown in Figure 3.1.

The module is a 6700 mm x 7300 mm x 5000 mm single story house which has a concrete basement, frame wall construction, and a gable roof on elevated roof trusses. Design details of the module are given in Table 3.1.

The solar collector was assembled using six flat plate air collectors[1] by connecting two in series and mounting three of these units in parallel, forming a gross area of 11.1 m^2. The collector has a double glazed cover, an enamelled steel absorber and provides a total air heating path length of about 3500 mm. This flat plate collector is mounted on an adjustable stand positioned adjacent to the south wall of the module and faces south. The slope of the collector was initially set at 68° to the horizontal but was adjusted to 88° in December 1983 to study the effect of attaching the collector to the south wall. The collector heat loss factor $F_r U_L$ and its transmittance- absorptance

---

[1]Solaron Corporation series 2000 air type solar collector.

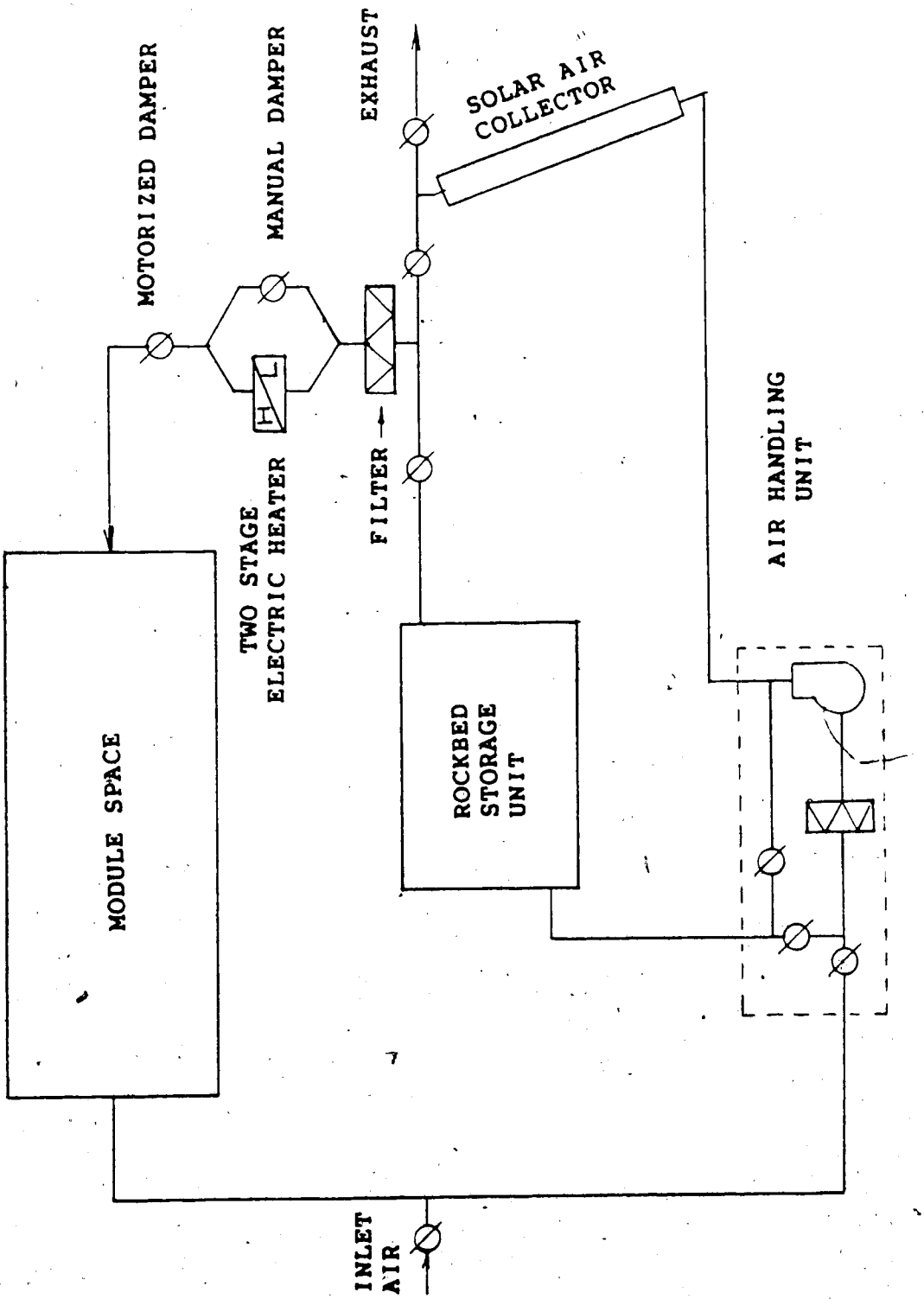

Figure 3.1 Schematic Solar Air System

Table 3.1 Design Details of Module Six

Floor Area(exterior) : 6700mm x 7300mm
(interior) : 6500mm x 7100mm

Main Floor Wall Height : 2400mm

Basement Height : 2400mm, 1800mm below grade

Roof : CMHC approved trusses with 600mm-150mm stub
: 210# asphalt shingles
: 10mm plywood Ext, GD sheathing

Ceiling : standard truss with 600mm bobtail rafters 600mm on center
: fiberglass insulation (RSI 5.46)
: 100 micrometre (4 mil) poly vapour barrier
: 13mm drywall painted

Wall Construction : 10mm plywood
: 89mm fiberglass insulation (RSI 1.76)
: 51mm x 102mm studs, 406mm on center
: 100 micrometre (4 mil) poly vapour barrier
: 13mm drywall painted

Wall Area / Floor Area : 1.39

Main Floor : 16mm fir plywood
: 51mm x 203mm studs, 406mm on center

Basement Wall : 13mm preservative treated plywood to 600mm below grade
: 51mm rigid insulation (RSI 1.76) to 600mm below grade
: 203mm concrete wall

Basement Floor : 102mm concrete slab on 150 micrometre (6 mil) poly vapour barrier

Windows North : 900mm x 1930mm double glazed sealed
South : None
East : 1020mm x 1930mm double slider
West : 1020mm x 1930mm double slider

Window Area / Floor Area : 11.9%

Door : 914mm x 2032mm insulated metal

(RSI - $m^2 °C/W$)

product factor $F_r(\tau\alpha)$ are given in Table 3.2.

The 1370 mm x 1370 mm x 1730 mm storage unit is located in the basement and contains 2 m^3 of 16 mm washed gravel. The unit is of 120 mm wood frame construction with fiberglass insulation and the interior surface is lined with 51 mm of rigid polystyrene insulation. Details are shown in Appendix E-3.

The air handling unit has internal by-pass dampers to permit a single fan to move the air in all of the system operation modes shown in Figure 3.3. The system operates at two different flow rates due to different path resistance. During collector operation mode, an airflow rate of 0.122 m^3/s is circulated through the collector to either the module space or the storage bed. When the collector is not operating, the air flows through the storage bed in the reverse direction to the space with an airflow rate of 0.218 m^3/s.

Other components include a control system with sensors and relays, motorized dampers for properly directing the flow, and a two stage electric heater. The electric heater is sized to handle the design heating load for the module and the first stage provides approximately half of the maximum heating capacity of 7.5 kW.

Table 3.2 $F_r U_L$ and $F_r(\tau a)$ of The Solar Collector

Curve *	$F_r(\tau a)$	$F_r U_L$ ($W/m^2 \cdot °C$)
Standard Test	0.50	2.90
Hourly	0.54	1.58
Monthly	0.56	2.61

* Collector performance is usually represented by a straight line plot of efficiency (η) versus the division of the difference between collector inlet air (T_{ci}) and ambient (T_a) temperatures by the incidence radiation (I_T), with intercept $F_r(\tau a)$ and slope $-F_r U_L$. That is:

$$\eta = F_r(\tau a) - F_r U_L (T_{ci} - T_a)/I_T$$

with $F_r(\tau a)$ and $F_r U_L$ assuming constant. These constant parameters were found by Fung(1983) using three different sets of data:

1. Standard test curve was calculated based on manufacturing data.
2. Hourly curve was obtained from the experimental data for the hours including solar noon.
3. Monthly curve was obtained from the monthly records of measurements.

(see Sections 4.3 and 6.1.1 for more description)

3.2 Control Criteria for Operation Modes

The control system is designed to operate the system in five modes and for implementing temperature level control. On the basis of three input temperatures (i.e., room temperature, collector outlet air temperature and the temperature at the top of the storage bed), the outputs of the controller will feed to the motorized dampers, heater and air handling unit to direct the flow through the correct loop with desired amount of electric energy provided for each mode. The control criteria are given in Figure 3.2 which shows every operating point of the solar air system. Figure 3.3 indicates the air-flow loop of each mode.

Based on Figure 3.2, the modes of operation are defined as follows:

1. **Heat From Collector(HFC)**

   If the room temperature T_r is below 21°C and the air temperature at collector outlet T_{co} is above 29°C, then air is circulated through the collector, by-passes the storage unit and is sent directly to the space as shown in Figure 3.3a. If the collector outlet air temperature is less than 33°C, the first stage electric heater is used to prevent uncomfortable cold drafts.

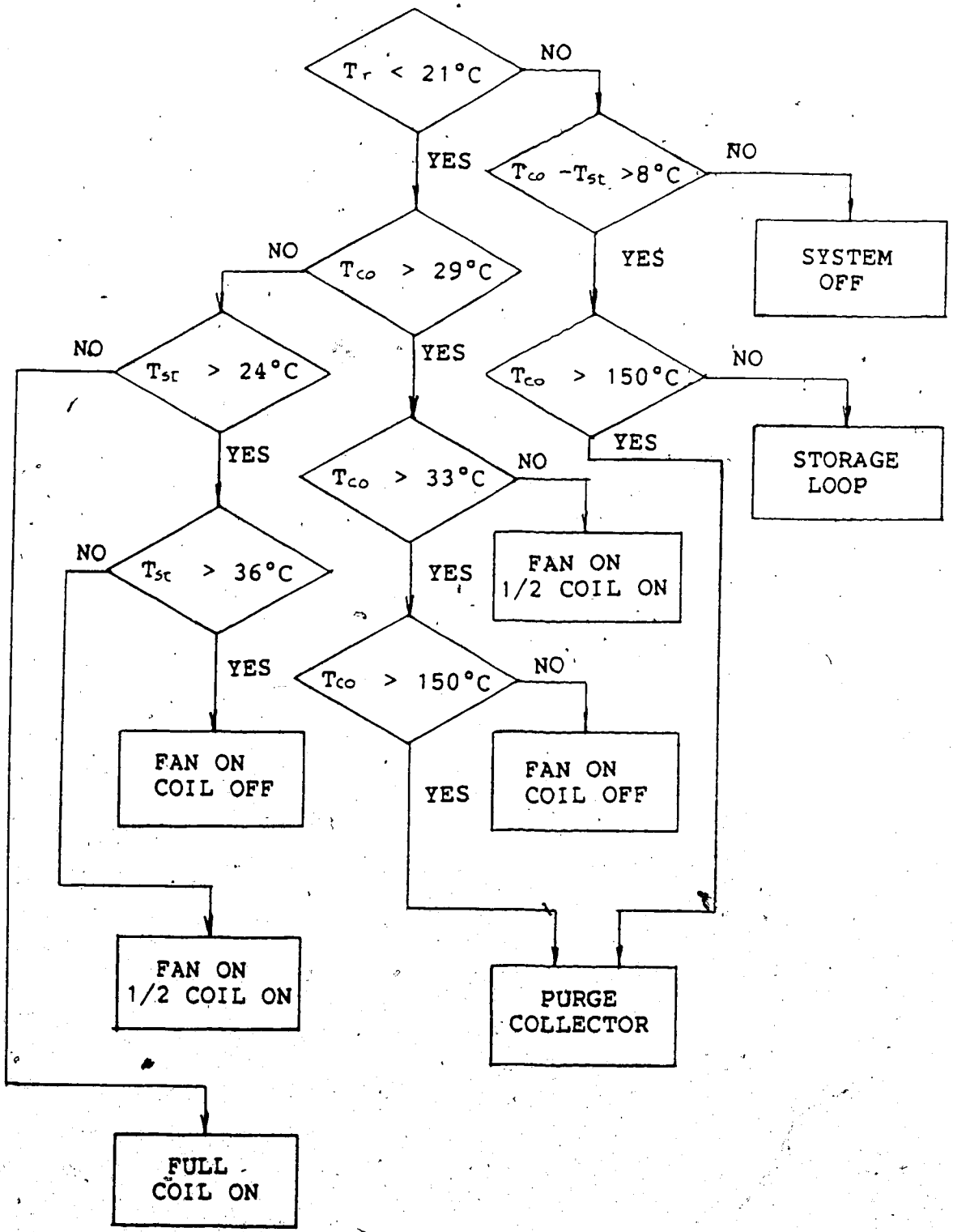

Figure 3.2 Control Criteria of The Solar Air System

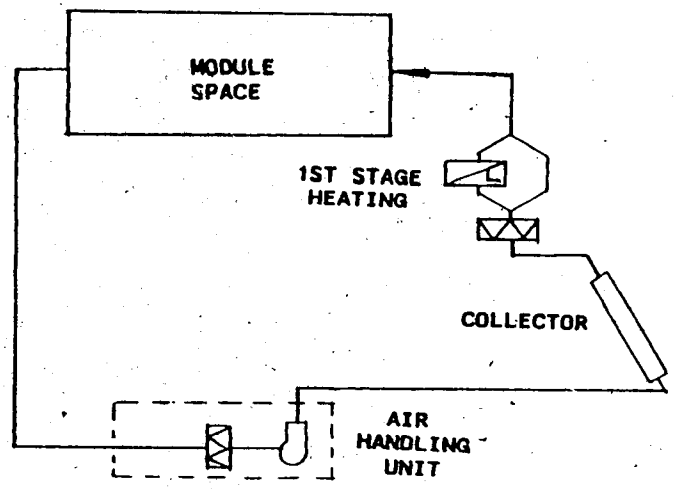

(a) Heat From Collector

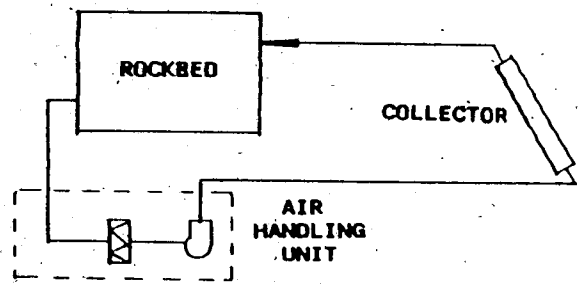

(b) Heat Collection

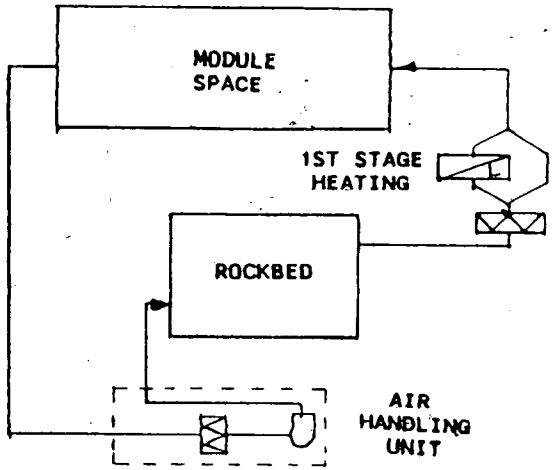

(c) Heat From Storage

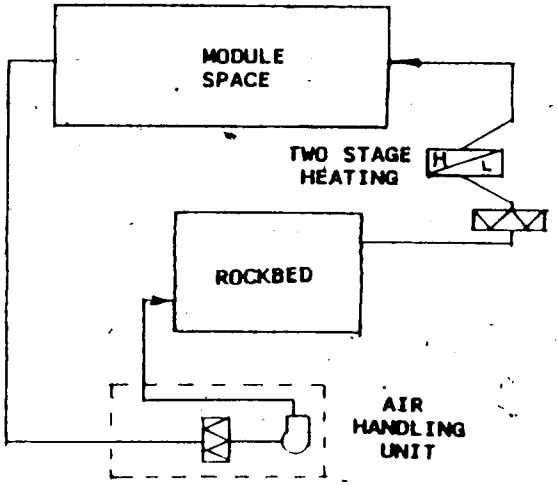

(d) Electric Heating

Figure 3.3 Schematic Air Flow Loop for Each Mode

2. **Heat Collection(COL)**

If the room temperature is above 21°C and the air temperature at collector outlet is 8°C above the temperature at the top of the storage unit T_{st}, air is circulated from the collector to the storage unit and returned to the collector as shown in Figure 3.3b. If the air temperature difference between the collector outlet and the top storage unit is less than 8°C, then the system is off.

3. **Heat From Storage(HFS)**

If the room temperature is below 21°C and energy is only available from the storage unit as indicated by a temperature above 24°C at the top of the storage bed, air is circulated in the opposite direction through the storage unit and sent directly to the room as shown in Figure 3.3c. If the air temperature at the top of the storage unit is less than 36°C, the first stage electric heater is used.

4. **Electric Heating(EH)**

If the room temperature is below 21°C, but little or no energy is available from either the collector or the storage unit, then both the first and second stage heaters are in operation with air circulating through the storage unit as shown in Figure 3.3d.

5. **System Purge**

If the collector temperature is above the maximum allowable limit, outside air can be circulated through the collector and exhausted to the outdoors in order to prevent the collector overheating.

In the following chapters, the abbreviations **HFC**, **COL**, **HFS** and **EH** will be used to refer to the operation modes defined above. The solar collector is in operation during **HFC** and **COL** and therefore these modes are known as collector operation modes. In **HFS** and **EH**, air is circulated through the storage bed. The modes of **HFS** and **EH** are then entitled as storage bed operation modes.

4. SIMULATION MODEL

As discussed in Chapter 2, subroutines are available in TRNSYS to represent the typical components in a solar energy system. If special components or operating sequences are present in the system, the user writes the appropriate subroutine and adds it to the program. Also, using typical components, the configuration of the simulation model may differ from the actual system.

4.1 The Modelling System

First of all, the system shown in Figure 3.1 should be modified so that the air flow loop of each mode governed by the motorized dampers can be handled by TRNSYS. Since the air in the duct connected to the top of the storage unit may flow either into or out of the storage unit depending on the mode of operation, the motorized damper at the top of the storage bed cannot simply be represented by a TRNSYS damper. The TRNSYS damper is actually a flow diverter or flow mixer for one directional flow control. For this system, it is necessary to replace the motorized damper by two TRNSYS dampers: a flow diverter and a flow mixer. This is shown in Figure 4.1 which indicates the solar heating system model. The flow diverter (Damper No.3) is used for inlet flow control to the storage bed and also directs the flow from the collector. Therefore, it replaces the motorized damper at the outlet of the collector in Figure 3.1 as well. The flow mixer (Damper No.4) is used for outlet flow control

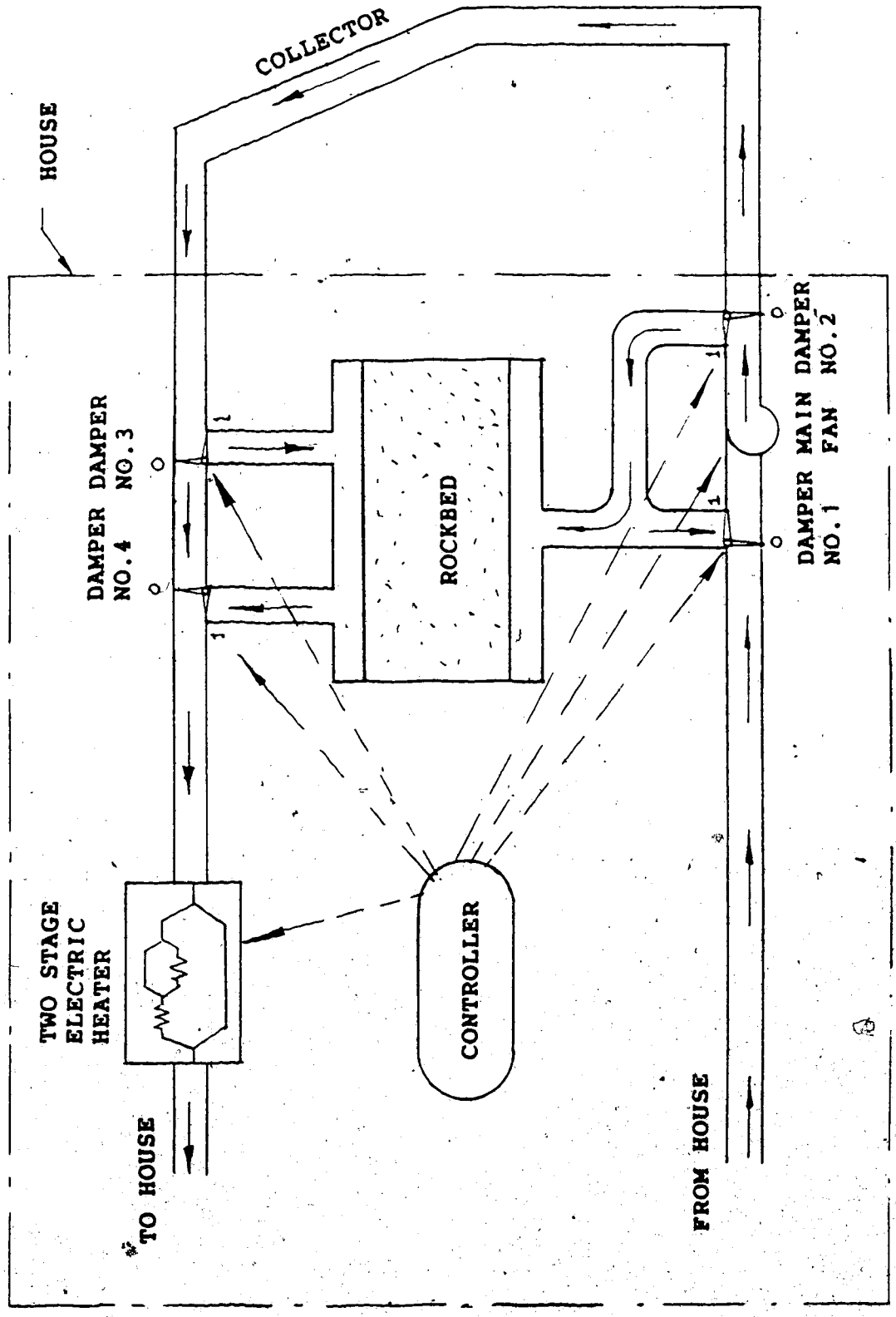

Figure 4.1 Solar Heating System Model

from the storage bed. In the air handling unit, another flow mixer (Damper No.1) and flow diverter (Damper No.2) are used to represent the three dampers in the actual system. The two dampers in the model are arranged in the way that they perform exactly the same functions of the three real dampers.

Experiments indicated that the system never operated in the System Purge mode, since the collector temperature never reached its maximum allowable limit even during summer period. Thus, the dampers for circulating outside air through the collector to the outdoors are omitted in the modelling system.

As seen in Figure 4.1, the positions of the dampers are designated by 1 and 0 which are the output values of the controller that operates the dampers in such a manner as to let the air flow through the same loops as those indicated in Figure 3.3. Thus, the damper positions under each system operation mode will be:

1. During HFC, all four dampers are open (position 1) so that air can flow through the collector by-passing the storage unit to the house module space.

2. During HFS and EH, Damper No.1 and No.3 are open (position 1); Damper No.2 and No.4 are closed (position 0). As a result, air is moved from bottom to the top of the storage unit, by-passing the collector to the space.

3. During COL, Damper No.1 and No.3 are closed (position 0). While Damper No.2 and No.4 are open (position 1) so that air is circulated from collector to the storage unit and returned to the collector.

The components of the system have been described in Chapter 3. Figure 4.1 indicates that the collector and two sections of duct are actually located outside the house. The space of the house itself is considered to be a component located within the module, i.e., the House Module described in Chapter 3. This component is represented by a TYPE 12 energy/(degree-hour) space heating load. In the system model, ducts connected to the collector outside the house are included for calculation of thermal losses. Thermal losses from ducts inside the house actually contribute to space heating and so are neglected. Further, simulations generally require some devices which are not ordinarily considered as parts of the system, for example, data reader, solar processor and algebraic operator. They are all treated as components in **TRNSYS**. Thus, in summary, the components to be used to analyze the system are:

1. a TYPE 9 data reader
2. two TYPE 16 solar radiation processors
3. two TYPE 31 ducts
4. a TYPE 1 air collector
5. a TYPE 3 fan

6. four TYPE 11 dampers
7. three TYPE 2 controllers
8. seven TYPE 15 algebraic operations
9. a TYPE 10 rockbed thermal storage
10. a TYPE 12 energy/(degree-hour) space heating load
11. a TYPE 36 system analyser

    A component, which is not from the standard **TRNSYS** library, has been written to identify the modes of operation, to supply electric energy for first and second stage heaters, and to analyze the energy distribution in the system. This component is described in Section 4.7.

12. printers, plotters and quantity integrators

    TRNSYS has printers, plotters and quantity integrators built in to the program. They will be used when needed.

Although, **TRNSYS** components are standard models that have been used for many years, their applications are worth mentioning. In addition, an integral part of a specified task of the system can be achieved by joining together a special group of components. This component group, as a whole, can be regarded as another component such as the data processor or system controller. They are discussed in the following sections.

4.2 Data Processor

Dynamic thermal behavior of a solar heating system depends on meteorological data such as ambient temperature and solar radiation. These time dependent conditions are considered to be the inputs of the system. For preparing the input data for simulations, a data processor formed by using three TRNSYS components (Figure 4.2) is used to read the data at each successive hour interval and make them available to other components as time varying functions.

The TYPE 9 data reader reads the month, date, year, hour and the hourly values of ambient temperature T_a, total radiation on collector I_T, total, beam and diffuse radiation on horizontal surface (indicated as I, I_b, and I_d respectively). The TYPE 9 component also linearly interpolates ambient temperature for each time step. Linear interpolation of solar radiation data was found to have several drawbacks[3]. Therefore, estimation of the actual radiation over a time step is done separately in two TYPE 16 solar radiation processors which use the curve for extraterrestrial radiation to interpolate radiation data. TYPE 16 is also designed to calculate several quantities related to the position of the sun, and estimate the radiation incident on various fixed and/or tracking surfaces. Since measurement of radiation on collector is available, the TYPE 16 components mainly serve the purpose of interpolating hourly solar radiation data from TYPE 9 and

---

[3]This is explained in Klein et al. (1983), P.4.1.4-1.

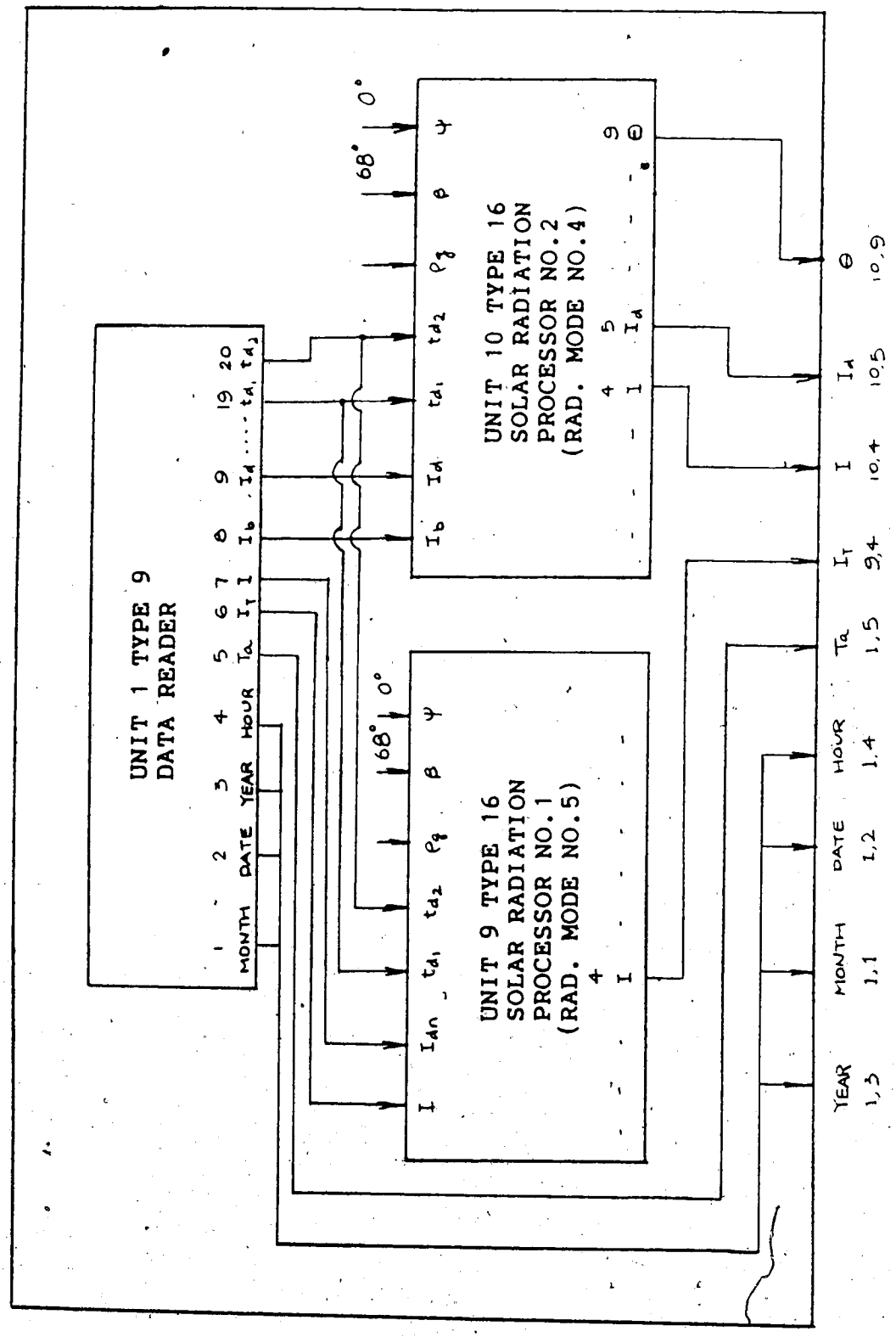

Figure 4.2 Data Processor

calculating the collector incidence angle θ which is required by the collector model to account for the effect of non-normal solar incidence (see Section 4.3).

However, a problem is encountered when concerning the interpolation of radiation incident on collector surface because TYPE 16 does not directly interpolate the radiation on tilted surface which is only estimated from the "interpolated" horizontal radiation data. To solve the problem, Radiation Mode No.5* in Solar Processor No.1 is used. The radiation data required as inputs in this mode are the horizontal total and direct normal beam radiation I_{dn}. Simply inputting the quantity of total radiation on collector I_T to the input position of horizontal total radiation I, the output of I will then become the "interpolated" total radiation on collector surface. The rest of the inputs (except the time of last data reading t_{d1} and the time of next data reading t_{d2}) to the unit is just for fulfilling the input requirement of the component.

Interpolation of horizontal total and diffuse radiation and calculation of the angle of incidence θ are performed in Solar Radiation Processor No.2 in which Radiation Mode No.4 is utilized. This mode takes horizontal beam and diffuse radiation as inputs.

Finally, the necessary quantities required by other components are "collected" together as the outputs of the

---

*TYPE 16 provides the user with several options for estimating radiation on tilted surface based on different sets of horizontal radiation data and each option is identified by a mode number.

component group. They are identified by (J,K), the Kth output of UNIT J.

4.3 Solar Collector Model

Solar collectors are modelled using the TYPE 1 TRNSYS component in which there are four possible collector operation modes. These operation modes model the thermal performance of a variety of collector types using either performance data or theory. For modelling the collector in the system, the first collector operation mode is used which is a linear efficiency model using the Hottel - Whillier equation:

$$\eta = \dot{Q}_u/A_c I_T = F_r(\tau\alpha) - F_r U_L(T_{ci} - T_a)/I_T \qquad (4.1)$$

where

η = overall collector efficiency

$\dot{Q}_u$ = rate of energy gain of collector

A_c = collector area

I_T = total incident radiation on collector per unit area

$F_r(\tau\alpha)$ = transmittance-absorptance product factor of collector

$F_r U_L$ = collector heat loss factor

T_{ci} = inlet temperature of fluid to collector

T_a = ambient temperature

Equation (4.1) is derived from an energy balance on a flat plate collector under steady state conditions. If $F_r(\tau\alpha)$ and $F_r U_L$ are constants, the performance data can be presented as straight line plot of η versus $(T_{ci} - T_a)/I_T$ with intercept $F_r(\tau\alpha)$ and slope $-F_r U_L$. Mode 1 assumes that efficiency vs. $(T_{ci} - T_a)/I_T$ is a straight line.

Equation (4.1) is a general equation in which the values of the collector parameters depend on the test conditions. Since standard tests of collector performance are done at solar noon on clear days, the parameter $F_r(\tau\alpha)$ determined under standard test conditions is nearly the normal incidence value $F_r(\tau\alpha)_n$. To account for non-normal incidence, Mode 1 corrects the intercept efficiency $F_r(\tau\alpha)_n$ using an incidence angle modifier defined as

$$K_{(\tau\alpha)} = (\tau\alpha)/(\tau\alpha)_n \qquad (4.2)$$

The incident radiation is composed of beam, diffuse, and ground-reflected radiation. Thus the incidence angle modifier for each of the three components is treated separately. For beam radiation, the incidence angle modifier outlined in ASHRAE Standard 93-77, 1977 is defined as

$$(\tau\alpha)_b/(\tau\alpha)_n = 1 - b_o(1/\cos\theta - 1) \qquad (4.3)$$

where

b_o = incidence angle modifier coefficient

θ = solar incidence angle

For diffuse and ground-reflected radiation, equivalent incidence angles for using Equation (4.3) are defined in Klein et al. (1983), P.4.2.1-11. These equivalent angles for beam radiaton are assumed to give the same transmittance as for diffuse and ground-reflected radiation.

Moreover, corrections applied to the slope and intercept parameters to account for 1) the presence of a heat exchanger, 2) identical collectors in series, and 3) flow rates other than those at test conditions are also included in collector mode 1. Since the system is not equipped with a heat exchanger, the first correction is ignored in the model.

4.4 Rockbed Model

The rockbed model currently in TYPE 10 is a modification of previous models. The first analytical study was by Schumann(1929) who assumed one dimensional "plug" flow, no axial conduction, constant properties, no heat loss to the environment and no temperature gradients within the solid particles for his formulations. The fluid (T_f) and bed (T_b) temperatures are related by energy balances on the fluid and bed as

$$\rho_f C_f \zeta \frac{\partial T_f}{\partial t} = - \frac{\dot{m} C_f}{A} \frac{\partial T_f}{\partial x} + h_v (T_b - T_f) \qquad (4.4)$$

$$\rho_b C_b (1-\zeta) \frac{\partial T_b}{\partial t} = h_v (T_f - T_b) \qquad (4.5)$$

where

ζ = void fraction of packed bed

A = cross sectional area of packed bed

x = position along the bed in the flow direction

h_v = volumetric heat transfer coefficient between the bed and the fluid

For an air based system, Hughes et al.(1976) assumed the fluid capacitance term in Equation (4.4) to be negligible so that the equations can be written as

$$\frac{\partial T_f}{\partial (x/L)} = Ntu\ (T_b - T_f) \tag{4.6}$$

$$\frac{\partial T_b}{\partial \theta} = Ntu\ (T_f - T_b) \tag{4.7}$$

where

Ntu = number of heat transfer units

$= (h_v AL)/(\dot{m}C_f)$

θ = dimensionless time

$= t(\dot{m}C_f)/[\rho_b C_b (1-\zeta)AL]$

$= t(\dot{m}C_f)/[\rho_r C_b AL]$

L = flow length of bed

ρ_r = apparent rock density (accounting for voids)

Hughes et al. indicated that the long term performance of a solar air heating system predicted by Equations (4.6) and (4.7) with Ntu greater than 10 is virtually the same as that

with Ntu equal to infinity. In this case for any rockbed with Ntu greater than 10, an infinite Ntu can be assumed. Thus Equations (4.6) and (4.7) can be reduced to a single equation since the bed and fluid temperatures are equal throughout the bed for infinite Ntu. With the additional terms of axial conduction and heat losses to the environment from the sides of the bed included, the resulting equation is

$$\frac{\partial T}{\partial \theta} = -L\frac{\partial T}{\partial x} + \frac{UPL}{\dot{m}C_f}(T_{env} - T) + \frac{kAL}{\dot{m}C_f}\frac{\partial^2 T}{\partial x^2} \qquad (4.8)$$

where

T = bed and fluid temperatures

P = perimeter of rockbed wall

U = loss coefficient from the rockbed to the environment

k = thermal conductivity of rockbed in the axial direction

To solve Equation (4.8) numerically, the rockbed is divided into segments. Using finite difference methods, an ordinary differential equation can be written for each segment in which the bed temperature is assumed to be uniform. Once the differential equation is solved, a detailed temperature profile can then be obtained.

4.5 Space Heating Model

To estimate the heating load of the house module, TYPE 12 energy/(degree-hour) space heating component is employed. In TRNSYS, the ASHRAE energy/(degree-day) concept is extended to estimate the hour by hour heating load (i.e., the so called energy/(degree-hour) space heating load model). There are four modes of operation in this component and Mode 4 is selected to calculate the heating energy requirement. This mode formulates a single lumped capacitance house compatible with temperature level control by the following equation

$$CAP \cdot dT_r/dt = \gamma \epsilon C_{min}(T_i - T_r) + \dot{Q}_{gain} - UA(T_r - T_a) + \dot{Q}_{aux} - (1-L_f)\dot{Q}_{cool} \qquad (4.9)$$

where

γ = heat exchanger control function

$$= \begin{cases} 1 \text{ if } \dot{m} > 0 \\ 0 \text{ otherwise} \end{cases}$$

CAP = lumped thermal capacitance of house

ϵC_{min} = product of the effectiveness and minimum capacitance rate of load heat exchanger

$\dot{Q}_{gain}$ = all time variant heat gains such as losses from storage tanks and fenestration

$\dot{Q}_{aux}$ = the instantaneous auxiliary energy

$\dot{Q}_{cool}$ = rate of cooling by air conditioner

L_f = ratio of latent load to total cooling load

UA = overall heat loss coefficient - area product of a structure

T_r = room temperature

T_a = ambient temperature

T_i = temperature of fluid from heat source

$\dot{m}$ = mass flow rate of fluid from heat source

Equation (4.9) is a general equation of an energy balance for a house. By solving the differential equation, the final and average room temperature for each time step can be obtained.

The rate of energy transferred across the load heat exchanger $\dot{Q}_T$, instantaneous heating load $\dot{Q}_L$, rate of sensible cooling $\dot{Q}_{sens}$, and rate of cooling used to reduce room humidity $\dot{Q}_{lat}$ are calculated as

$$\dot{Q}_T = \gamma \cdot \epsilon C_{min}(T_i - T_r) \tag{4.10}$$

$$\dot{Q}_L = UA(T_r - T_a) - \dot{Q}_{gain} \tag{4.11}$$

$$\dot{Q}_{sens} = (1 - L_f)\dot{Q}_{cool} \tag{4.12}$$

$$\dot{Q}_{lat} = \dot{Q}_{cool} - \dot{Q}_{sens} \tag{4.13}$$

Since only heating is of interest, $\dot{Q}_{cool}$ is set to zero in the simulation. Therefore $\dot{Q}_{sens}$ and $\dot{Q}_{lat}$ are zero. For estimating the UA factors of the house, the method of energy/(degree-day) is modified in the model by defining the house as an analysis control volume. The heating load is assumed to be the total energy required by the system to

cover the balanced effect of all losses and internal heat gains of the control volume. The UA factor is then evaluated by dividing the measured total energy requirement by the summation of the average hourly difference between the room and ambient temperatures. The losses through the collector and ducts outside the module are beyond the control volume[4] and therefore not taken into account. Since $\dot{Q}_{gain}$ is covered by the estimated UA factor[5], $\dot{Q}_{gain}$ in Equations (4.9) and (4.11) is ignored by setting it to zero. Hence, Equation (4.9) becomes

$$Cap \cdot dT_r/dt = \dot{Q}_T + \dot{Q}_{aux} - UA(T_r - T_a) \qquad (4.14)$$

For computational purposes, the sum of $\dot{Q}_T$ and $\dot{Q}_{aux}$ is replaced by $\dot{Q}_H$, the rate of total energy supply for space heating which is discussed in Section 4.7. During simulation, this can be done by 1) assigning a zero value to ϵC_{min} so that $\dot{Q}_T$ becomes zero, and 2) feeding $\dot{Q}_H$ into the input position of $\dot{Q}_{aux}$.

---

[5] Justification of the estimated UA factor is done in Chapter 6.

4.6 Control System

For simulating the control strategy, it is necessary to understand how the system responds to the input temperatures. The input temperatures signal the controller to identify the modes of operation according to the control criteria of the system, and the outputs govern the fan, dampers and the electric heater.

The control criteria, modes of operation, the corresponding mass flow rate, damper positions and conditions for first and second stage heating have been defined previously. It will be helpful to summarize all these into a table (Table 4.1). The first four columns of Table 4.1 give the control criteria based on Figure 3.2. It can be seen that dead band temperature differences for giving a hysteresis effect are used to promote stability. For example, the room temperature in the first column indicates a dead band temperature difference of 1.5°C. That is, a heating system may be turned off if the room temperature is over 21.5°C, but not turned on until the room temperature is less than 20°C. If the difference between the set temperature (21.5°C) and the room temperature lies within the dead band difference (1.5°C), the controller remains in its previous state. Column 5 assigns a mode number to each of the seven system operation modes which are re-classified in column 6 to distinguish whether stage heating is required. Finally, columns 7 to 11 give the control strategy outputs.

Table 4.1 Summary of Control Strategy

Control Criteria				Mode		Control Strategy outputs				
Room Temp.	Collector Outlet Air Temp.	Top Storage Bed Temp.		No.	Operation	Main Fan Control Function	Damper No.1 Position	Damper No.2 Position	Damper No.3 Position	Damper No.4 Position
T_r (°C)	T_{co} (°C)	T_{st} (°C)	$T_{co}-T_{st}$ (°C)			γ_F	γ_1	γ_2	γ_1	γ_2
<20.0	>29.0 ≤33.0	/	/	1.0	HFC-1st stage heater on	0.56	1	1	1	1
<20.0	>33.0	/	/	1.1	HFC-heater off	0.56	1	1	1	1
<20.0	<22.0	≥24.0 ≤36.0	/	2.0	HFS-1st stage heater on	1	1	0.04	1	0.04
<20.0	<22.0	>36.0	/	2.1	HFS-heater off	1	1	0.04	1	0.04
<20.0	<22.0	<24.0	/	3.0	EH-two stage heater on	1	1	0.04	1	0.04
>21.5	/	/	>10.0	4.0	COL	0.56	0	1	0	1
>21.5	/	/	<-1.0	5.0	System Off	0	0	1	0	1

Since the mass flow rate during collector operation mode (HFC and COL) is approximately 56% of the mass flow rate during storage bed operation mode (HFS and EH), it is computed using a variable control function having values of 0, 1 and 0.56. This control function indicates whether the fan should be off, operated at maximum flow or 56% of the maximum flow. Furthermore, the experimental data showed that there is leakage through the dampers to the collector during storage bed operation mode. In the modelling system (Figure 4.1), this leakage can be manipulated by assuming that Damper No.2 and No.4 cannot be closed completely. However, the amount of leakage is very difficult to quantify experimentally. The model assumes that the percentage of leakage is approximately 4%*.

From Table 4.1, the positions of Damper No.1 and No.3 are always the same, thus one control function γ_1 is enough to describe the positions of these two dampers. For Damper No.2 and No.4, another control funtion γ_2 is used. Together with the main fan control function γ_F, these three functions are the control strategy outputs. It is now natural to ask how to model the control system in order to 1) identify the modes of operation and 2) produce the three control functions. The latter is achieved by using a system controller whose information flow diagram is represented as follow:

---

*Determination of leakage is described in Chapter 6.

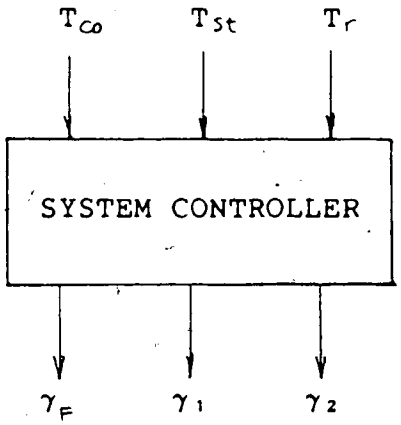

Note that T_{co} , T_{st} and T_r are the three control strategy inputs of the system and are used to generate those values of γ_F , γ_1 and γ_2 shown in Table 4.1. They can be grouped into four combinations:

	γ_F	γ_1	γ_2	
1.	0.56	1	1	for **HFC**
2.	1	1	0.04	for **HFS** and **EH**
3.	0.56	0	1	for **COL**
4.	0	0	1	for **System Off**

The control functions from the system controller together with the input temperatures were fed to a system analyzer to identify the modes of operation and supply electric energy for stage, heating if necessary (This is discussed in the next section).

The system controller is modelled using nine TRNSYS components. Figure 4.3 shows the interconnection of the components. The three TYPE 2 temperature controllers test the room temperature, collector outlet air temperature and top storage bin temperature, and produce the output control functions on the basis of two dead band temperature differences (ΔT_H and ΔT_L), with the input (γ_i) and output (γ_o) control functions connected giving a hysteresis effect. The mathematical description of the TYPE 2 controller is:

if $\gamma_i = 1$ and $\Delta T_L \leq (T_H - T_L)$, $\gamma_o = 1$

if $\gamma_i = 1$ and $\Delta T_L > (T_H - T_L)$, $\gamma_o = 0$

if $\gamma_i = 0$ and $\Delta T_H < (T_H - T_L)$, $\gamma_o = 1$

if $\gamma_i = 0$ and $\Delta T_H \geq (T_H - T_L)$, $\gamma_o = 0$

where

ΔT_H = upper dead band temperature difference

ΔT_L = lower dead band temperature difference

T_H = upper input temperature

T_L = lower input temperature

A more complete description of this component is given in Klein et al.(1983), Section 4.4.

Table 4.1 indicates that whenever the room temperature is less than 20°C, γ_1 is 1, otherwise it is 0. Since the room temperature is tested by UNIT 16, the positions of Damper No.1 and Damper No.3 are directly controlled by UNIT 16. In order to find γ_F and γ_2, the outputs of the

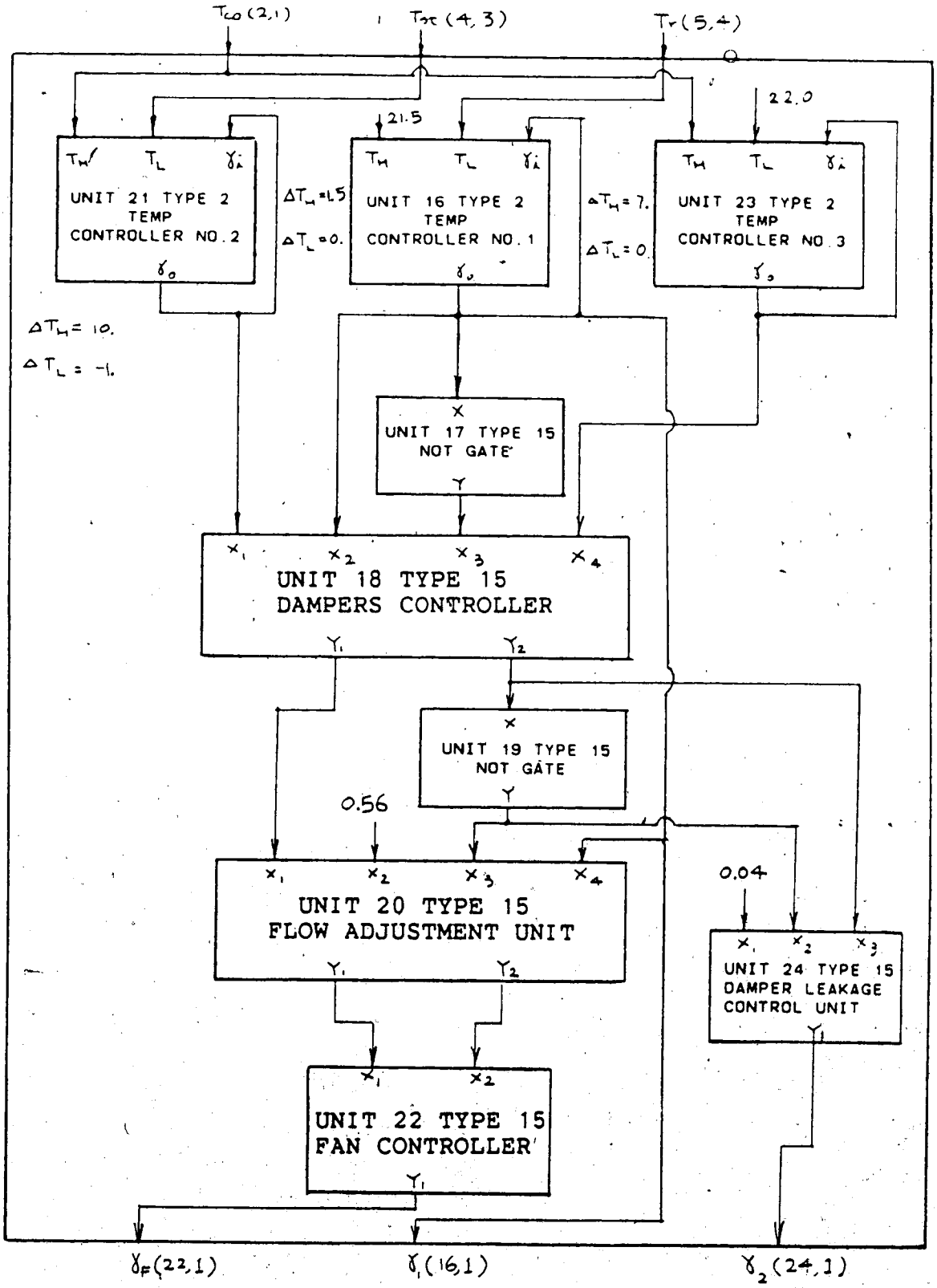

Figure 4.3 System Controller

three TYPE 2 controllers go through a series of logical operations by using the following TYPE 15 algebraic operators:

1. UNIT 17 and 19 are "NOT" gates which are formulated by:

$$Y = 1 - X$$

2. UNIT 18 contains two "OR" gates which are described as follow:

$$Y_1 = \max(X_1, X_2)$$

$$Y_2 = \max(X_3, X_4)$$

3. UNIT 20 is a flow adjustment unit. It consists of a multiplication operator and an "AND" gate. The mathematical description of the component is:

$$Y_1 = X_1 X_2 \ , \ X_2 = 0.56$$

$$Y_2 = \min(X_3, X_4)$$

4. UNIT 22, the fan controller, is an "OR" gate which controls the operation of the fan in the air handling unit and so produces the control function γ_F —

5. Finally, γ_2 is determined by UNIT 24. The positions of Damper No.2 and No.4 are justified by the following equation:

$$Y = \max(X_1 X_2 \ , \ X_3) \ , \ X_1 = 0.04$$

where X_i is the ith INPUT value and Y_i is the ith OUTPUT of the operators.

To see how the system controller performs, a truth table showing the outputs of each component of the system under each category of operation modes are shown in Table 4.2.

4.7 System Analyzer

The system analyzer is an author-written subroutine not included in the standard TRNSYS library. To be compatible with TRNSYS components, a UNIT number 6 and TYPE number 36 are assigned to the model. This component not only identifies the modes of operation and electric energy for first and second stage heating $\dot{Q}_{aux}$, it also determines the rates of energy distributed to the rockbed $\dot{Q}_{store}$, total energy actually supplied from the thermal system to space heating $\dot{Q}_H$, total energy supplied to the thermal system $\dot{Q}_{sys}$, the radiation incident on the collector during collector operation mode I_{TC}, and energy losses.

The energy $\dot{Q}_H$ is considered to be the total of the net solar energy directly sent from the collector to the module space, the energy supplied from the storage unit $\dot{Q}_S$ and the electric energy provided. The energy $\dot{Q}_{sys}$ is regarded as the sum of the useful solar energy collected by the collector $\dot{Q}_u$ and the electric energy supplied.

In this component, two kinds of energy losses are taken into account. One is the energy loss through ducts outside the house during collector operation mode $\dot{Q}_{DUCT}$. The other is the energy loss due to leakage of dampers $\dot{Q}_{DLL}$. During

Table 4.2 Outputs of Each Component of The System Controller

Operation Mode	UNIT 16 δ_0	UNIT 21 δ_0	UNIT 23 δ_0	UNIT 17 Y	UNIT 18 Y_1, Y_2	UNIT 19 Y	UNIT 20 Y_1, Y_2	UNIT 22 Y_1	UNIT 24 Y_1	δ_F	δ_1	δ_2
HFC	1	*	1	0	1, 1	0	0.56, 0	0.56	1	0.56	1	1
HFS, EH	1	*	0	0	1, 0	1	0.56, 1	1	0.04	1	1	0.04
COL	0	1	*	1	1, 1	0	0.56, 0	0.56	1	0.56	0	1
SYSTEM OFF	0	0	*	1	0, 1	0	0, 0	0	1	0	0	1

* A dummy unit whose output value, whether 1 or 0, will not affect the final outputs of the system controller

storage bed operation mode, there is little or no solar radiation. If air leaks through the dampers to the collector, the energy $\dot{Q}_u$ is negative. In this case, $\dot{Q}_u$ is considered to be part of the losses and treated separately from the useful solar energy gained.

4.7.1 Information Flow Diagram

The information flow of the system analyzer is summarized in the following diagram. As shown, the model requires nine inputs and six parameters to produce nine outputs:

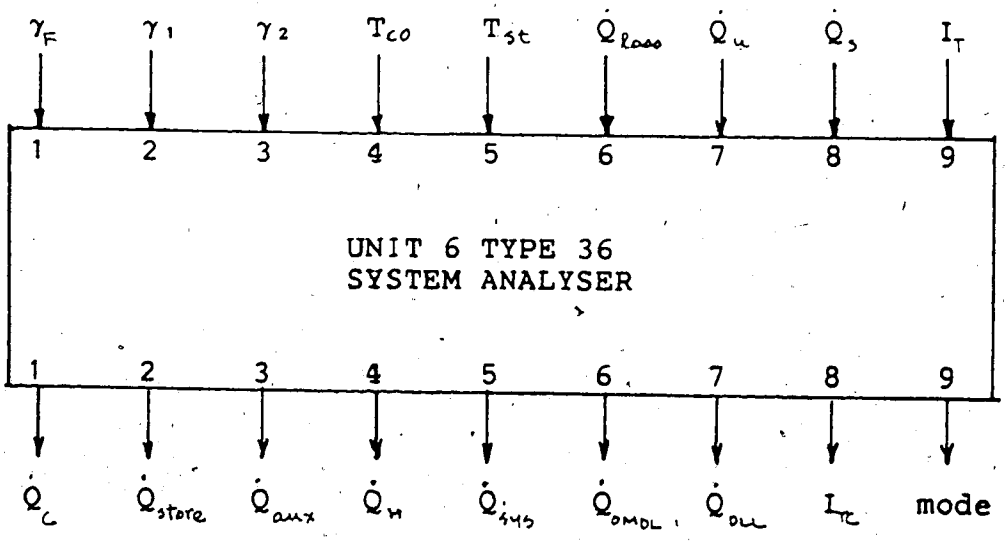

Parameters

1. T_{s1} 2. T_{s2} 3. T_{co_2}
4. P_1 5. P_2 6. P_{min}

The PARAMETERS, INPUTS and OUTPUTS are defined in sequential order as:

PARAMETERS

1. T_{S1} - set temperature of top storage bed for HFS with 1/2 electric coil on, 24°C
2. T_{S2} - set temperature of top storage bed for HFS with electric coil off, 36°C
3. T_{co_2} - air set temperature at collector outlet for HFC with electric coil off, 33°C
4. P_1 - electric power supply for first stage heating, 3.75 KW
5. P_2 - electric power supply for two stage heating, 7.50 KW
6. P_{min} - minimum power supply to keep the fan on, 0.63 KW

INPUTS

1. γ_F - main fan control function
2. γ_1 - control function of Damper No.1 and No.3
3. γ_2 - control function of Damper No.2 and No.4
4. T_{co} - collector outlet air temperature
5. T_{St} - top storage bed temperature
6. $\dot{Q}_{Loss}$ - rate of energy losses from the ducts outside of the house
7. $\dot{Q}_u$ - rate of useful solar energy collected from collector

8. $\dot{Q}_S$ - rate of energy supplied from storage bed
9. I_T - incident solar radiation on collector

OUTPUTS

1. $\dot{Q}_C$ - rate of solar energy gain of collector during collector operation mode
2. $\dot{Q}_{store}$ - rate of energy stored in rockbed
3. $\dot{Q}_{aux}$ - rate of auxiliary energy supply
4. $\dot{Q}_H$ - rate of total energy supply to space heating
5. $\dot{Q}_{sys}$ - rate of total energy supply to the system
6. $\dot{Q}_{DUCL}$ - rate of energy losses through ducts during collector operation mode
7. $\dot{Q}_{DLL}$ - rate of energy losses due to leakage of dampers
8. I_{TC} - incident solar radiation on collector during collector operation mode
9. mode - mode number of operation

4.7.2 Mathematical Description

The system analyzer uses control functions and temperature set points to define its mode of operation so that energy flow for the heating system can be determined as follows:

1. For heating from collector operation mode, HFC the control functions are:

$$\gamma_1 = \gamma_2 = 1$$

If $T_{co} \leq T_{co_2}$

mode = 1

1st stage heater on

$\dot{Q}_{aux} = P_1$

Otherwise

mode = 1.1

min. power supply to keep the fan running

$\dot{Q}_{aux} = P_{min}$

Then, the energy flow is defined as:

$I_{TC} = I_T$

$\dot{Q}_{store} = 0$

$\dot{Q}_H = \dot{Q}_{aux} + \dot{Q}_u - \dot{Q}_{loss}$

$\dot{Q}_{sys} = \dot{Q}_{aux} + \dot{Q}_u$

$\dot{Q}_{comb} = \dot{Q}_{loss}$

$\dot{Q}_{DLL} = 0$

$\dot{Q}_C = \dot{Q}_u$

2. For heating from storage and electric heating operation modes, HFS and EH

the control functions are:

$\gamma_1 = 1$ and $\gamma_2 < 1$

If $T_{S2} \geq T_{st} \geq T_{S1}$

mode = 2

1st stage heater on

$\dot{Q}_{aux} = P_1$

If $T_{st} > T_{S2}$

mode = 2.1

min. power supply

$\dot{Q}_{aux} = P_{min}$

If $T_{st} < T$

mode = 3

both stage heaters on

$\dot{Q}_{aux} = P_2$

Then, the energy flow is defined as:

$I_{TC} = 0$

$\dot{Q}_{store} = 0$

$\dot{Q}_H = \dot{Q}_{aux} + \dot{Q}_s$

$\dot{Q}_{sys} = \dot{Q}_{aux}$

$\dot{Q}_{ondl} = 0$

$\dot{Q}_{DLL} = \dot{Q}_{loss} - \dot{Q}_u$

$\dot{Q}_c = 0$

3. For heat collection operation mode, COL the control function are:

$\gamma_1 = 0, \ \gamma_2 = 1, \ \gamma_F \neq 0$

Then

mode = 4

$I_{TC} = I_T$

$\dot{Q}_{aux} = P_{min}$

$\dot{Q}_{store} = \dot{Q}_u - \dot{Q}_{loss}$

$\dot{Q}_H = \dot{Q}_{aux}$

$\dot{Q}_{sys} = \dot{Q}_{aux} + \dot{Q}_u$

$\dot{Q}_{ondl} = \dot{Q}_{loss}$

$\dot{Q}_{DLL} = 0$

$\dot{Q}_c = \dot{Q}_u$

4. System Off if $\gamma_F = 0$

Then

mode = 5, and

all energy quantities are zero

The subroutine program is given in Appendix B.

4.8 Information Flow of System

Now that the components of the system are known, it is necessary to join all of them together to form an information flow diagram of the system. The information flow of the active a[redacted] solar heating system is shown in two figures. Figure 4.4 shows the interconnection of the components outside the house module. Figure 4.5 considers only the components inside the house. As described previously, each component is represented as a box with information flowing in the directions indicated by the arrows. The INPUTS and OUTPUTS, presented in the order defined by TRNSYS, for each component are shown. The outputs identified by a numbered circle are the results of interest. These outputs are connected to TYPE 25 printers (not shown). The printers basically print the instantaneous values at the end of each hour. If integrated quantities are required, then TYPE 24 quantity integrators are used to integrate the instantaneous quantities over a period of time before printing (also not shown).

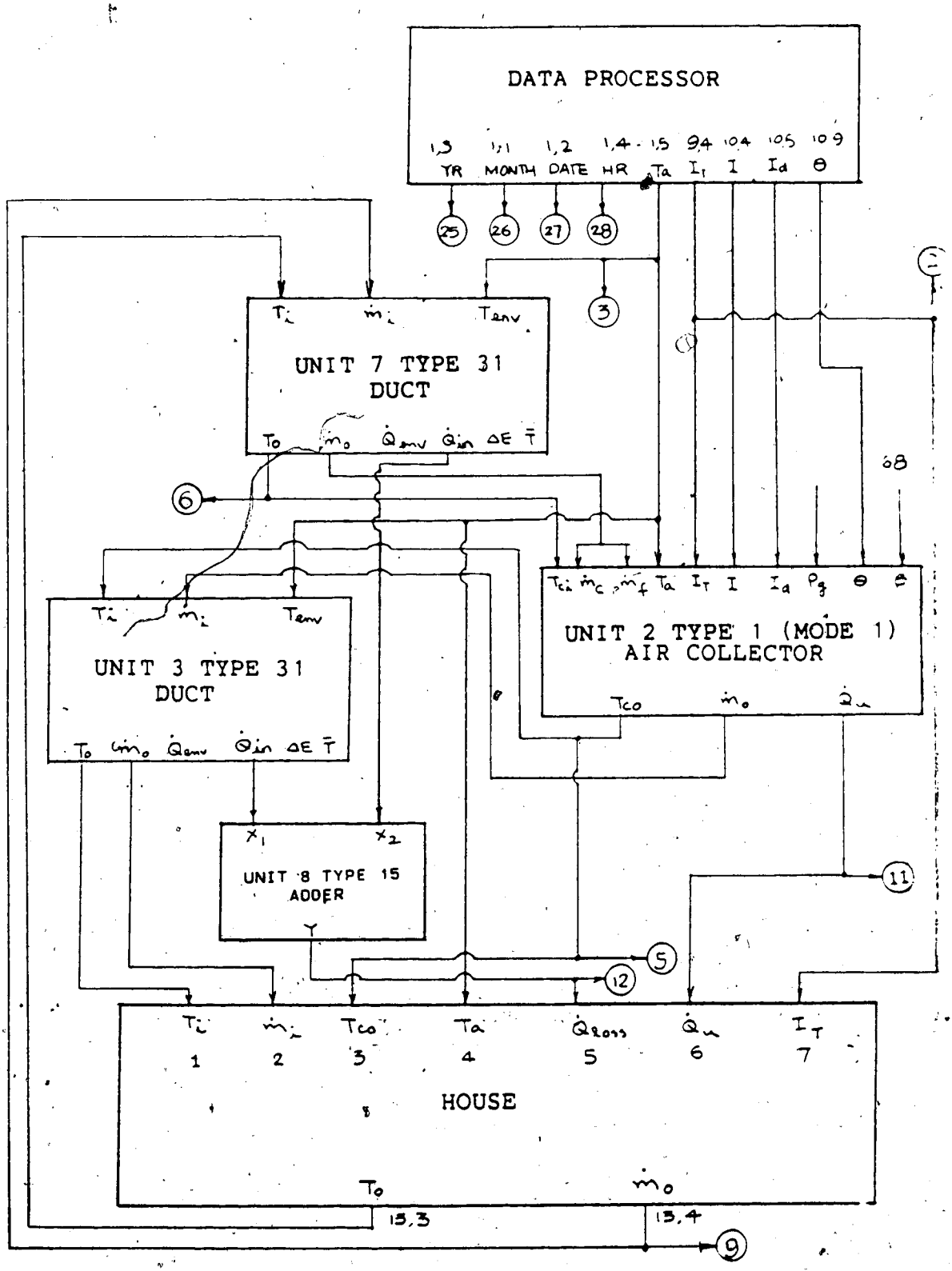

Figure 4.4 Information Flow Diagram of Components Outside The House

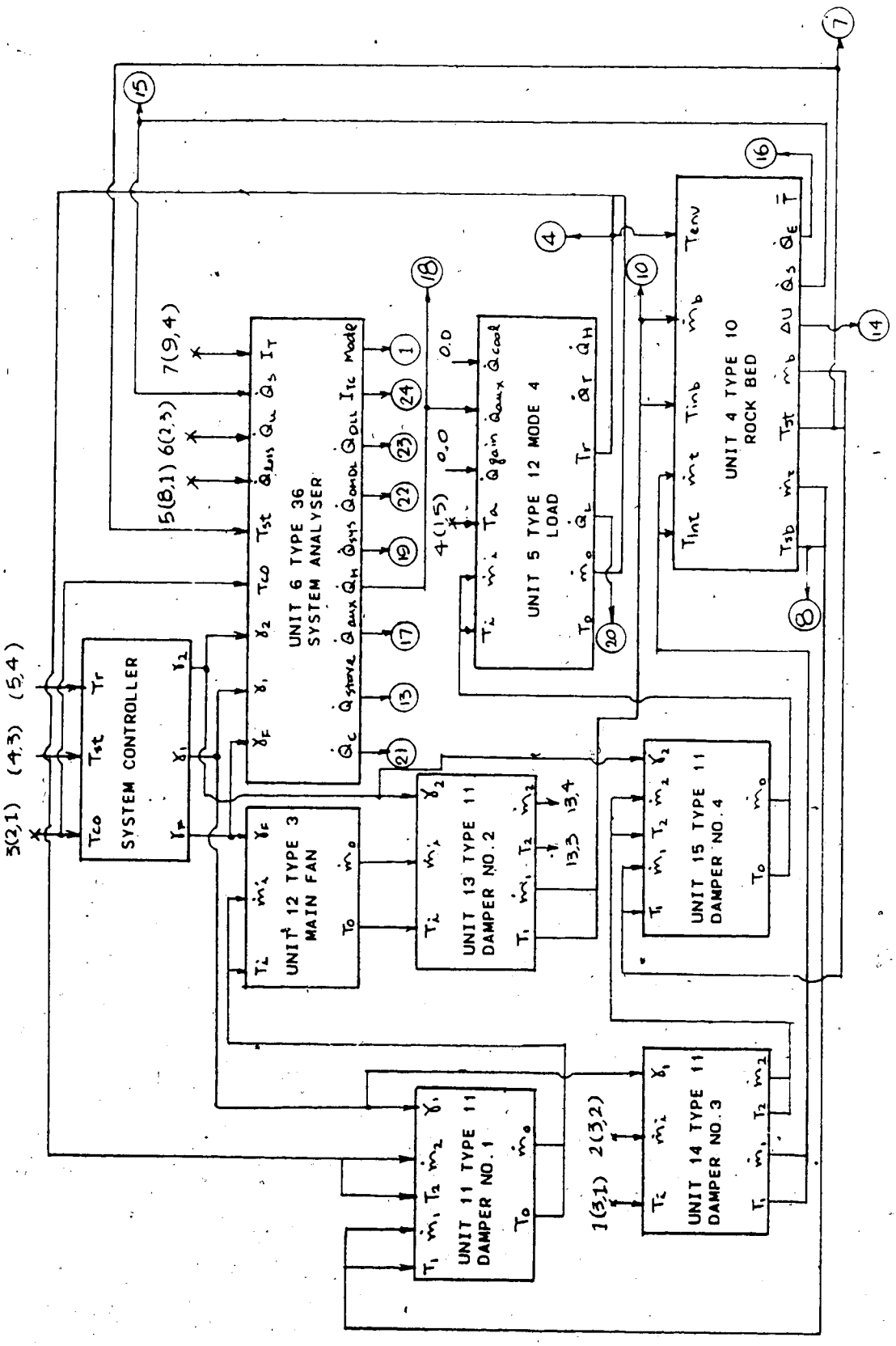

Figure 4.5 Information Flow Diagram of Components Within The House

For the components outside the module (Figure 4.4), there are actually two identical duct sections and an air collector. UNIT 7 is the section of duct connected from the module to the inlet of the collector. UNIT 3 is connected from the collector outlet to the house. Each unit is represented by a TYPE 31 component, a "plug-flow" model, which estimates the rate of energy $\dot{Q}_{in}$ gained or lost for each duct section. The energy $\dot{Q}_{in}$ from UNITS 3 and 7 is summed by a TYPE 15 adder to give $\dot{Q}_{loss}$ (the fifth input to the house), the total energy lost from or gained by the two duct sections outside the residence. The data processor which is described in Section 4.2 provides all the necessary inputs to the components and TYPE 1 calculates T_{co} and $\dot{Q}_u$. The air flow loop is indicated by the paths connecting $\dot{m}_o$, outlet mass flow rate from a component, to the next unit. Thus, as shown in Figure 4.4, air is sent from the house to UNIT 7, and then through the collector to UNIT 3. The outlet air from UNIT 3 is returned to the room and circulated back to UNIT 7 to complete the loop. The seven inputs to the house are the information required by the components inside the house. The locations of the seven inputs being sent are indicated in Figure 4.5 by I(J,K), the Ith input to the house from the Kth output of UNIT J (i.e., inputs 1(3,1), 2(3,2), 3(2,1), 4(1,5), 5(8,1), 6(2,3) and 7(9,4)). Finally, the temperature and flow rate of the returned air from Damper No.2, UNIT 13, are transmitted to UNIT 7 to complete the information flow of the system. The

returned air temperature and flow rate are the third and fourth outputs of UNIT 13 respectively.

For the components within the structure (Figure 4.5), there are the system controller, main fan, four dampers, two stage electric heater and the rockbed storage unit. The heater is modelled in TYPE 36 system analyser which has been described in Section 4.7. The TYPE 12 component is included to determine the space heating load and the room temperature (described in Section 4.5). As mentioned previously, the system controller produces three control functions (γ_F, γ_1 and γ_2). They are sent to the fan, the four dampers and the system analyzer. The fan controls the flow rate by the following equation

$$\dot{m}_o = \gamma_c \dot{m}_{max} \qquad (4.15)$$

where

$\dot{m}_{max}$ = maximum flow rate

and the flow is directed by two types of dampers:

1. A mixer is modelled by

$$\dot{m}_o = \dot{m}_1(1-\gamma_k) + \dot{m}_2\gamma_k \qquad (4.16)$$

where

γ_k = γ_1 for Damper No.1

= γ_2 for Damper NO.4

$\dot{m}_1, \dot{m}_2$ = inlet flow rates to the mixer

2. A diverter is described by

$$\dot{m}_1 = \dot{m}_i(1-\gamma_k) \tag{4.17}$$

$$\dot{m}_2 = \dot{m}_i\gamma_k \tag{4.18}$$

where

γ_k = γ_1 for Damper No.3

= γ_2 for Damper NO.2

$\dot{m}_1, \dot{m}_2$ = outlet flow rates from the diverter

As a result, if $\gamma_1 = 1$, Damper No.1 directs the flow from the space heating model to the fan; if $\gamma_1 = 0$, air is sent from the rockbed. If $\gamma_2 = 1$, Damper No.2 leads the air to the collector; if $\gamma_2 = 0.04$, 96% flow is diverted to the rockbed and 4% to the collector. Damper No.3 takes the air from the collector to either Damper No.4 when $\gamma_1 = 1$ or the rockbed when $\gamma_1 = 0$. Similarly, Damper No.4 takes the air from Damper No.3 to the space heating model when $\gamma_2 = 1$; if $\gamma_2 = 0.04$, then a mixing of air from both Damper No.3 and the rockbed will be sent to the space heating model.

It is found that mixing of air due to leakage from dampers will create unexpected loss of returned flow from Damper No.4. For example, if a flow rate of 100 Kg/s is originally supplied by the fan during storage bed operation mode with 4% leakage of both Damper No.2 and No.4, then the air after being split by Damper No.2 will finally reach Damper No.4 at a rate of 96 Kg/s from the rockbed and 4 Kg/s from Damper No.3. Mixing of air at Damper No.4 using

Equation (4.16) gives a flow rate of 92.3 Kg/s in return. Although, the returned flow rate is about 7.7% lower, it will not affect the simulation results because the first two inputs to TYPE 12 space heating model are dummy inputs if a heat exchanger is not present. Further, $\dot{m}_o$, which is equal to $\dot{m}_i$, of TYPE 12 will be re-adjusted by Equation (4.15) after passing through Damper No.1 to the fan.

The rockbed storage unit is the TYPE 10 component, an "infinite" Ntu model, described in Section 4.4. This model is applied directly to determine the dynamic behavior of the storage bin. As shown in Figure 4.5, the component requires five inputs to generate eight outputs. They are:

INPUTS

1. T_{int} - temperature of air entering the rockbed from the top
2. $\dot{m}_t$ - flow rate of air entering the rockbed from the top
3. T_{inb} - temperature of air entering the rockbed from the bottom
4. $\dot{m}_b$ - flow rate of air entering the rockbed from the bottom
5. T_{env} - basement room temperature

OUTPUTS

1. T_{sb} - bottom segment air and rockbed temperature
2. $\dot{m}_t$ - flow rate of air entering the rockbed from the top

3. T_{St} - top segment air and rockbed temperature
4. $\dot{m}_b$ - flow rate of air entering the rockbed from the bottom
5. ΔU - change in internal energy of the rockbed between any time and time = 0.0
6. $\dot{Q}_S$ - rate at which energy is removed from the rockbed to meet the load
7. $\dot{Q}_E$ - rate of energy losses from bed
8. $\bar{T}$ - average rockbed and air temperature

As a whole, the overall configuration of the active air solar heating system can be simply regarded as a single box shown in Figure 4.6. The input data required by the whole system are those read by the TYPE 9 data reader and the outputs are those identified by a numbered circle. They are:

INPUTS

1. Month
2. Date
3. Year
4. Hour
5. T_a - ambient temperature
6. I_T - total radiation on collector
7. I - total radiation on horizontal surface
8. I_b - beam radiation on horizontal surface
9. I_d - diffuse radiation on horizontal surface

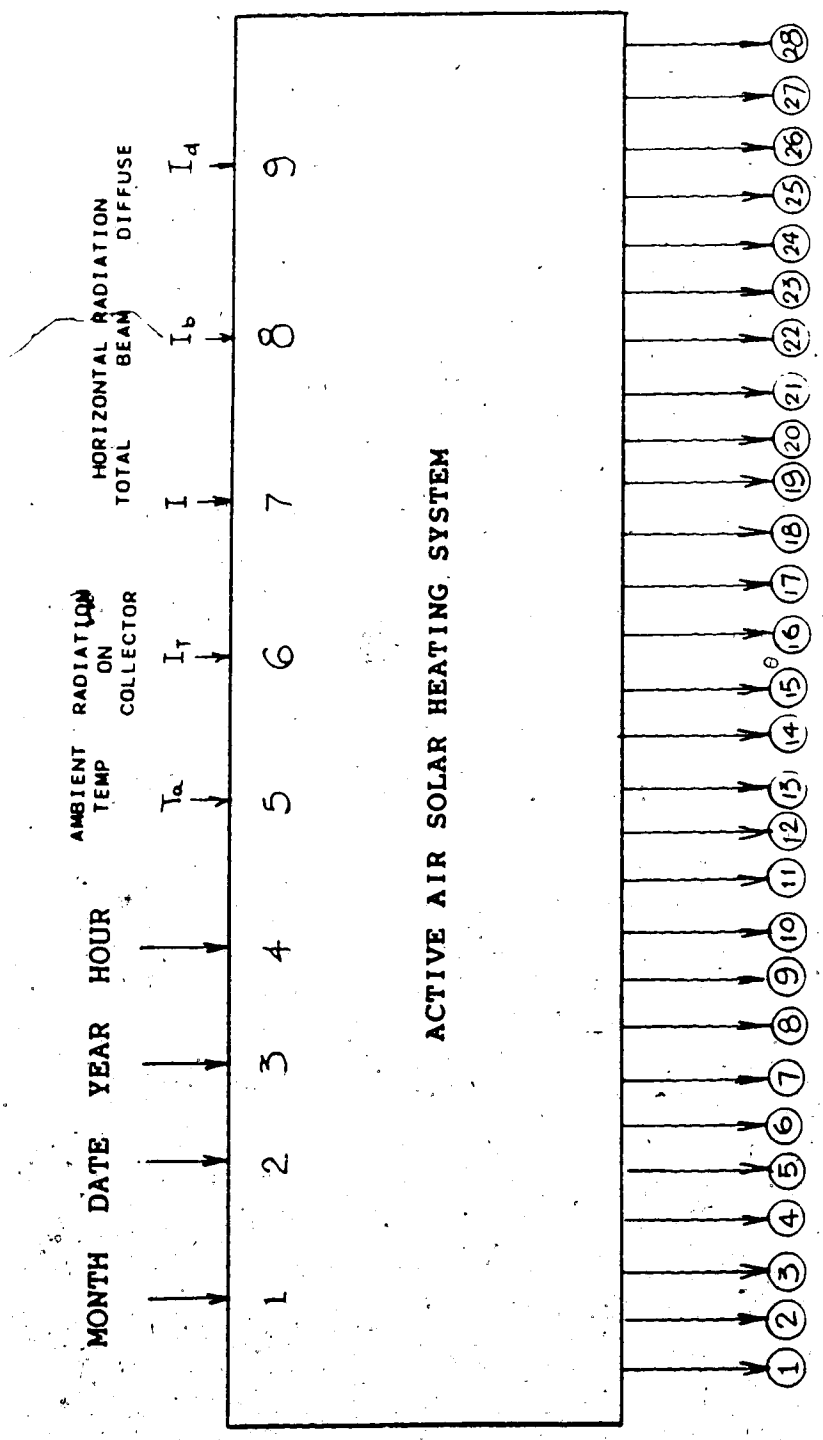

Figure 4.6 Overall Configuration of The Active Air Solar Heating System

OUTPUTS

1. Mode number
2. I_T - radiation on collector
3. T_a - ambient temperature
4. T_r - room temperature
5. T_{co} - collector outlet air temperature
6. T_{ci} - collector inlet air temperature
7. T_{st} - top storage bin temperature
8. T_{sb} - bottom bin temperature
9. $\dot{m}_c$ - mass flow rate through collector
10. $\dot{m}_b$ - mass flow rate through the rockbed entering from the bottom
11. $\dot{Q}_u$ - rate of energy gain of collector
12. $\dot{Q}_{loss}$ - rate of energy losses from ducts outside the residence
13. $\dot{Q}_{store}$ - rate of energy stored in rockbed
14. ΔU - change in internal energy of the rockbed between any given time and time =0.0
15. $\dot{Q}_s$ - rate at which energy is removed from the rockbed to space heating
16. $\dot{Q}_E$ - rate of energy losses from bed
17. $\dot{Q}_{aux}$ - electric power supply
18. $\dot{Q}_H$ - rate of total energy supply from system to space heating
19. $\dot{Q}_{sys}$ - rate of total energy supply to the system
20. $\dot{Q}_L$ - heating load of the residence
21. $\dot{Q}_c$ - rate of energy gain of collector during

collector operation mode

22. $\dot{Q}_{DMDL}$ - rate of energy losses through ducts during collector operation mode

23. $\dot{Q}_{DLL}$ - rate of energy losses due to leakage of dampers

24. I_{TC} - total radiation on collector during collector operation mode

25. Year

26. Month

27. Date

28. Hour

The order of the outputs is not necessarily that shown above. It depends on the order of the outputs connected to the printers. The output numbers are used only for identification. They are assigned arbitrarily.

Once the above outputs are known, investigation of the characteristics of the system using the methods developed in Chapter 5 can then be accomplished. The constant PARAMETERS required by the system for each of the components are given in Appendix A.

5. METHODS OF SYSTEM PERFORMANCE ANALYSIS

In this thesis, the analysis will focus on the evaluation of the solar contribution and on determination of component energy losses. Since the simulations of the system performance are based on the given performance data of the collector (see Section 4.3), shown in Table 3.2, determination of the collector performance will not be included, but evaluation of its losses and comparison of the performance data found under different conditions will be discussed. The performance of the storage unit will be studied by evaluating the heat losses from the unit and its energy flows. Energy flows of the solar heating system will also be analyzed. This chapter simply highlights the methods used in the analysis to assess the performance of the solar heating system in terms of solar contribution and component energy losses.

5.1 Solar Contribution

The energy sources contributing to the total heating load are the solar and electric energy. Therefore, the solar contribution expressed in percentage is evaluated as:

$$\begin{aligned} \%\ \text{solar} &= \text{solar}/(\text{solar} + \text{electric}) \times 100\% \\ &= \text{solar}/\text{total heating load} \times 100\% \end{aligned} \qquad (5.1)$$

Several methods may be used to assess the solar contribution. The methods are either directly based on the solar energy supplied to the module or, indirectly, based on

an estimate of the module energy loss by assuming a constant UA factor for the house. The method selected here considers the maximum solar contribution by assuming that all solar energy collected by the collector will be contributed to the load. Thus, the solar energy supplied to the module is $\dot{Q}_c$[21]', and the total heating load becomes $\dot{Q}_{sys}$ [19]. The solar contribution over a time period can then be estimated using Equation (5.1). That is:

$$\% \text{ solar} = \int \dot{Q}_c \, dt / \int \dot{Q}_{sys} \, dt \times 100\% \qquad (5.2)$$

5.2 Component Energy Losses

Energy losses from components play a prominent role in the investigation of the characteristic of the system. Component heat losses to the outside of the module are wasteful heat losses. However, losses from the components to the space within the module are part of the useful energy transfers which help to satisfy the building heating load or might overheat the module in summer as detrimental heat losses. Wasteful heat losses mainly are those lost through the collector and ducts located outside of the heated space, and due to damper leakage. Useful or detrimental heat losses are those transferred by the ductwork inside the house and by the rockbed storage unit. Unfortunately, simulations might not be able to predict completely all kinds of losses.

'The number inside the square bracket indicates the ouput number of the system model.

In the model, predictions of losses through the collector and ducts outside the house, from the storage bin and due to leakage of dampers are available. Energy lost from ducts inside the room occurs mainly in the heating modes in which the energy lost from the ductwork is actually part of the energy delivered to space heating. During COL and SYSTEM OFF, the model assumes the duct loss within the room is zero.

5.2.1 Collector Loss

Due to the temperature set points of the control system, the collector may not be in operation whenever there is incident solar radiation. When the collector is off, solar energy cannot be delivered to the room and so it is wasted. When the collector is on, part of the incident radiation will be reflected back to the surroundings due to the optical properties of the collector and part of it will be lost by conduction, convection and infrared radiation. The sum of the losses Q_{CL} can be determined by substracting the collected solar energy $\dot{Q}_c$[21] from the total incidence radiation I_T[2] over the period of simulation. Therefore, the total collector loss (CL) is:

$$CL = Q_{CL} = \int I_T A_c dt - \int \dot{Q}_c dt \qquad (5.3)$$

or

$$\% \; CL = Q_{CL} / \int I_T A_c dt \times 100\% \qquad (5.4)$$

where

A_c = collector area

5.2.2 Bin Loss

The rockbed storage unit is one of the principal components in the solar air heating system. Determination of its perfomance is essential. One way to study the rockbed performance is by evaluating the heat losses and energy flows of the unit.

The charging of the bed occurs in COL, and energy is stored at a rate of $\dot{Q}_{store}$ [13] by air flowing downward. The discharging occurs in HFS and EH in which energy is removed at a rate of $\dot{Q}_s$ [15] with air flowing in the upward direction. The difference between the input and output energy over a period of operation reflects both losses $\int \dot{Q}_E dt$ and net energy accumulated in the bed ΔU. Due to instrumentation limitations, experimental determination of $\dot{Q}_E$ and ΔU is difficult. However, simulated results of $\dot{Q}_E$ [16] and ΔU[14] are available. The percentage of energy lost from the energy stored in the bin is therefore:

$$\% \text{ bin loss} = \int \dot{Q}_E dt / \int \dot{Q}_{store} dt \times 100\% \qquad (5.5)$$

5.2.3 Damper Leakage Loss

Damper Leakage Loss is defined as the energy $\dot{Q}_{DLL}$ [23] lost to the environment from the air in the collector and ducts located outside of the module after leaking through the dampers from the module during storage bed operation mode. Since this loss increases the module heating requirement $\dot{Q}_H$ [18], Damper Leakage Loss (DLL) is expressed

as the percentage of the amount of total heating requirement contributed by the loss. That is:

$$\% \text{ DLL} = \int \dot{Q}_{DLL}\, dt / \int \dot{Q}_{H} dt \times 100\% \qquad (5.6)$$

5.2.4 Outside Module Duct Loss

Outside Module Duct Loss refers only to the energy losses $\dot{Q}_{OMDL}$ [22] from the two sections of duct connecting the collector and the module during collector operation mode. Since the module is defined as a control volume, the net solar energy delivered to the module is the difference between the useful solar energy collected by the collector and the losses. In order to see the fraction of energy lost from the energy collected by the collector, Outside Module Duct Loss (OMDL) is evaluated by:

$$\% \text{ OMDL} = \int \dot{Q}_{OMDL}\, dt / \int \dot{Q}_{c} dt \times 100\% \qquad (5.7)$$

6. RESULTS AND DISCUSSION

This chapter consists of three sections. In the first section, the model is tested against data from some clear days, cloudy days, cold months and warm months. This includes:

1. justification of percent damper leakage, comparison of the hourly, monthly and standard test of the collector thermal efficiency curves, evaluation of the effect of incidence angle modification (IAM), and study of the response of system temperatures to the operation modes on a hourly basis over a two-day period for the sunny and cloudy days
2. justification of the module UA factor and monthly collector efficiency curve by comparing the simulated and measured consumptions of solar and electric energy on a daily basis over a month for the cold and warm months

The second section presents the analysis of the monthly performance of the system for three heating seasons (81-82, 82-83 and 83-84) by using the methods developed in Chapter 5 and compares the results with the available experimental measurements. Finally, a parametric study which includes the investigation of the effects of changes of collector area, storage volume and collector tilt angle is done in the last section.

6.1 Model Testing

6.1.1 Clear Day Test

The model was first tested by using the hourly collector efficiency curve with incidence angle modification* included for two consecutive sunny days, February 20th and 21st, 1982. Experiments indicated that the solar collector approaches steady state conditions about or shortly after solar noon. Therefore, the hourly efficiency curve obtained from the data for the hours including solar noon closely approaches the steady state performance of the collector. Ignoring damper leakage, the collector outlet and inlet air temperatures predicted by the curve are compared with the measured temperatures for the two sunny days in Figure 6.1. The predicted temperature profile of the air at collector outlet is found to shift to the left of the measured temperature profile. The shift of the profile appears to be due to the storage and release of energy by the mass of the collector. Under dynamic conditions, the thermal mass of the collector affects the performance of the collector in a way that solar energy absorbed during the forenoon is partly used to heat the components of the collector, so the useful energy collected is smaller and the outlet air temperature is lower. The opposite effect occurs in the afternoon with the stored

---

* Test of incidence angle modifier coefficient (b_o) is not available for our collector, but a value of 0.17 for two cover plates obtained from Duffie and Beckman (1980), Figure 7.4.2, is used.

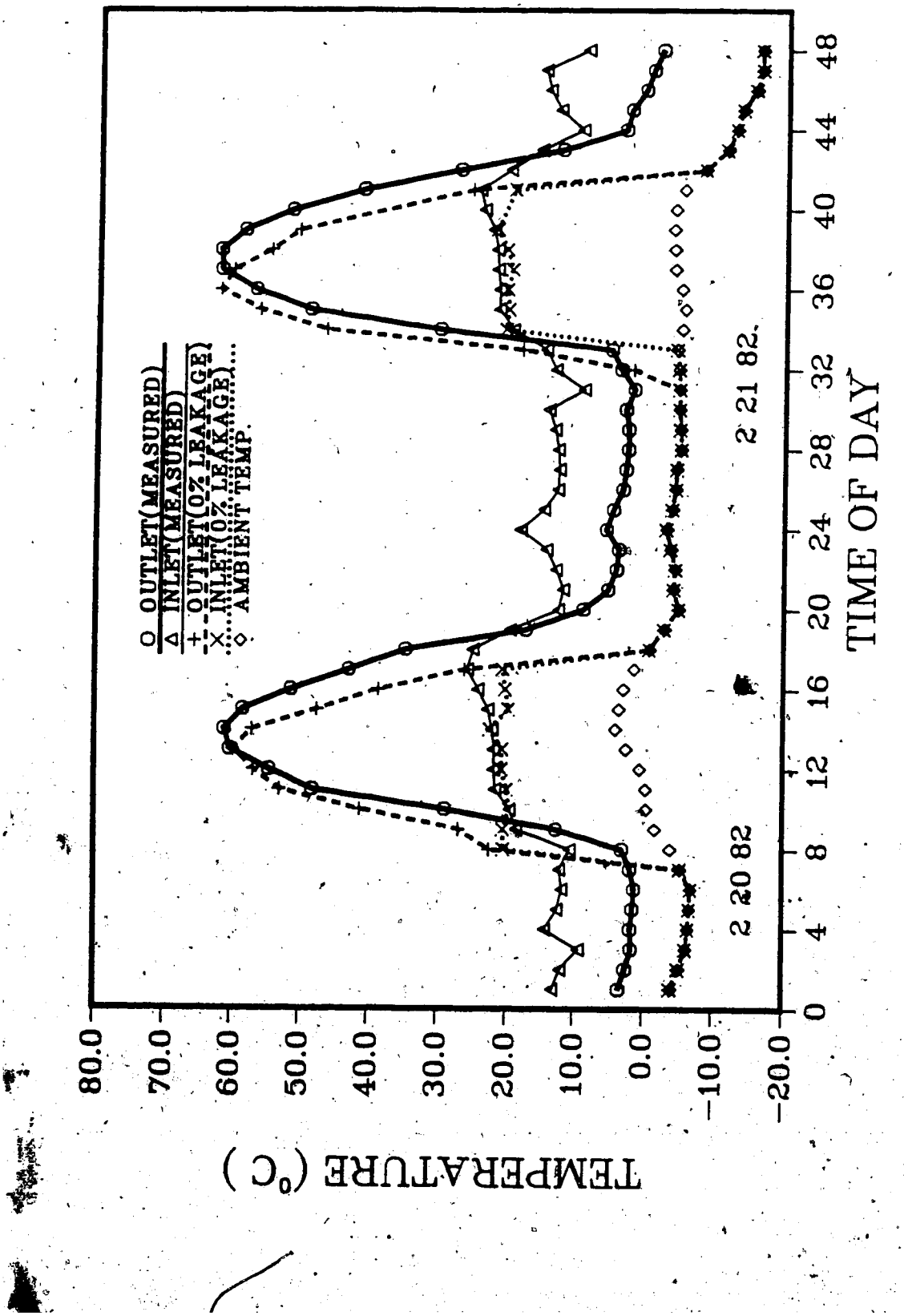

Figure 6.1 Measured and Simulated Collector Temperatures for 0% Leakage

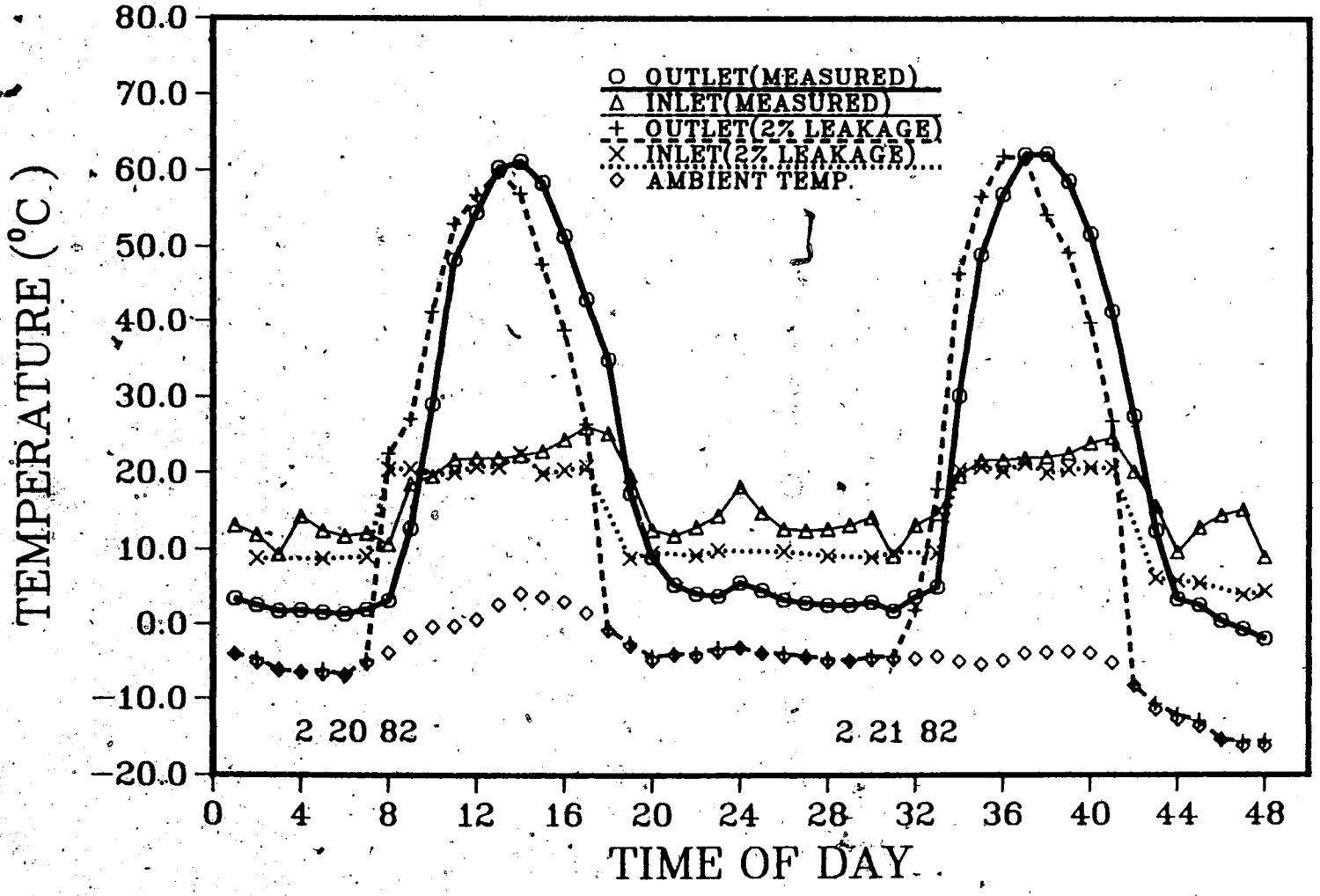

Figure 6.2 Measured and Simulated Collector Temperatures for 2% Leakage

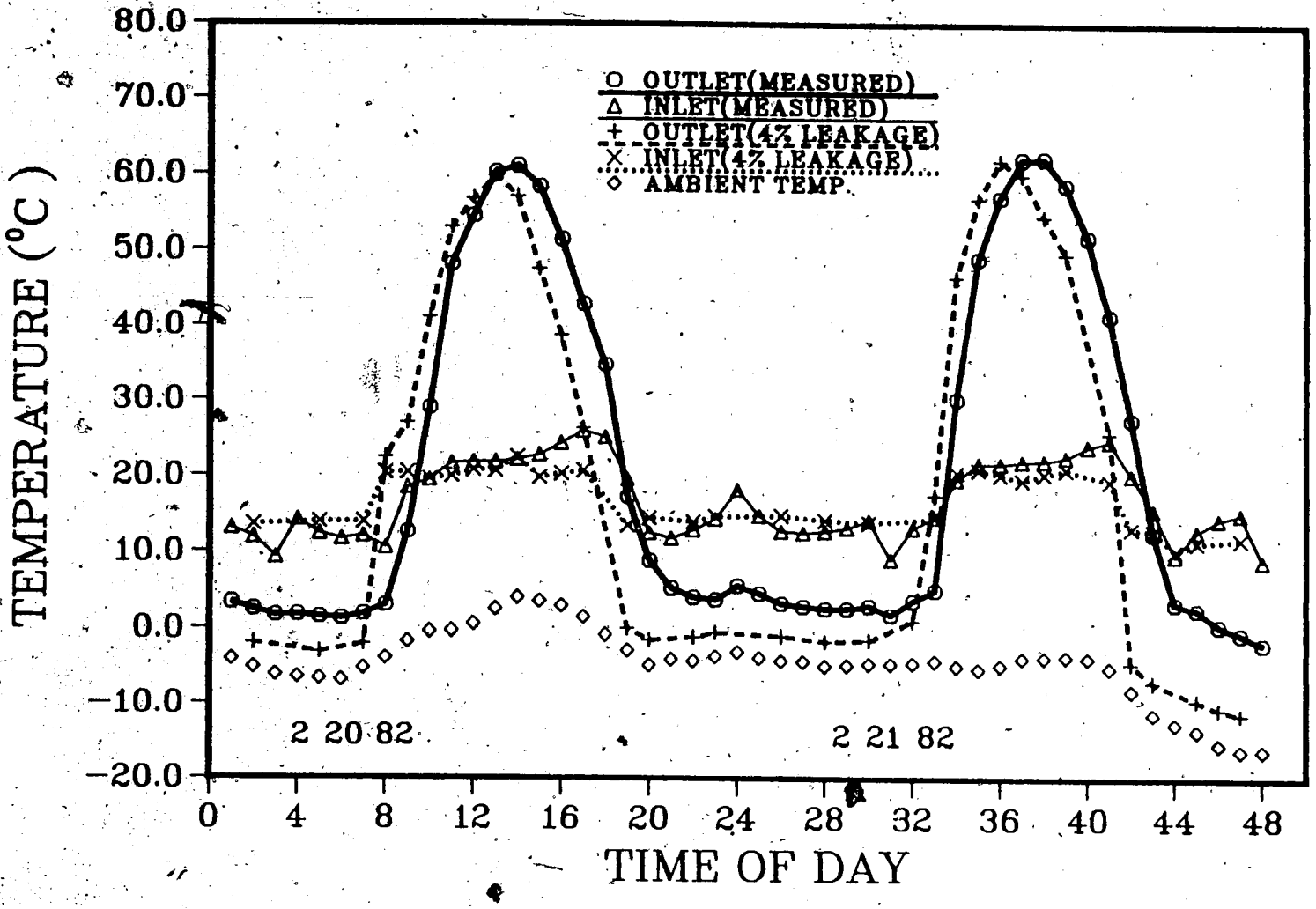

Figure 6.3 Measured and Simulated Collector Temperatures for 4% Leakage

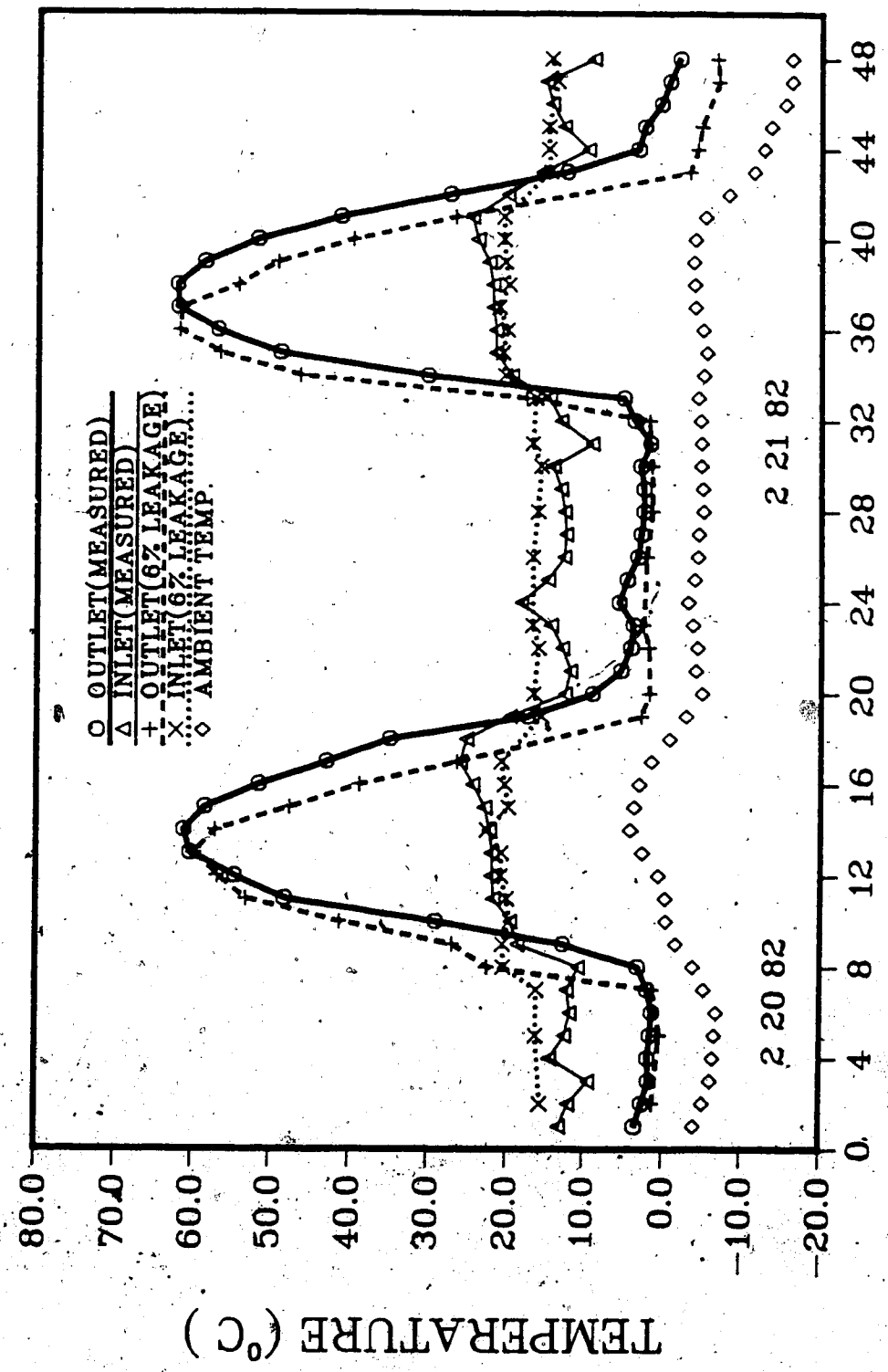

Figure 6.4 Measured and Simulated Collector Temperatures for 6% Leakage

energy released so that more energy is collected and higher outlet air temperature is obtained. With the absence of the effect of energy storage and release, the collector responds immediately to the incident solar radiation. Consequently, the rise and fall of the predicted outlet air temperature profile occurs earlier.

Theoretically, the collector temperature should drop to the ambient temperature at night when there is no flow through the collector as shown by the simulated collector inlet and outlet air temperatures in Figure 6.1. This phenomenon cannot be observed experimentally. This indicates that warm air inside the module probably leaks through the dampers to the cold collector. If the system leaked constantly, the collector temperature during storage bed operation mode should change more or less proportionally to the ambient temperature. The variation of the measured inlet temperature suggests that the amount of air leaking through the damper to the collector varied throughout the night. It is very difficult to simulate a system with changing leakage. The model simply assumes that the system leaks constantly. Expetimental determination of the amount of leakage is not easy due to inadequate instrumentation. A trial and error method was therefore used to estimate the leakage by graduately changing the percent leakage of the dampers in the model until the simulated collector temperature is close to the measured temperature. The difference between the simulated collector temperature

profiles for 2, 4 and 6% leakage and the measured temperature profiles are shown in Figure 6.2 through Figure 6.4 respectively. As expected, the collector temperatures increase with the leakage during the night time period. With increasing leakage, the difference between the simulated temperature profiles and the ambient temperature profile increases. At 4% leakage, the simulated inlet temperature is found to be close to the measured inlet temperature.

The leakage was justified based on the collector inlet temperature, but not the outlet temperature due to the fact that the collector heat loss factor was averaged from a wide range of data distribution by the method of least squares (Fung 1983). Instantaneous or hourly collector heat losses calculated by the average factor may be significantly in error. However, over a period of time, the curve may provide reasonable estimate of overall heat losses.

The energy quantities for each percent leakage over the two day period are shown in Table 6.1. The Energy Q_c, Q_{aux} and Q_H for each case are found to fluctuate within 3% difference probably due to simulation controller stability problems. The energy quantities appear not to be affected by the change of leakage since leakage loss is already covered by the UA factor of the module. However, the percentage of the amount of energy attributed to the loss (% DLL) increases from 0 to 3.2 within the test range. Since experimental results of Q_{DLL} are not available, the

Table 6.1 Comparison of Measured and Simulated Energy Quantities for 0, 2, 4 and 6% Leakage

	Experiment	Simulation			
		% Leakage			
		0	2	4	6
Q_c (MJ)	238.4	237.0	243.6	237.4	243.6
Q_{aux} (MJ)	323.6	364.0	370.3	362.0	368.9
Q_H (MJ)	579.0	588.2	600.8	586.5	599.3
Q_{DLL} (MJ)	/	0.0	8.0	14.5	19.2
% Solar	42.4	39.4	39.7	39.6	39.8
% DLL	/	0.0	1.3	2.5	3.2

Q_c = solar energy collected during collector operation mode

Q_{aux} = auxiliary energy supplied by electric heater

Q_H = total energy supplied to space heatng

Q_{DLL} = damper leakage loss

% DLL cannot be compared. The hourly collector efficiency curve with IAM coupled with the control system provides a good estimate of the collected solar energy Q_c with an error between -0.6% and 2% for these days. The energy required for space heating Q_H is about 2 to 4% over-predicted. As a consequence, the model requires more auxiliary energy to meet the load and therefore predicts approximately 3% less of solar contribution.

The preceding test considered only the hourly collector efficiency curve including incidence angle modification. It is of interest to see what happens if incidence angle modification is omitted or other efficiency curves are used such as monthly or standard test curve. The simulation and experimental results are shown in Table 6.2.

The standard test curve was obtained by ASHRAE Standard Test Method and represents the steady state performance of a single Solaron 2000 solar collector at a test flow rate per unit collector area of 0.0102 $m^3/s \cdot m^2$. Using this curve to predict the collector performance, corrections for identical collectors in series and flow rates other than those at test conditions have to be applied. For the same two sunny days, the standard test curve appears to collect approximately 10% to 15% less solar energy because the standard test curve was obtained before the addition of more insulation to the back of the collector array. As a result, more auxiliary energy is required and less solar contribution is obtained. The hourly efficiency curve represents the *IN SITU* steady state

Table 6.2 Comparison of The Hourly, Monthly and Standard Test of The Collector Thermal Efficiency Curves

	Experiment	Simulation				
		Standard Test		Hourly		Monthly
		With IAM	No IAM	With IAM	No IAM	
Q_c (MJ)	238.4	201.7	213.1	237.4	256.2	247.9
Q_{aux} (MJ)	323.6	403.8	394.3	362.0	347.2	360.4
% Solar	42.4	33.3	35.1	39.6	42.5	40.8

performance of the collector array and gives reasonable estimates of overall energy quantities and the solar contribution.

The transmittance-absorptance product of the collector ($\tau\alpha$) is incidence angle dependent. Theoretically, the collector cover transmits maximum solar radiation at normal incidence. As the angle between the rays of the sun and the normal to the collector increases, the amount of solar energy transmitted and collected decreases. Since both the standard test curve and the hourly curve were determined based on the data obtained at solar noon, correction should be applied to account for off-normal incidence. Table 6.2 indicates that without off-normal incidence effect, the model predicts that the collector would collect approximately 6% more solar energy over the two days by the standard test curve and 8% by the hourly curve. The difference between the air temperatures at collector outlet predicted by the hourly curve with and without incidence angle modification is shown in Figure 6.5*.

In order to eliminate the effects due to off-normal incidence, instantaneous changes in cloud cover, wind speed, radiation, and transient response of collector mass; the collector performance was evaluated on a monthly basis to obtain the monthly collector efficiency curve. Since less data scatter appears in the monthly efficiency plot*, monthly efficiency is believed more steady and more

---

*Shown in Figure 5.9 of Fung(1983).

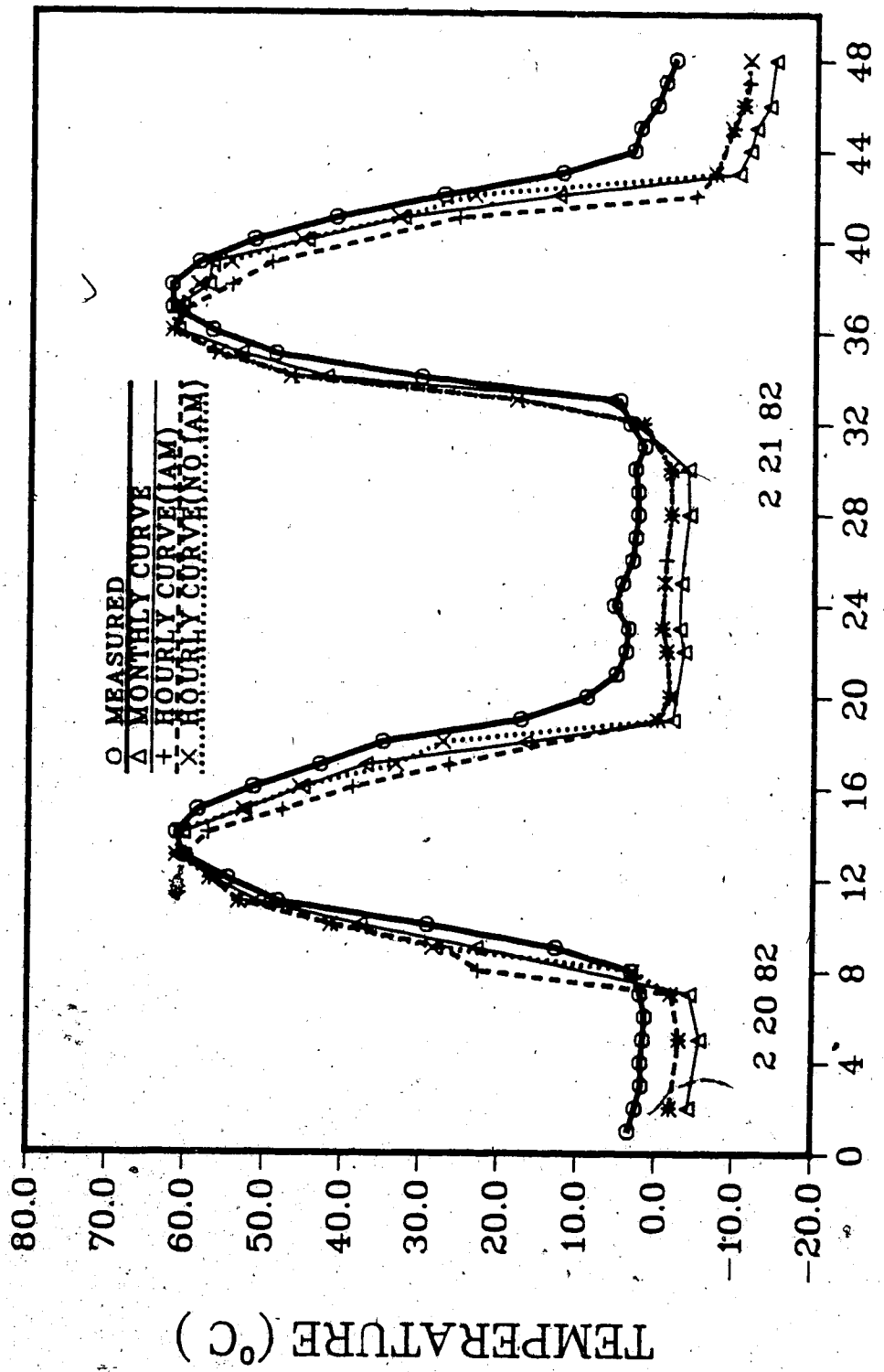

Figure 6.5 Comparison of The Collector Outlet Air Temperatures Predicted by Different Methods

representative of the overall collector performance. The collected solar energy and the outlet air temperature predicted by the monthly curve for the two sunny days are also shown in Table 6.2 and Figure 6.5 respectively. It is found that the monthly curve is able to simulate the collector performance over the two day period with an accuracy of 4%, and the outlet temperature estimated in this manner is close to the measured temperature.

Except for the standard test curve which predicts low collected solar energy, both the hourly and monthly efficiency curves provide reasonable estimates of the collector performance. The hourly curve requires consideration of incidence angle modification to improve accuracy. However incidence angle modification is not required by the monthly curve since it, theoretically, covers the effect of non-normal solar incidence. As a result, calculation of the angle of incidence for collector surface by Solar Radiation Processor No.2 is not necessary if monthly curve is used. Thus, the two solar radiation processors in the model can be omitted for reducing computational effort.

Once a percent leakage has been assumed (4%) and a collector efficiency curve has been chosen (monthly curve), it is necessary to see how the simulation model predicts the behavior of the rockbed for the two clear days by comparing the measured and simulated system temperatures. The measured system temperatures with the mode of operation

indicated on top are shown in Figure 6.6 in which the temperature at the top of the bin is the air temperature in the upper plenum above the rockpile. During COL, the temperature of the air entering the bin continuously increased in the morning due to increase in incident solar radiation on the collector. As solar radiation decreased in the afternoon, the air delivered to the bin cooled the top of the rockbed and carried the energy towards the bottom of the bin. Eventually, the bottom temperature was raised when the thermal wave reached there. When space heating was required in the late afternoon and little or no solar radiation was available from the collector, the system switched to the mode of HFS with air flowing in an upward direction to remove the stored energy from the rocks through the top of the bin to the room. The reverse process resulted in an increase in temperature of the air at the upper plenum at the beginning of the discharging process, and a decrease occurred afterward as the stored energy in the rocks was graduately used up.

The predicted system temperatures are shown in Figure 6.7 in which the sudden drop of the top bin temperature due to the change of operation mode from COL to HFS does not appear. This is because the rockbed model defines the top bin temperature as the top segment temperature of the rockpile'° instead of the air temperature

---

'°For solving the differential equation describing both air and rock temperatures, the rockpile was divided into segments and the temperature within each segment was assumed to be uniform.

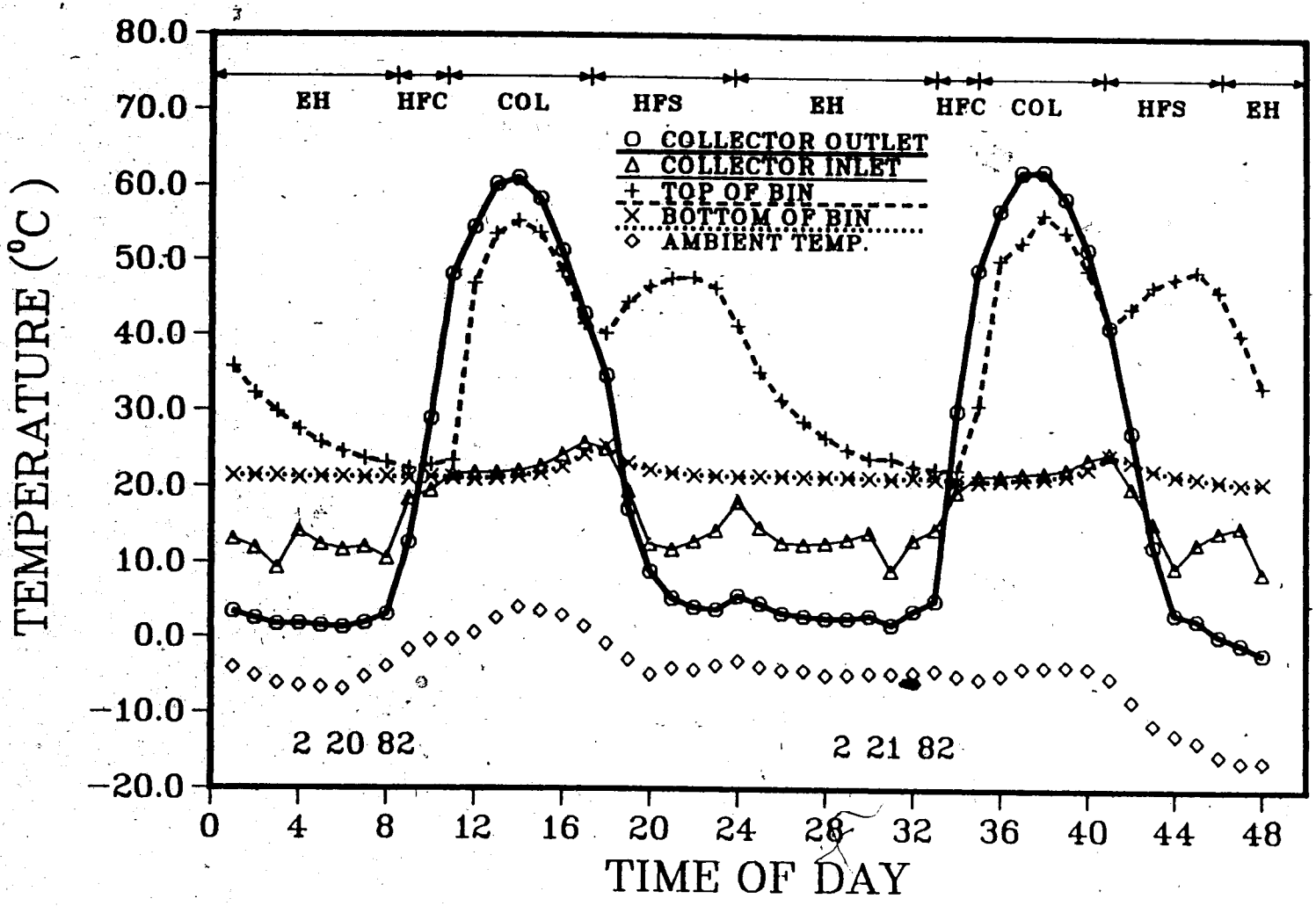

Figure 6.6 Measured System Temperatures for 2 Consecutive Sunny Days, February 20th and 21st, 1982

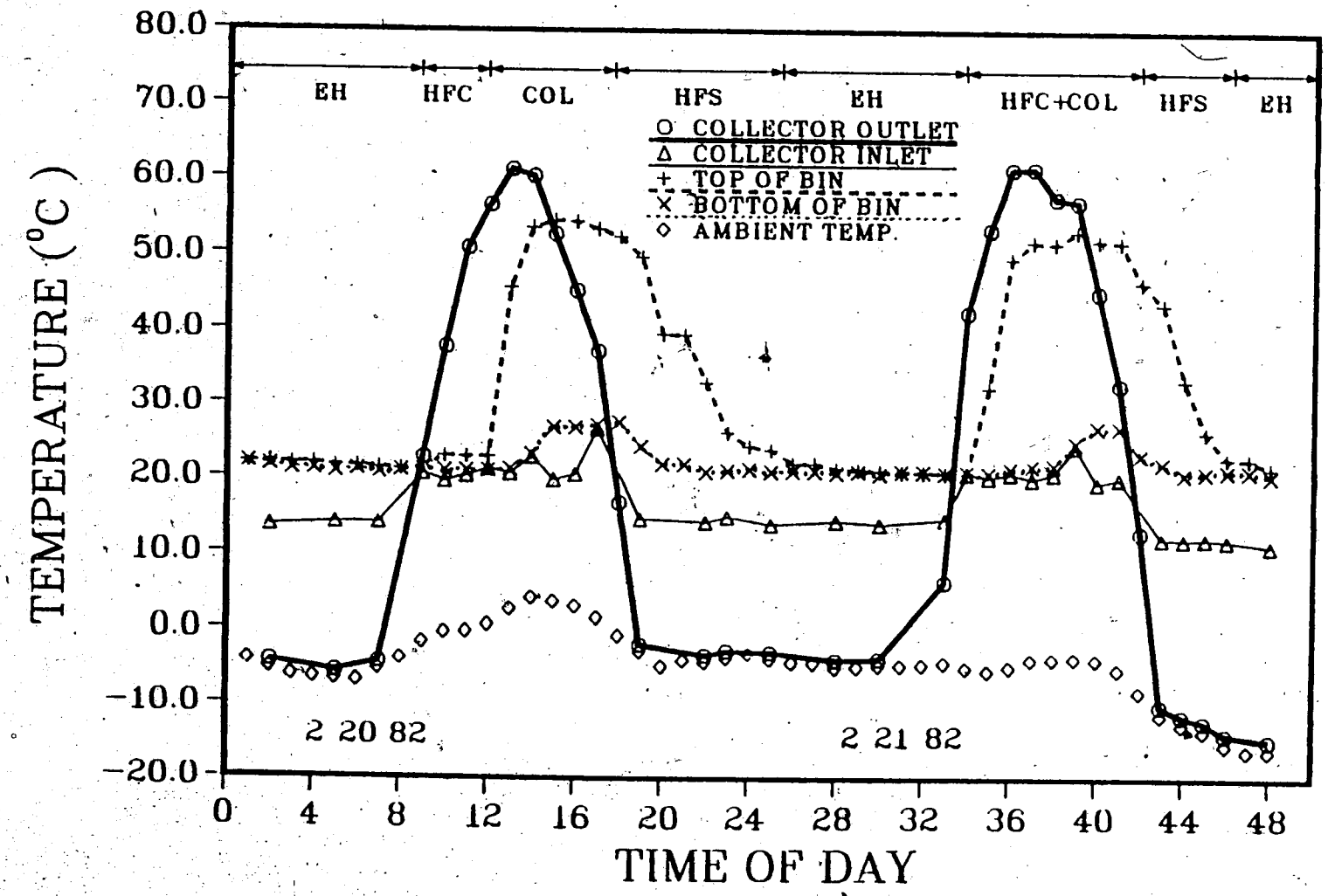

Figure 6.7 Predicted System Temperatures for 2 Consecutive Sunny Days, February 20th and 21st, 1982

in the upper plenum. Further, the bin is about 60% filled. The location of the thermocouple for measuring the top bin temperature shown in Figure 6.6 is above the rocks. In this case, the simulated top bin temperature does not behave the same way as the measured temperature at the beginning of the discharging process but drops gently until the bin is empty. Like the measured temperature at the bottom of the bin, the simulated bottom bin temperature remains nearly constant at 21°C unless the thermal wave has penetrated to the bottom. Due to shortage of data channels, detailed study of thermal wave propagation through rockbed during charging and discharging operations could not be accomplished.

6.1.2 Cloudy Day Test

The simulation model was tested further by selecting two cloudy days: January 1st and 2nd, 1982. Figure 6.8 shows the measured system temperatures for the two days. The predicted system temperatures (assuming 4% leakage) is given in Figure 6.9. As shown from both experiment and simulation that the solar radiation incident on the collector on the first day was not intense enough to raise the air temperature at the collector outlet over the set temperature for the system to operate in collector operation mode. When more sunlight appeared on the next day, the system switched to HFC to deliver the collected energy from the collector directly to the room. Since there was no energy storage over the two days, the temperature gradient

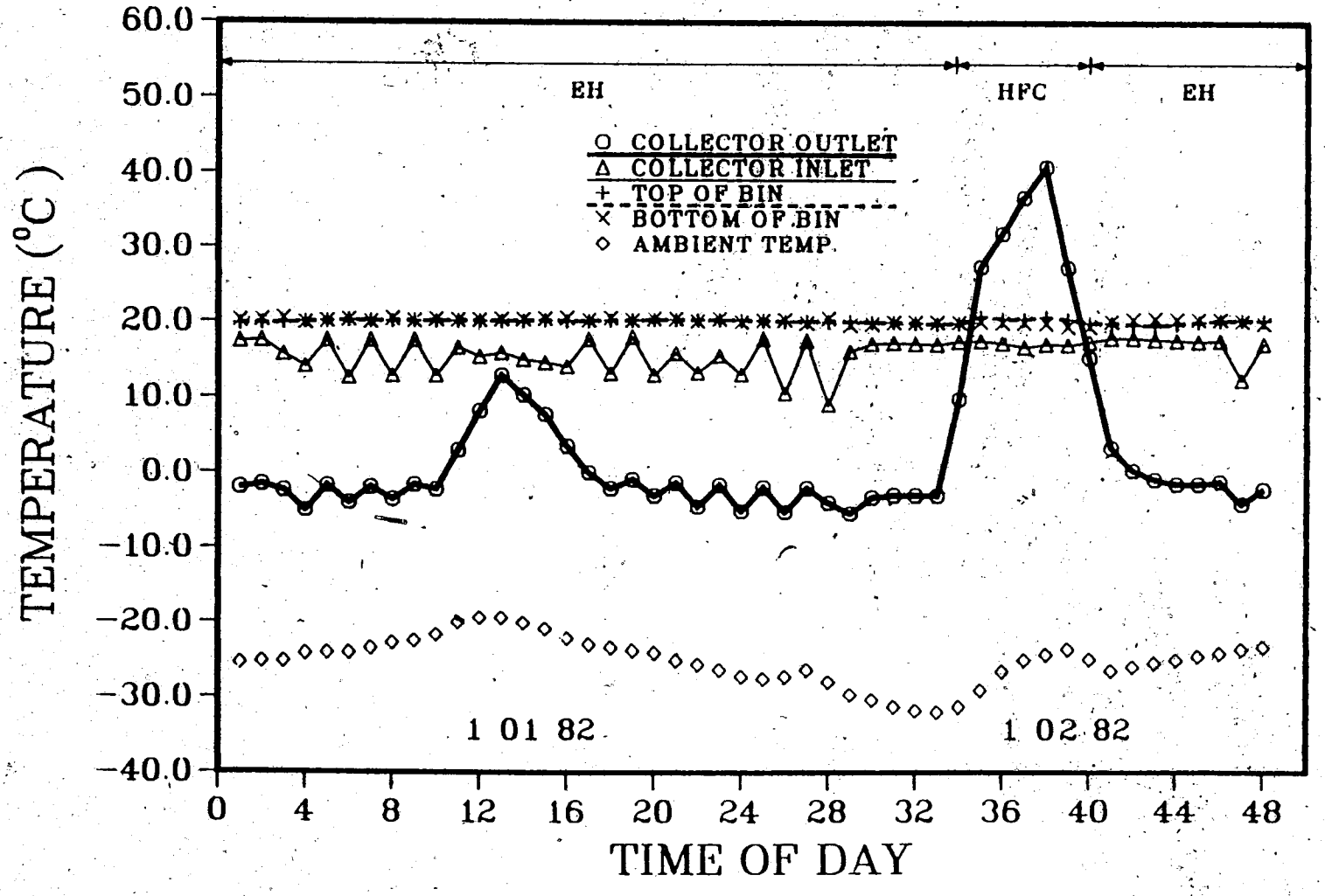

Figure 6.8. Measured System Temperatures for 2 Consecutive Cloudy Days, January 1st and 2nd, 1982

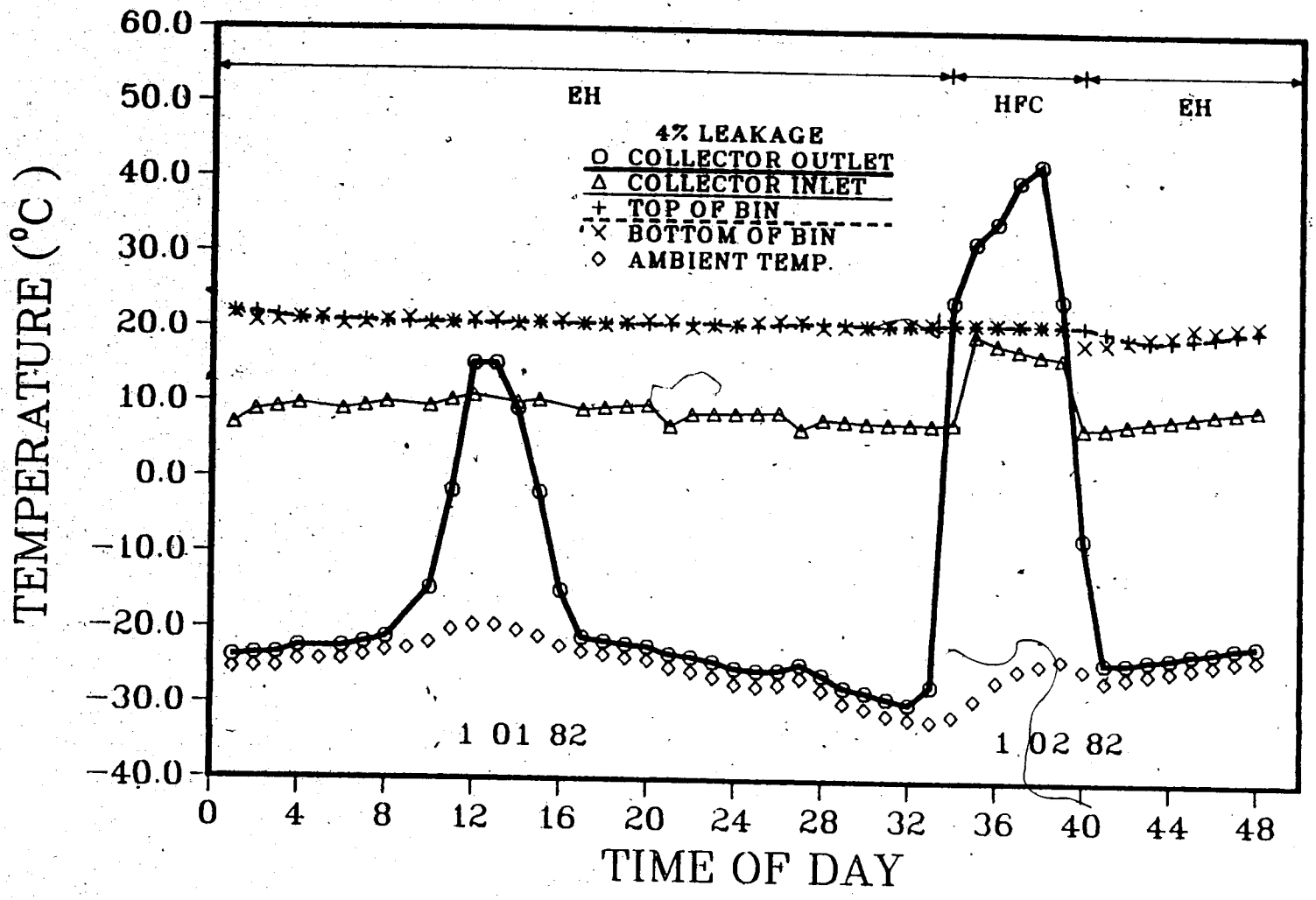

Figure 6.9 Predicted System Temperatures for 4% Leakage for The 2 Cloudy Days

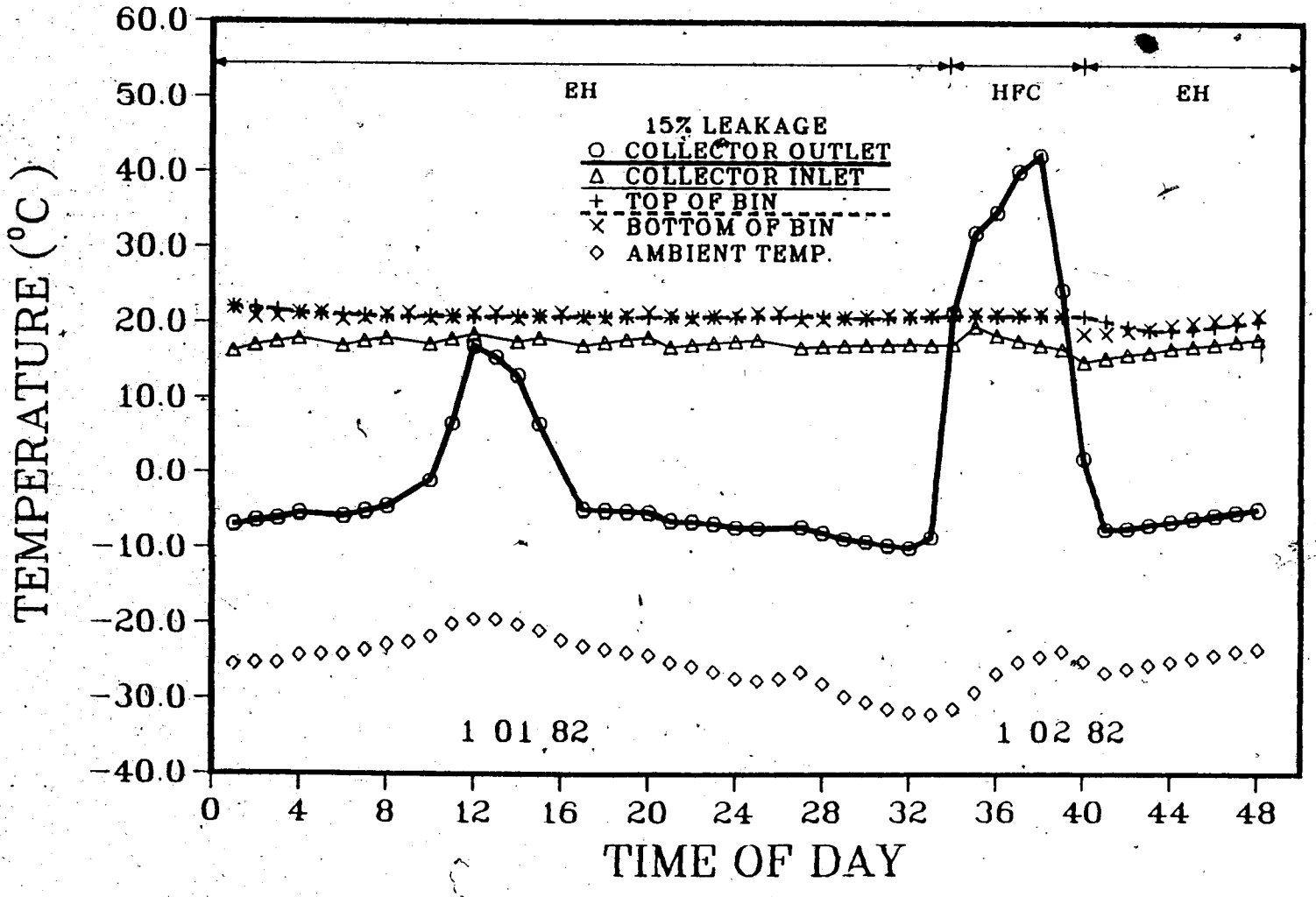

Figure 6.10 Predicted System Temperature for 15% Leakage for The 2 Cloudy Days

across the bin was zero as indicated in both Figure 6.8 and Figure 6.9. As a result, the system operated mainly in EH mode.

So far, the way the system operates and the way the temperatures respond to the modes of operation shown by both experiment and simulation are consistent. However, the accuracy of the predicted collector temperatures depends on the accuracy of the assumed percent leakage. It is surprising to see from Figure 6.8 that the temperature of the air at the collector inlet did not drop at all towards the ambient temperature when the collector was not in operation. This implies that the system leaked quite seriously on these two days. Assuming a 4% leakage, the predicted collector temperatures shown in Figure 6.9 are found to be far below the measured temperatures during the collector off period, indicating that the system leaked more than the previous assumed percent leakage. The leakage was therefore re-adjusted. In Figure 6.10, the predicted temperatures using a leakage of 15% are in better agreement with the measured temperatures in Figure 6.8. The fluctuations of the inlet and outlet air temperatures of the collector in Figure 6.8 are due to the on and off cycling of the heating system by the thermostat.

Obviously, the system leaked badly on these two cloudy days. Therefore assuming a constant 4% leakage fails to describe the temperatures of the air inside the collector during the off period of the collector for these specific

days. However, the predicted energy consumptions, both solar and electric energy, for 4% and 15% leakage are found to be almost identical as shown in Table 6.3, except that the amount of energy contributed to the loss increases from 5.3% to 12.6%.

6.1.3 Cold and Warm Month Test

Justication of the module UA factor and the monthly collector efficiency curve was done by comparing the daily variations of the simulated and measured energy consumptions of Q_{sys} and Q_c for some cold and warm months. This is shown in Figure 6.11 to Figure 6.15 in which the ambient temperature is included and the difference between Q_{sys} and Q_c represents the electric energy Q_{aux} supplied to the load.

In the simulations, the total energy consumption is predicted according to the estimated heating load Q_L by using an average module UA factor based on three heating seasons as shown in Appendix E-1. As mentioned in Section 4.5, this average UA factor represents the average rate of overall heat losses of the control volume, including the losses such as conduction heat loss through building structure, basement loss, infiltration, leakage loss, etc. and the gains such as passive solar gain, bin loss, duct loss inside house, etc., for each degree difference between the room and the ambient temperatures under average environmental conditions of the three heating seasons. The model assumes that the average UA factor of 140 W/°C is

Table 6.3 Comparison of Measured and Simulated Energy Quantities for 4% and 15% Leakage for The 2 Cloudy Days

	Experiment	Simulation	
		% Leakage	
		4	15
Q_C (MJ)	39.4	44.4	44.3
Q_{aux} (MJ)	1028.1	1041.0	1044.0
Q_H (MJ)	1069.1	1083.0	1085.0
Q_{DLL} (MJ)	/	57.8	137.3
% Solar	3.7	4.1	4.1
% DLL	/	5.3	12.6

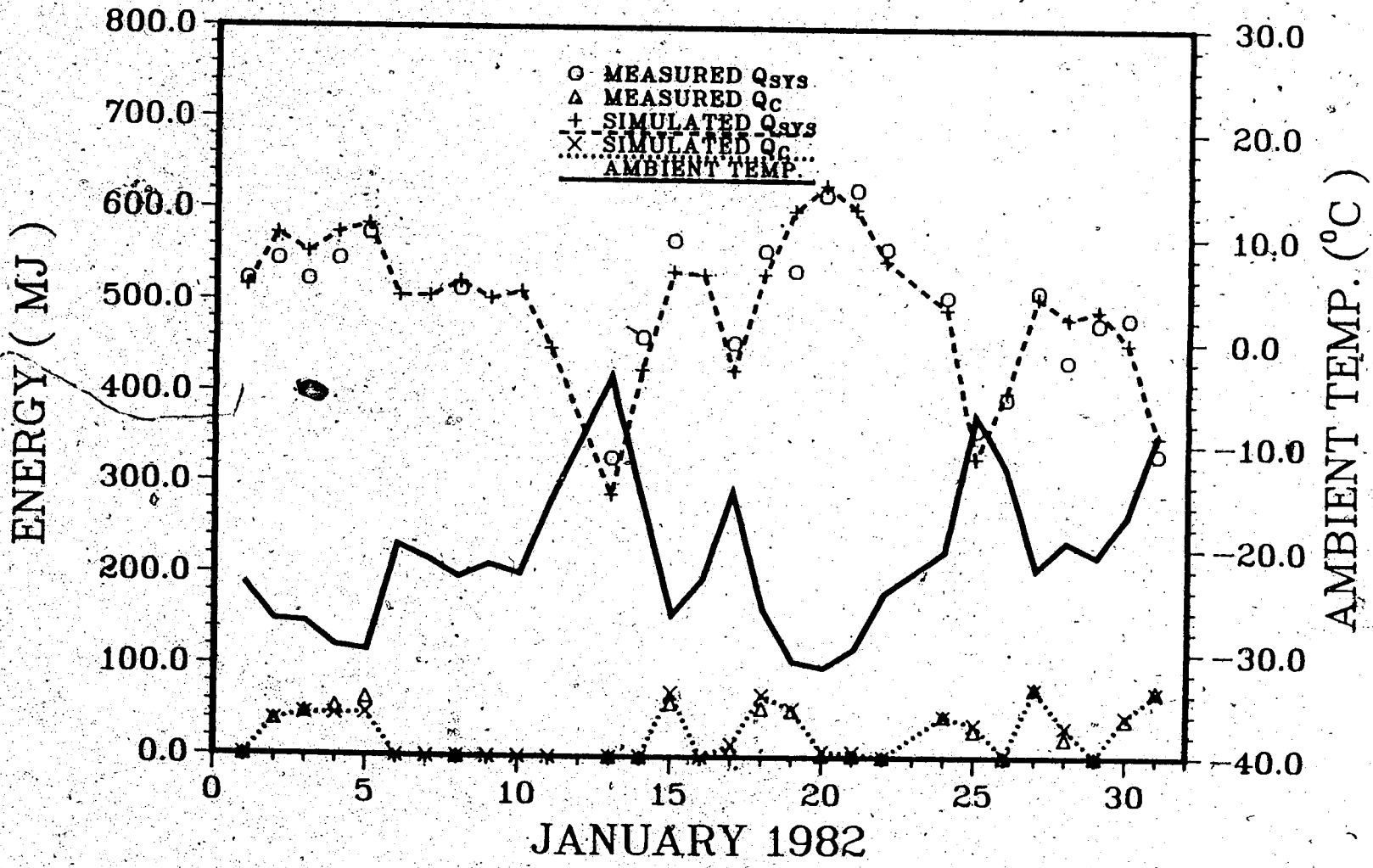

Figure 6.11 Daily Variations of Collected Solar Energy and Total Energy Supplied to The System for January 1982

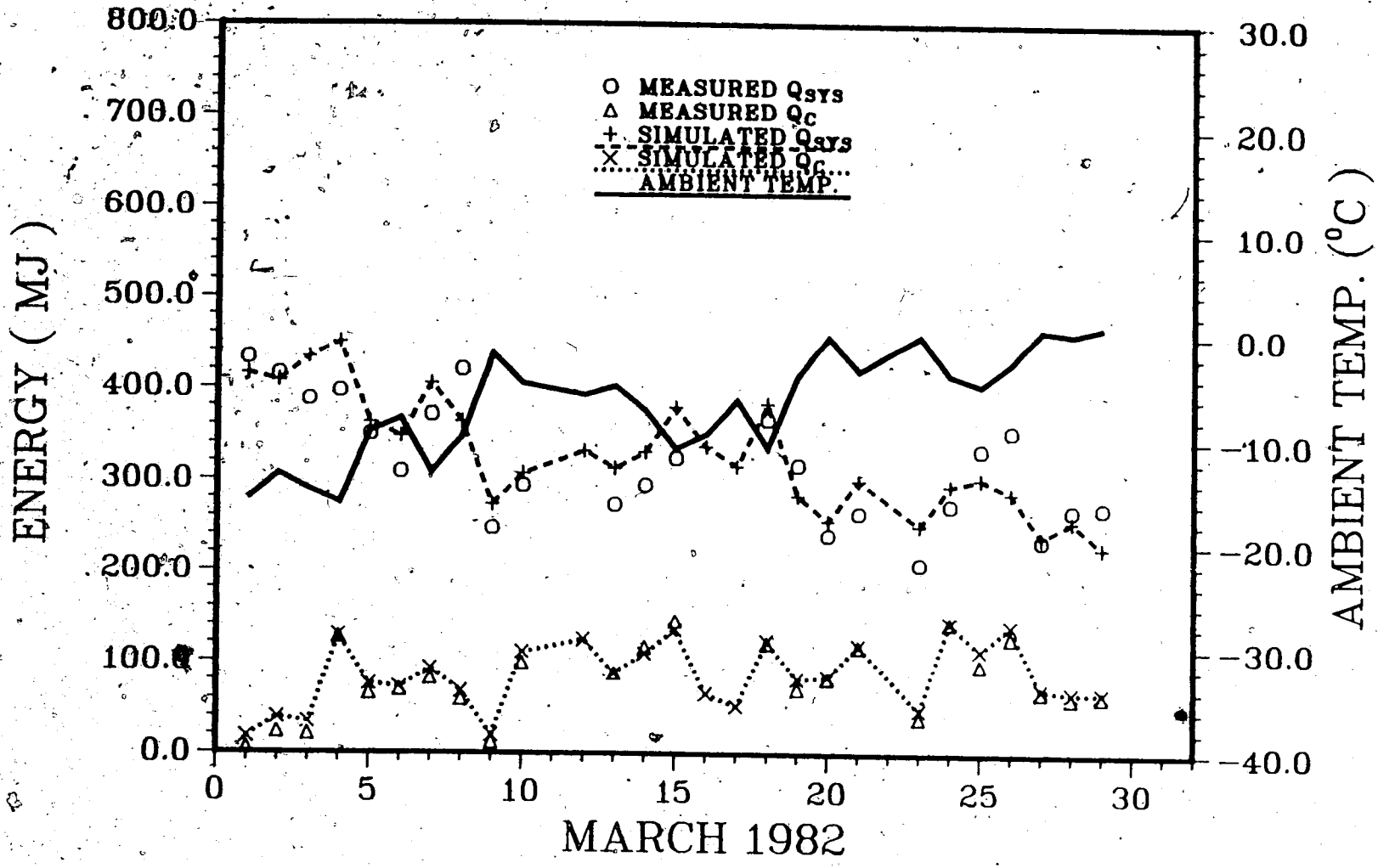

Figure 6.12 Daily Variations of Collected Solar Energy and Total Energy Supplied to The System for March 1982

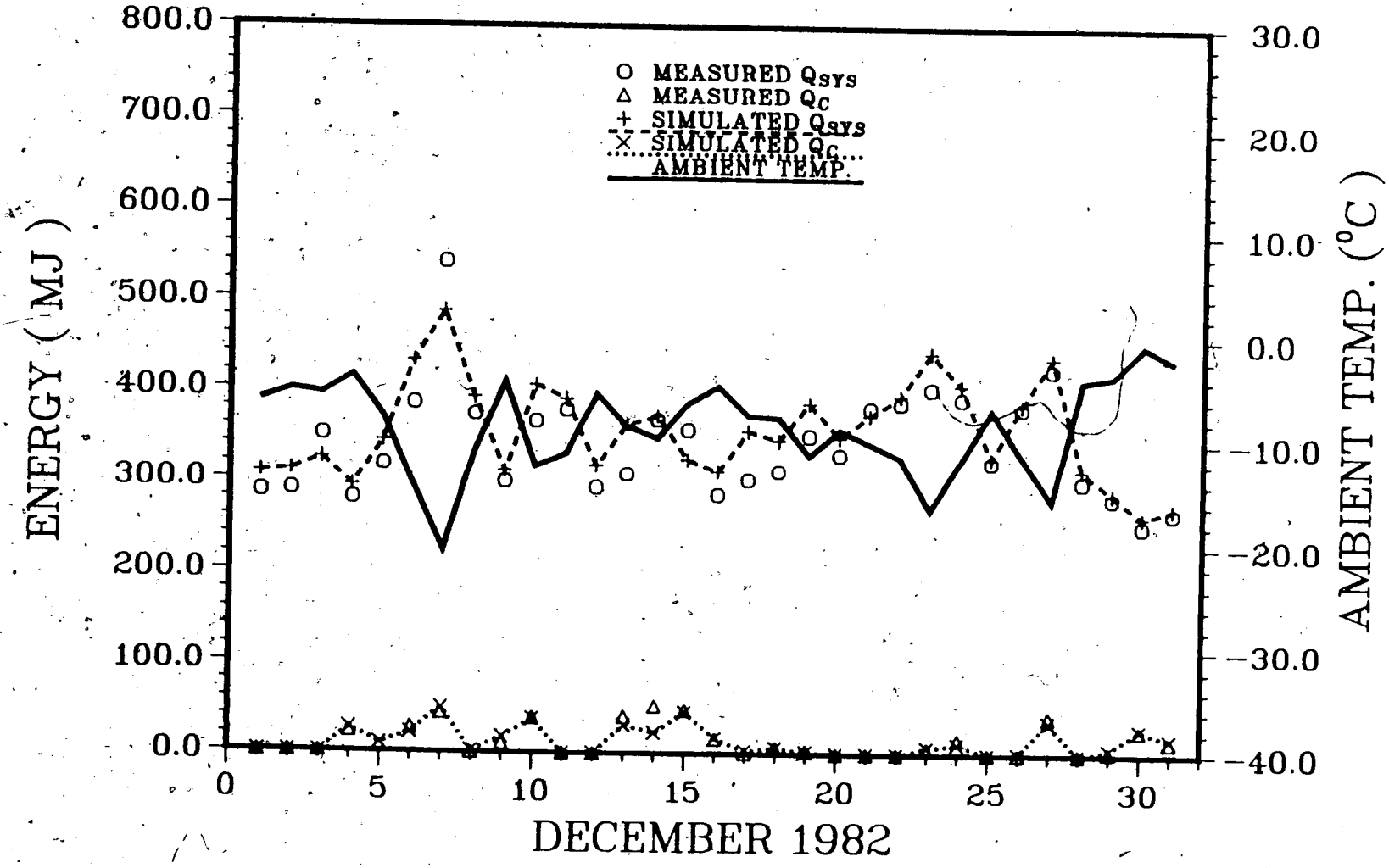

Figure 6.13 Daily Variations of Collected Solar Energy and Total Energy Supplied to The System for December 1982

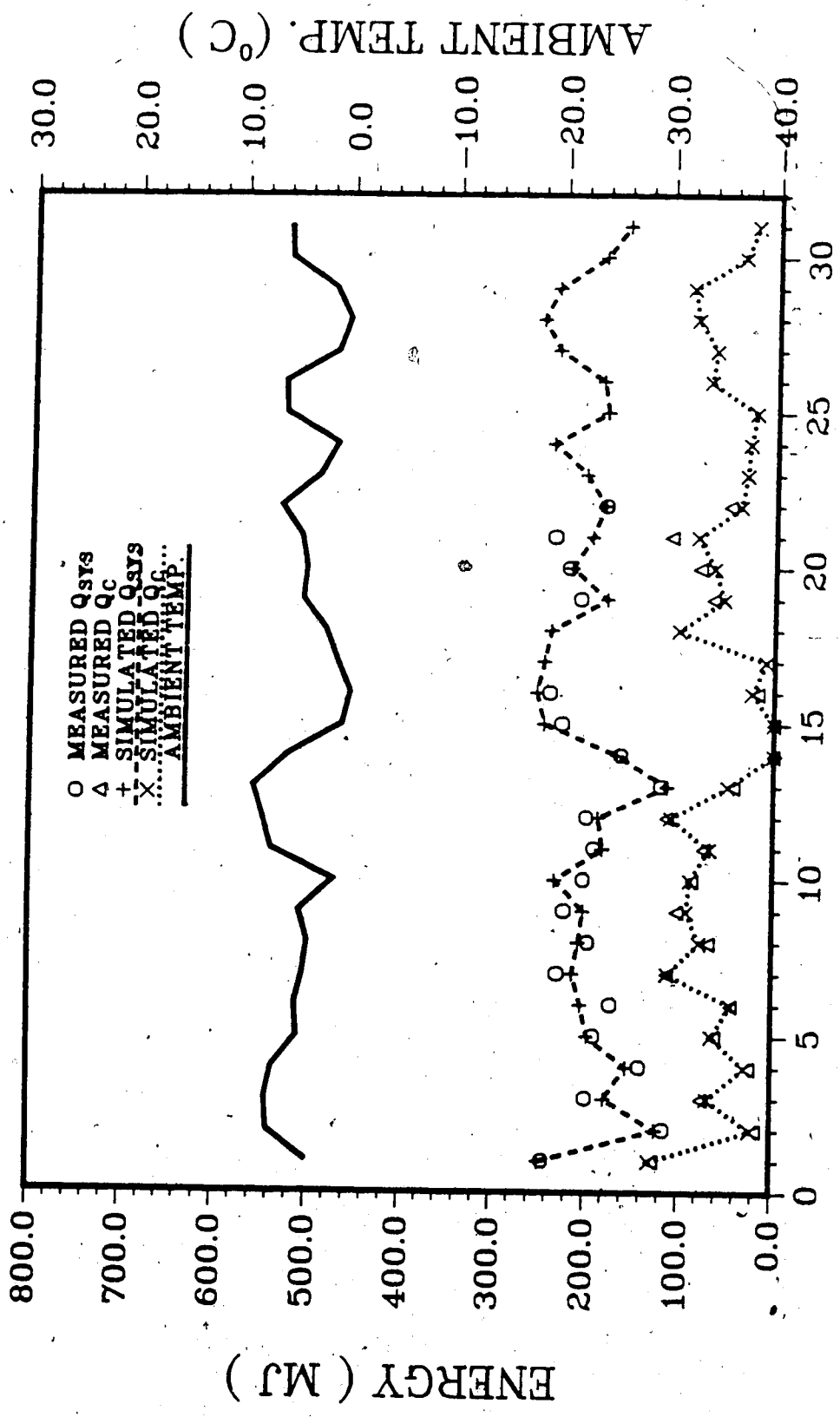

Figure 6.14 Daily Variations of Collected Solar Energy and Total Energy Supplied to The System for October 1983

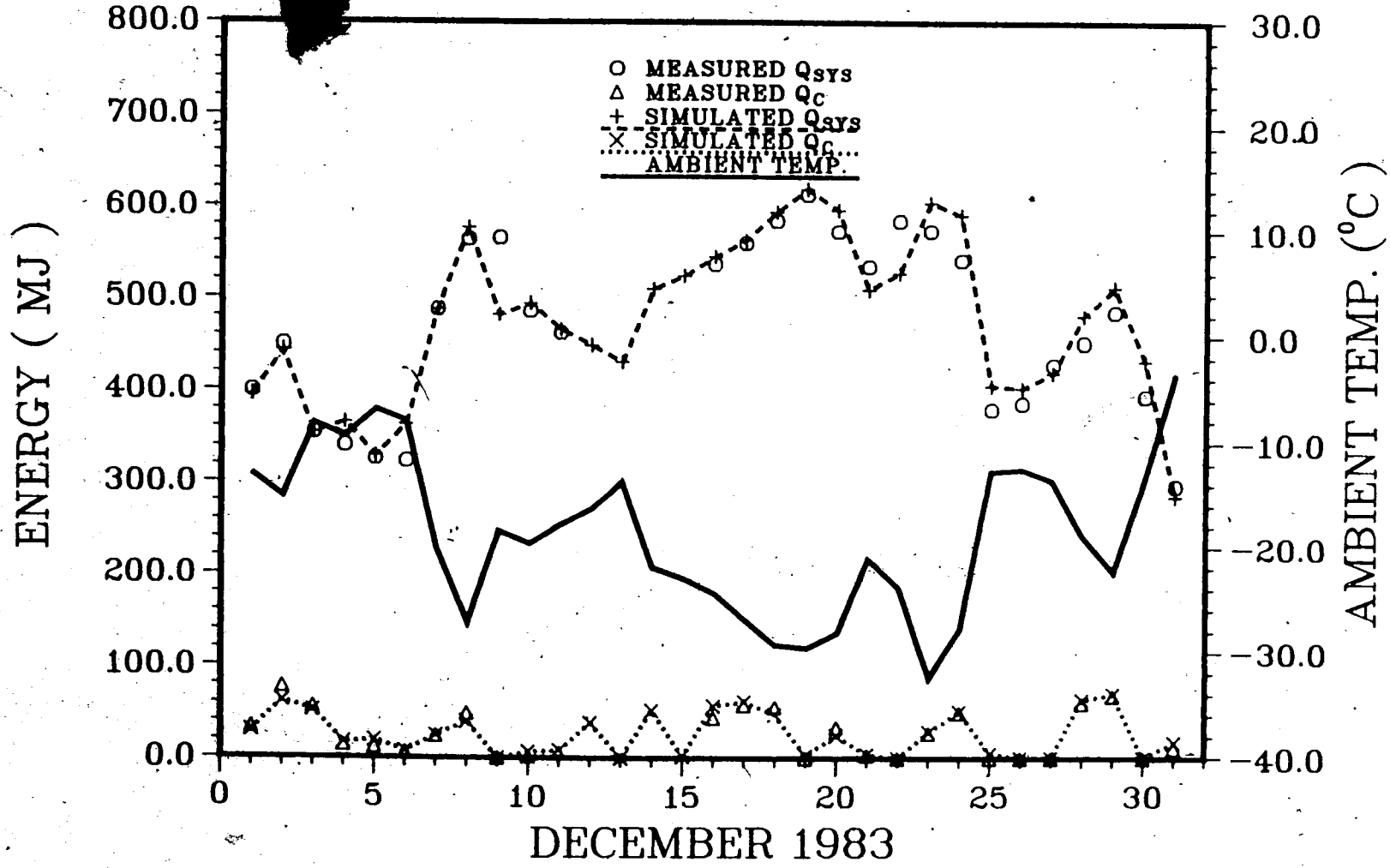

Figure 6.15 Daily Variations of Collected Solar Energy and Total Energy Supplied to The System for December 1983

applicable for all days and months. Therefore, the predicted energy consumption by the system becomes mainly a function of ambient temperature and increases as ambient temperature decreases and vice versa. As a result, the profile of the predicted Q_{sys} has almost a reverse shape of the ambient temperature profile for each month as shown from Figure 6.11 to Figure 6.15.

Theoretically, the resistance to conduction energy transfer should be relatively constant unless there is a major change in moisture content for the materials. Using heat flux meters, the basement loss during the heating season has also been found to be relatively constant (Zaheeruddin 1983). But the wind speed, wind direction and the ambient temperature alter the infiltration energy component. The passive solar gain also varies due to different radiation levels in summer and winter even though there is no south facing window in the module and the small windows in the east and west walls are almost completely shaded. Thus, the constant UA factor, while representative of the average overall heat losses, may differ from the actual UA factor for particular days if there was a major change in the balance of the time variant heat losses and gains. Nevertheless, the method appears to provide reasonable estimate of Q_{sys} for most of the days.

The amount of solar energy collected by the collector depends mainly on the radiation level. The daily variations of both measured and predicted Q_c are found to be in good

agreement. This indicates that the monthly efficiency curve is not only able to simulate the monthly collected energy but also the daily collection with reasonable accuracy.

For the cold months like January 1982 and December 1983, the system obviously needed much energy to maintain the room temperature within a comfort zone. Since little solar energy was available for these months, a large portion of energy was supplied by electricity as shown in Figures 6.11 and 6.15. The contrary is observed in October 1983 (Figure 6.14) in which the weather was warm and the average radiation level was comparatively high, so that less Q_{sys} was required but more Q_c was obtained. Figures 6.12 and 6.13 indicate that March 1982 and December 1982 had almost the same range of ambient temperature such that the energy supplied to the system for these two months were nearly in the same level. However, there were less hours of sunshine in December 1982, the major energy contribution in this month was electricity.

6.2 Monthly Performance Analysis

The problem of damper leakage exists in most analyses of solar heating systems. In the literature, the problem is usually ignored by simply assuming that the leakage is zero or extremely low. In this system, the observed damper leakage ranged from a low of about 2% to a high of about 15%. Since it is impracticable to change the percent leakage for the defective dampers, the simulation model assumes the system operates under a constant normal leaking condition of 4% for storage bed operation mode and no leakage for the other operation modes for the following analysis.

During the three heating seasons, some experimental data were missing owing to system malfunction and instrumentation problems. The quantity of hourly data available for analysis for each month over the three heating seasons are shown in Table 6.4. To estimate the monthly value of each energy quantity from the incomplete monthly records of hourly data, each measured energy quantity was adjusted to its monthly sum by multiplying a factor equal to the ratio of the number of hours in a month to the number of available hourly data for that month.

The application of the simulation model in the following anaylsis is mainly based on the methods described in Chapter 5. The adjusted monthly measurements will also be presented if available.

Table 6.4 Number of Hourly Records Available per Month

Month	81 - 82 Heating Season	82 - 83 Heating Season	83 - 84 Heating Season
Sep	577	317	/
Oct	/	513	496
Nov	686	681	591
Dec	717	740	666
Jan	663	665	534
Feb	655	529	/
Mar	652	729	/

6.2.1 Solar Contribution

Tables 6.5, 6.6 and 6.7 present the solar energy delivered by the collector, the electric energy supplied by the heater, the sum of the solar and electric energy and the calculated solar contribution for each month of the three heating seasons. It is apparent that the solar energy collected during the cold months like December and January was usually less than that collected during the warm months such as September and March, with the amount varying between a maximum of 2.62 GJ(2.43 GJ from experiment) in March 1982 and a minimum of 0.40 GJ(0.42 GJ) in December 1982. The auxiliary energy, however, varied in an opposite way with a maximum of 14.63 GJ(14.22 GJ) in January 1982 and a minumum of 1.89 GJ(2.03 GJ) in September 1981. As a result, the solar contribution obtained from both experiments and simulations for each heating season ranged from about 4 to 5% in December or January to about 50% in September and the maximum possible solar contribution for a whole heating season was approximately 15 to 16% (except for 83-84 heating season in which some of the months were absent).

6.2.2 Solar Distribution

From the total incidence radiation on the collector, only part of the energy will be collected. The rest will be lost by reflection, conduction, convection and infrared radiation plus a small portion that cannot be collected during the collector off period. While delivering to the

Table 6.5 Monthly Solar Contribution for 81-82 Heating Season

Month	Experiment				Simulation			
	Q_c (GJ)	Q_{aux} (GJ)	Q_{sys} (GJ)	%Solar	Q_c (GJ)	Q_{aux} (GJ)	Q_{sys} (GJ)	%Solar
Sep 81	1.84	2.03	3.87	47.5	1.88	1.89	3.77	49.9
Nov 81	1.03	5.97	7.00	14.7	1.05	6.63	7.68	13.7
Dec 81	0.90	9.89	10.79	8.3	0.97	10.52	11.49	8.4
Jan 82	0.72	14.22	14.94	4.8	0.75	14.63	15.38	4.9
Feb 82	1.51	9.76	11.27	13.4	1.61	10.04	11.65	13.8
Mar 82	2.43	7.32	9.75	24.9	2.62	7.54	10.16	25.8
Total	8.43	49.19	57.62	14.6	8.88	51.25	60.13	14.8

Table 6.6 Monthly Solar Contribution for 82-83 Heating Season

Month	Experiment				Simulation			
	Q_c (GJ)	Q_{aux} (GJ)	Q_{sys} (GJ)	%Solar	Q_c (GJ)	Q_{aux} (GJ)	Q_{sys} (GJ)	%Solar
Sep 82	2.30	2.14	4.44	51.8	2.19	2.34	4.53	48.3
Oct 82	2.37	3.56	5.93	40.0	2.34	3.91	6.25	37.4
Nov 82	0.96	8.68	9.64	9.9	0.93	9.66	10.59	8.8
Dec 82	0.42	10.11	10.53	4.0	0.40	10.60	11.00	3.6
Jan 83	1.05	9.98	11.03	9.5	1.07	10.53	11.60	9.2
Feb 83	1.35	7.83	9.18	14.7	1.35	8.44	9.79	13.8
Mar 83	1.49	7.08	8.57	17.4	1.67	7.56	9.23	18.1
Total	9.94	49.38	59.32	16.7	9.95	53.04	62.99	15.8

Table 6.7 Monthly Solar Contribution for 83-84 Heating Season

Month	Experiment				Simulation			
	Q_c (GJ)	Q_{aux} (GJ)	Q_{sys} (GJ)	%Solar	Q_c (GJ)	Q_{aux} (GJ)	Q_{sys} (GJ)	%Solar
Oct 83	1.97	4.14	6.11	32.2	1.80	4.46	6.26	28.8
Nov 83	0.68	8.69	9.37	7.3	0.64	7.95	8.59	7.5
Dec 83	0.77	13.75	14.52	5.3	0.78	13.95	14.73	5.3
Jan 84	0.84	9.89	10.73	7.8	1.02	9.71	10.73	9.5
Total	4.26	36.47	40.73	10.5	4.24	36.07	40.31	10.5

module, part of the collected energy will be lost along the insulated ductwork. The net energy sent to the house will be distributed either to the storage unit or directly to the room. Tables 6.8 to 6.10 give the monthly amount of each of the energy quantities and their percent distributions. They are indicated by the symbols; $I_T A_C$, total monthly incidence radiation; Q_{CL}, collector energy loss; Q_C, collected solar energy; Q_{OMDL}, energy loss from ducts outside the module; Q_{store}, energy delivered to storage unit; %CL, percent collector loss; %OMDL, percent outside module duct loss; and %STORE, percent storage.

During each of the heating seasons, the percentage of energy losses from both the collector and the duct sections increased towards the cold months. In general, the collector loss ranged from about 55 to 70% of the incidence radiation and was an average of about 60% for each season. The outside module duct loss ranged from about 6 to 13% of the collected solar energy and was an average of approximately 8%. Due to instrumentation limitations, it was impossible to obtain the experimental heat loss from the ductwork. Therefore, the outside module duct loss can only be estimated by simulations.

Since less heating is required in the warm months, more than half of the collected energy was sent to storage in September and March. While in the cold months, a large portion of the solar energy delivered from the collector would be used immediately for space heating and therefore

Table 6.8 Distribution of Solar Energy for 81-82 Heating Season

		Experiment					Simulation						
Month	$I_T A_C$ (GJ)	Q_{CL} (GJ)	%CL	Q_C (GJ)	Q_{stove} (GJ)	%STORE	Q_{CL} (GJ)	%CL	Q_C (GJ)	Q_{OMDL} (GJ)	Q_{store} (GJ)	%OMDL	%STORE
Sep 81	4.81	2.97	61.7	1.84	0.95	51.6	2.93	60.9	1.88	0.13	1.48	6.9	78.7
Nov 81	2.46	1.43	58.1	1.03	0.57	55.3	1.41	57.3	1.05	0.07	0.44	6.7	41.9
Dec 81	2.53	1.63	64.4	0.90	0.15	16.7	1.56	61.7	0.97	0.10	0.12	10.3	12.4
Jan 82	2.37	1.65	69.6	0.72	0.05	6.9	1.62	68.4	0.75	0.09	0.00	12.0	0.0
Feb 82	4.05	2.54	62.7	1.51	0.43	28.5	2.44	60.2	1.61	0.15	0.25	9.3	15.5
Mar 82	5.95	3.52	59.1	2.43	1.42	58.4	3.33	56.0	2.62	0.19	0.88	7.2	33.5
Total	22.17	13.74	62.0	8.43	3.57	42.3	13.29	60.0	8.88	0.73	3.17	8.2	35.7

Table 6.9 Distribution of Solar Energy for 82-83 Heating Season

		Experiment					Simulation						
Month	$I_T A_c$ (GJ)	Q_{cL} (GJ)	%CL	Q_c (GJ)	Q_{store} (GJ)	%STORE	Q_{cL} (GJ)	%CL	Q_c (GJ)	Q_{dmdL} (GJ)	Q_{store} (GJ)	%DMDL	%STORE
Sep 82	5.25	2.95	56.2	2.30	1.42	61.7	3.06	58.3	2.19	0.12	1.71	5.5	78.1
Oct 82	5.34	2.97	55.6	2.37	1.78	75.1	3.00	56.2	2.34	0.13	1.43	5.6	61.1
Nov 82	2.63	1.67	63.5	0.96	0.32	33.3	1.70	64.6	0.93	0.09	0.13	9.7	14.0
Dec 82	1.51	1.09	72.2	0.42	0.04	9.5	1.11	73.5	0.40	0.05	0.05	12.5	12.5
Jan 83	3.05	2.00	65.6	1.05	0.24	22.8	1.98	64.9	1.07	0.11	0.04	10.3	3.7
Feb 83	3.58	2.23	62.3	1.35	0.80	59.2	2.23	62.3	1.35	0.12	0.32	8.9	23.7
Mar 83	4.33	2.84	65.6	1.49	0.91	61.1	2.66	61.4	1.67	0.14	0.42	8.4	25.1
Total	25.69	15.7	61.3	9.94	5.51	55.4	15.74	61.3	9.95	0.76	4.10	7.6	41.2

Table 6.10 Distribution of Solar Energy for 83-84 Heating Season

		Experiment					Simulation						
Month	$I_{T,AC}$ (GJ)	Q_{cL} (GJ)	%CL	Q_c (GJ)	Q_{store} (GJ)	%STORE	Q_{cL} (GJ)	%CL	Q_c (GJ)	Q_{OMDL} (GJ)	Q_{store} (GJ)	%OMDL	%STORE
Oct 83	4.25	2.28	53.6	1.97	1.40	71.1	2.45	57.6	1.80	0.10	1.05	5.6	58.3
Nov 83	1.83	1.15	62.8	0.68	0.21	30.9	1.19	65.0	0.64	0.05	0.18	7.8	28.1
Dec 83	2.59	1.82	70.3	0.77	0.01	1.3	1.81	69.9	0.78	0.10	0.02	12.8	2.6
Jan 84	2.87	2.03	70.7	0.84	0.19	22.6	1.85	64.5	1.02	0.10	0.16	9.8	15.7
Total	11.54	7.28	63.1	4.26	1.81	42.5	7.30	63.3	4.24	0.35	1.41	8.2	33.3

little energy was stored in the rockbed in December or January. Although, the predictions of the collected solar energy are shown to follow very closely to those measured, the energy sent to storage is found to be around 10% less over a heating season. In other words, the simulation model distributed 10% more of energy directly to the room in the operation mode of HFC. The deviation of energy storage from experiments is probably because a different control criterion was used in the simulations.

During simulation, the controller's tendency to oscillate between its on and off states caused a problem. The controller model uses operational hysteresis and dead band temperature difference to promote stability. The use of hysteresis in general does not guarantee convergence on an output state in a finite number of iterations because control decisions can only be made at intervals of the simulation timestep. Thus, unlike real systems, a TRNSYS simulation involves dead bands in time and in temperature. To prevent the simulation from terminating in error due to excessive number of oscillations, the output control function η_o of the controller model ceases to change after a permitted number of oscillations, thereby hastening numerical convergence of the system but this may decrease the accuracy of the simulatiom. In the real system, the control of energy storage is based on the difference between the air temperature at collector outlet and the temperature at the top of the storage unit. When the difference is over

8°C and space heating is not required, the solar energy available from the collector will be stored in the rockbed. Otherwise, the mode of energy storage will be off. Simulations based on this criterion were found to be unstable and frequently terminated in error. To alleviate the problem, the dead band temperature difference was increased until instability was removed. Increasing the dead band difference represents a change in the system being simulated. Thus, the simulated percentage of energy stored was obtained on the basis of a new criterion. Energy storage occurred when the collector outlet air temperature was 10°C above the top bin temperature, and was terminated when the difference was less than -1°C as shown in Table 4.1.

6.2.3 Rockbed Storage

It was difficult to determine the energy flows of the storage unit experimentally. Since only the average hourly temperature in the rockbed adjacent to the top and bottom of the rockbed was measured, an energy analysis was not pratical although the qualitative behavior could be examined. The air flow through the bed varied between 0.122 m^3/s and 0.218 m^3/s depending on system mode as mentioned in Section 3.1. The calculations of energy flows showed that the discharge energy Q_s was usually greater than the storage energy Q_{store} for most months and even for a whole heating season. In this case, a negative monthly heat

loss would be obtained. This is theoretically impossible unless energy was gained from somewhere to the bin. It is suggested energy probably leaked to the rockbed during HFC. With the available instrumentation, it was impossible to determine the leakage, the conduction heat loss Q_ε or the internal energy change ΔU. Therefore the causes of energy imbalance could not be identified.

Although experiments failed to describe the rockbed storage performance, simulations can be used as a substitute to study the energy balance. The model used here for simulation is the infinite Ntu rockbed model which is currently used in the TRNSYS simulation program. The model is able to provide adequate temperature profile information, so that the conduction heat loss and the internal energy change can be estimated. However, simulation of leakage to and from the rockbed requires additional and complicated modelling as well as sufficient experimental information. Due to lack of knowledge regarding leakage, the model assumes leakage is negligible.

The infinite Ntu rockbed model has been proven by Persons et al.(1979) to be capable of simulating the storage and discharge energy flows with an accuracy of 5% for the rockbed with the value of Ntu, the number of heat transfer units, greater than 10 which includes most rockbeds in current use. The value of Ntu for the rockbed is 22 (calculated in Appendix E-3). It is believed the model is capable of giving reasonable estimates of the energy flows

but its use is restricted to negligible leakage.

The simulated energy flows for the three heating seasons are given in Tables 6.11 to 6.13. The energy balance for the simulated energy quantities closes within 0.5% of the stored energy. The monthly negative change of internal energy is due to the initial set temperature of 22°C for the rockbed for each monthly simulation. The average bin loss for a heating season from September to March is about 5 to 6% of the storage energy with usually more energy lost in the warm months and less in the cold months (except for those months with almost no energy storage).

6.2.4 Damper Leakage Loss

Preceding sections indicated that air leaks from the module to the collector even though the collector is off. In this case part of the energy supplied from the rockbed and electric heater during the collector off period will be lost from the module through the collector and the ducts to the outside of the module. The monthly energy loss and the total energy supplied for space heating Q_H for the three heating seasons are shown in Tables 6.14, 6.15 and 6.16. For a 4% constant leakage, the predicted energy loss ranges from about 1% in September to approximately 5% in December or January. The average loss over a heating season is approximately 3 to 4%.

Table 6.11 Simulated Energy Flows of The Storage Unit for 81-82 Heating Season

Month	Q_{store} (MJ)	Q_s (MJ)	Q_E (MJ)	ΔU (MJ)	Imbalance (MJ)	%BinLoss
Sep 81	1480.0	1321.3	157.6	-0.2	1.3	10.6
Nov 81	442.8	435.4	9.9	-3.1	0.6	2.2
Dec 81	119.0	124.3	2.6	-7.8	-0.1	2.2
Jan 82	1.4	3.5	1.0	-3.3	0.2	71.4
Feb 82	250.9	247.8	6.4	-3.5	0.2	2.6
Mar 82	876.2	857.7	20.7	-2.7	0.5	2.4
Total	3170.3	2990.0	198.2	-20.6	2.7	6.3

Table 6.12 Simulated Energy Flows of The Storage Unit for 82-83 Heating Season

Month	Q_{store} (MJ)	Q_s (MJ)	Q_E (MJ)	ΔU (MJ)	Imbalance (MJ)	%BinLoss
Sep 82	1706.3	1516.2	113.1	76.1	0.9	6.6
Oct 82	1433.0	1374.7	60.9	-3.8	1.2	4.2
Nov 82	127.6	127.9	2.9	-3.4	0.2	2.3
Dec 82	54.5	56.4	1.2	-3.2	0.1	2.2
Jan 83	41.3	43.9	1.4	-3.9	-0.1	3.4
Feb 83	321.2	315.4	7.0	-1.3	0.1	2.2
Mar 83	414.9	406.5	9.9	-1.5	0.0	2.4
Total	4098.8	3841.0	196.4	59.0	2.4	4.8

Table 6.13 Simulated Energy Flows of The Storage Unit for 83-84 Heating Season

Month	Q_{store} (MJ)	Q_S (MJ)	Q_E (MJ)	ΔU (MJ)	Imbalance (MJ)	%BinLoss
Oct 83	1054.0	1024.0	31.8	-3.2	1.4	3.0
Nov 83	176.1	175.5	4.2	-3.8	0.2	2.4
Dec 83	18.2	20.1	1.3	-3.2	0.0	7.1
Jan 84	161.1	161.8	3.3	-4.3	0.3	2.0
Total	1409.4	1381.4	40.6	-14.5	1.9	2.9

Table 6.14 Damper Leakage Loss for 81-82 Heating Season

Month	Q_H (GJ)	Q_{DLL} (GJ)	%DLL
Sep 81	3.49	0.04	1.1
Nov 81	7.60	0.19	2.5
Dec 81	11.41	0.42	3.7
Jan 82	15.30	0.75	4.9
Feb 82	11.49	0.42	3.7
Mar 82	9.93	0.28	2.8
Total	59.22	2.10	3.5

Table 6.15 Damper Leakage Loss for 82-83 Heating Season

Month	Q_H (GJ)	Q_{DLL} (GJ)	%DLL
Sep 82	4.22	0.05	1.2
Oct 82	6.07	0.12	2.0
Nov 82	10.50	0.35	3.3
Dec 82	10.95	0.38	3.5
Jan 83	11.50	0.40	3.5
Feb 83	9.66	0.30	3.1
Mar 83	9.07	0.21	2.3
Total	61.97	1.81	2.9

Table 6.16 Damper Leakage Loss for 83-84 Heating Season

Month	Q_H (GJ)	Q_{DLL} (GJ)	%DLL
Oct 83	6.13	0.12	1.9
Nov 83	8.55	0.25	2.9
Dec 83	14.63	0.68	4.6
Jan 84	10.62	0.36	3.4
Total	39.93	1.41	3.5

6.2.5 Summary of System Energy Flows

To permit meaningful interpretation of the performance of the system for a period of a heating season, the simulated and the available experimental results are summarized in the energy flow charts (Figures 6.16 to 6.18) for each of the three heating seasons. The charts are not to scale and all values are in GJ. The experimental results are shown inside the brackets underneath the simulated quantities.

The overall performance of the system for each heating season is relatively the same. From the total incidence energy, approximately 37 to 40% was collected at the array. The remaining 60 to 63% was lost to the environment demonstrating that in flat plate collectors the major loss occurs at the collector array. From the collected energy, approximately 8% was lost through the insulated ductwork connecting the collector to the module; 35 to 40% was delivered to storage (40 to 55% from experiments); the rest was sent directly to space heating. During storage bed operation mode, about 94% of the stored energy was drawn by the load and 5 to 6% was lost from the storage unit. The storage loss was mainly transferred to the heated space and therefore is actually part of the useful energy which helps to satisfy the building heating load. Energy lost through the basement floor was assumed to be negligible.

The auxiliary energy is actually the major source of supply and contributed approximately 85% of the total load

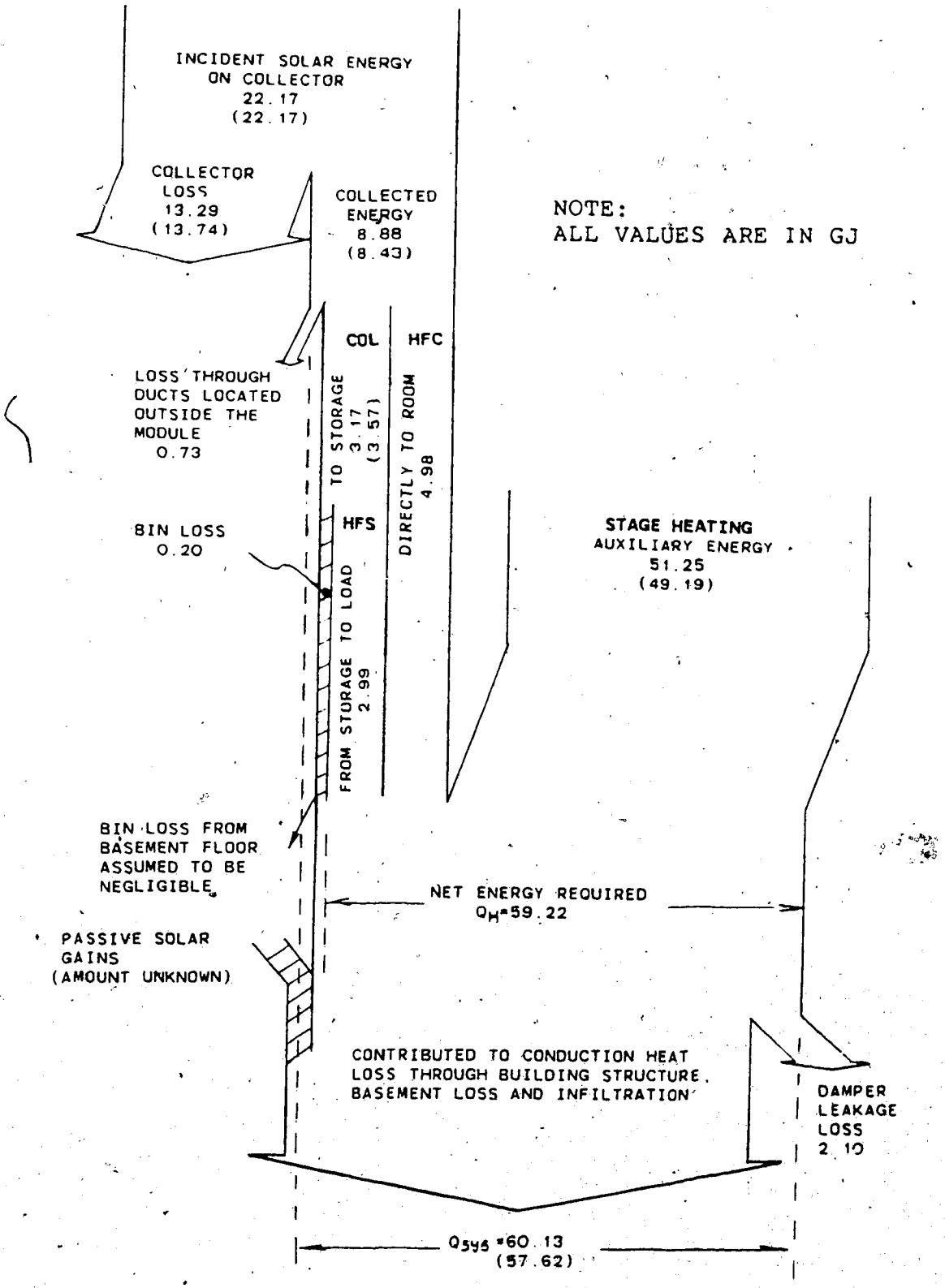

Figure 6.16 Energy Flows for 81-82 Heating Season

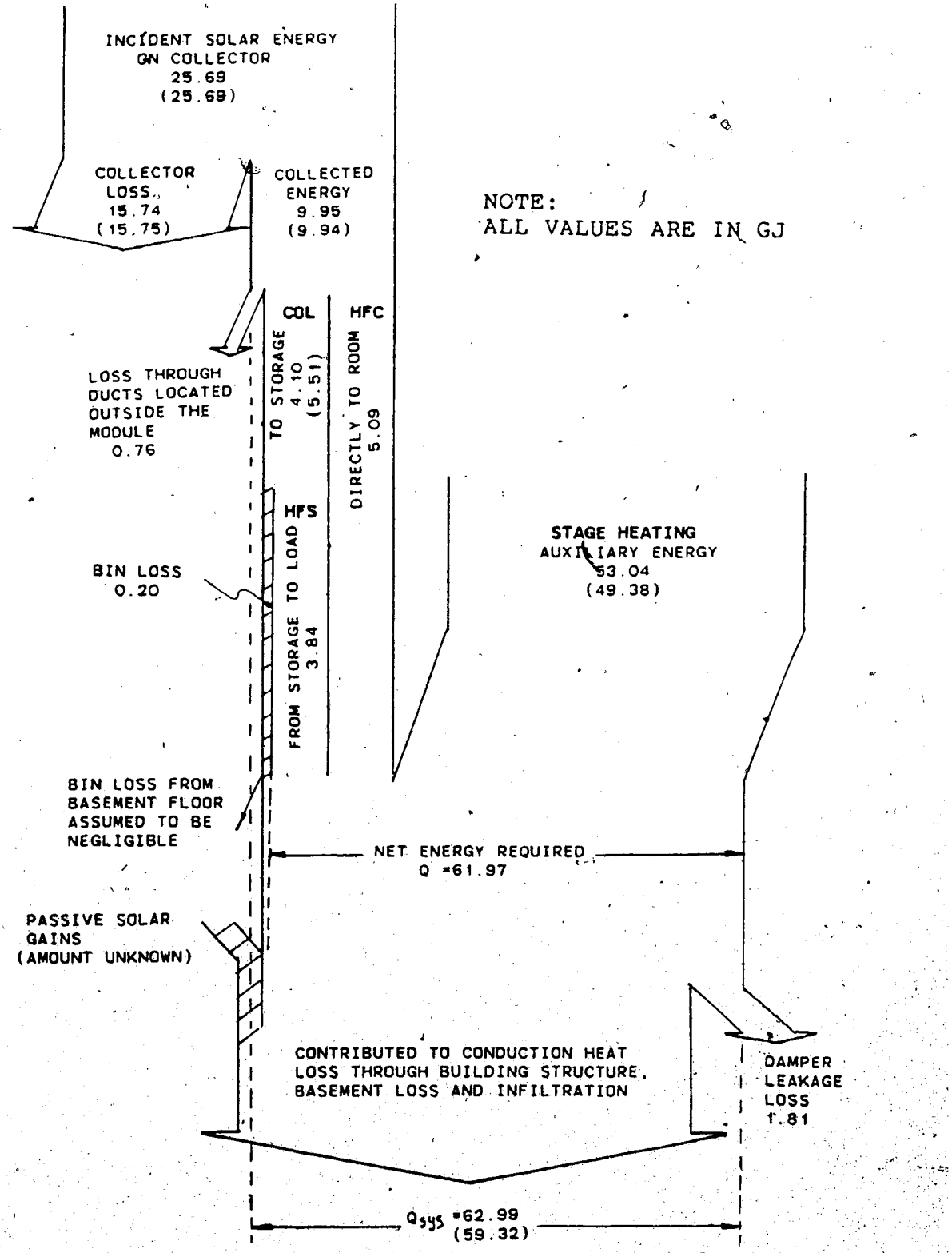

Figure 6.17 Energy Flows for 82-83 Heating Season

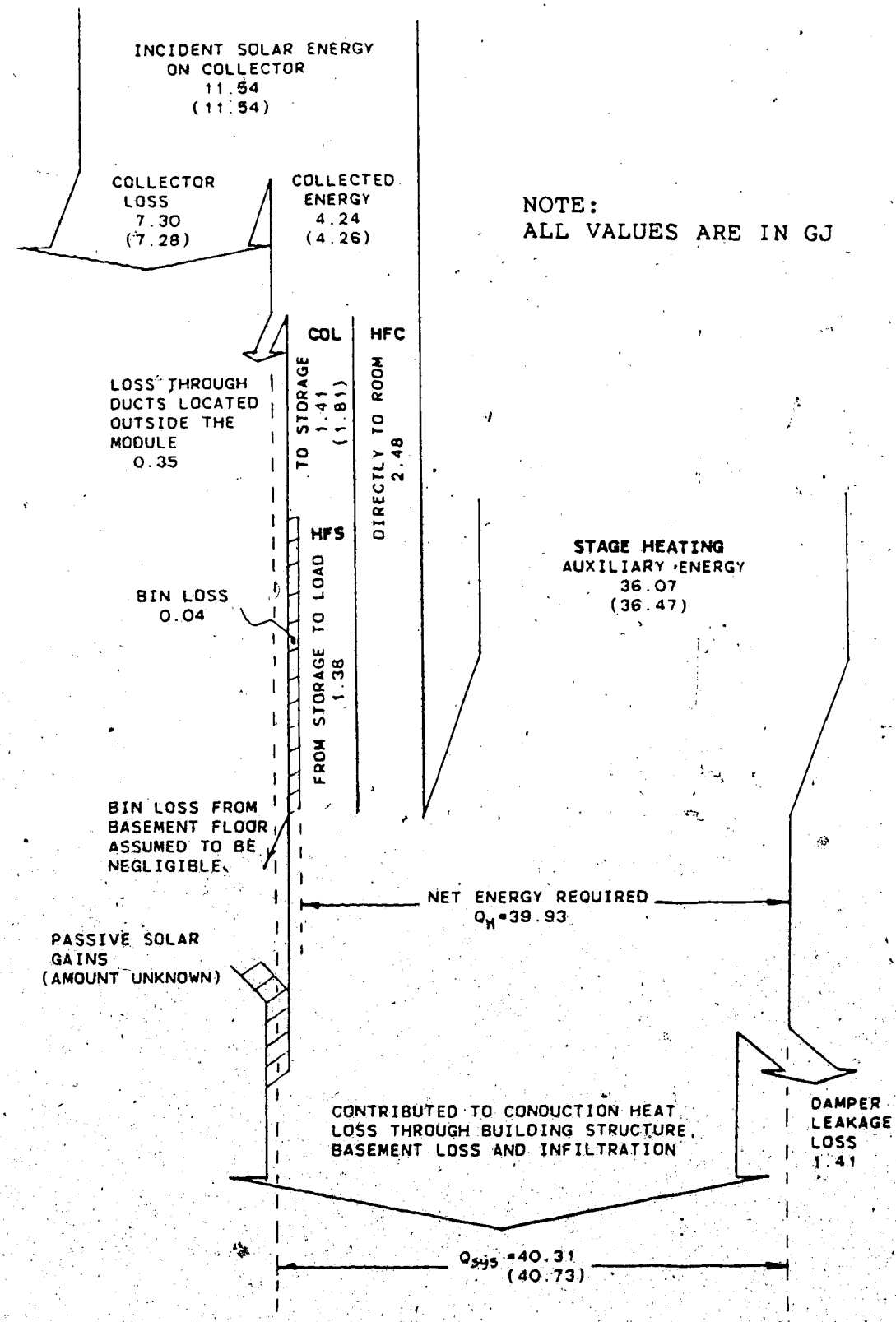

Figure 6.18 Energy Flows for 83-84 Heating Season

(based on Q_{sys}) for the period of a heating season. Besides the active solar gain and electric energy supply, a small portion of energy should be directly gained by passive solar energy (amount unknown). Damper leakage loss based on 4% leakage was about 3 to 4% of the net energy requirement Q_H over each of the periods of study. At the time of writing, the conduction heat loss, basement loss and infiltration could not be separated.

6.2.6 Justification Of The Simulation Model

The percent errors of the simulated quantities will be examined in this section to determine the accuracy of the simulations. Since not all measured quantities are available, the accuracy of the model can only be justified by comparing the major energy terms (Q_c, Q_{c_L}, Q_{aux} and Q_{sys}) which represent the collector performance and the load. The errors were calculated on a monthly basis by subtracting the measured quantities (the adjusted quantities to account for missing data) from the simulated values. Thus, positive error indicates over-estimation and negative refers to the under-prediction by the model. The percent error relative to the measurement of each energy quantity for each month of the three heating seasons is plotted in Figures 6.19 to 6.22.

Section 6.2.2 showed that the prediction of the percent energy storage is about 10% less than measurement over a heating season. The rest of the simulations however follow

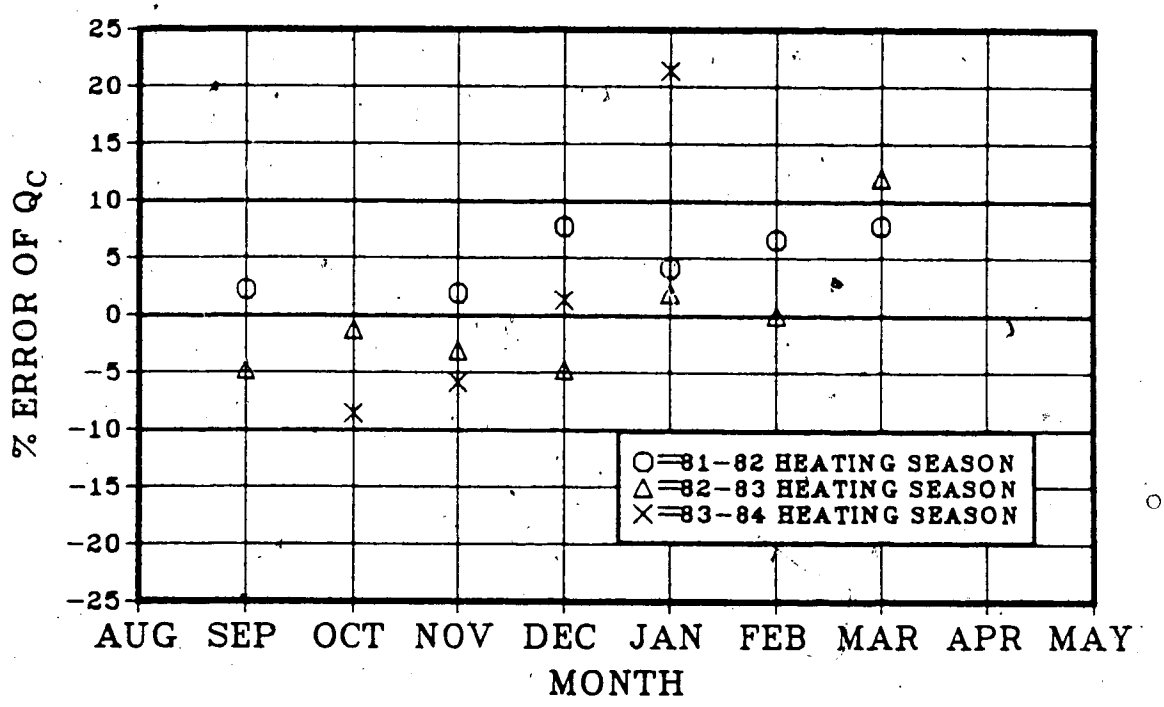

Figure 6.19 Percent Error of Collected Solar Energy

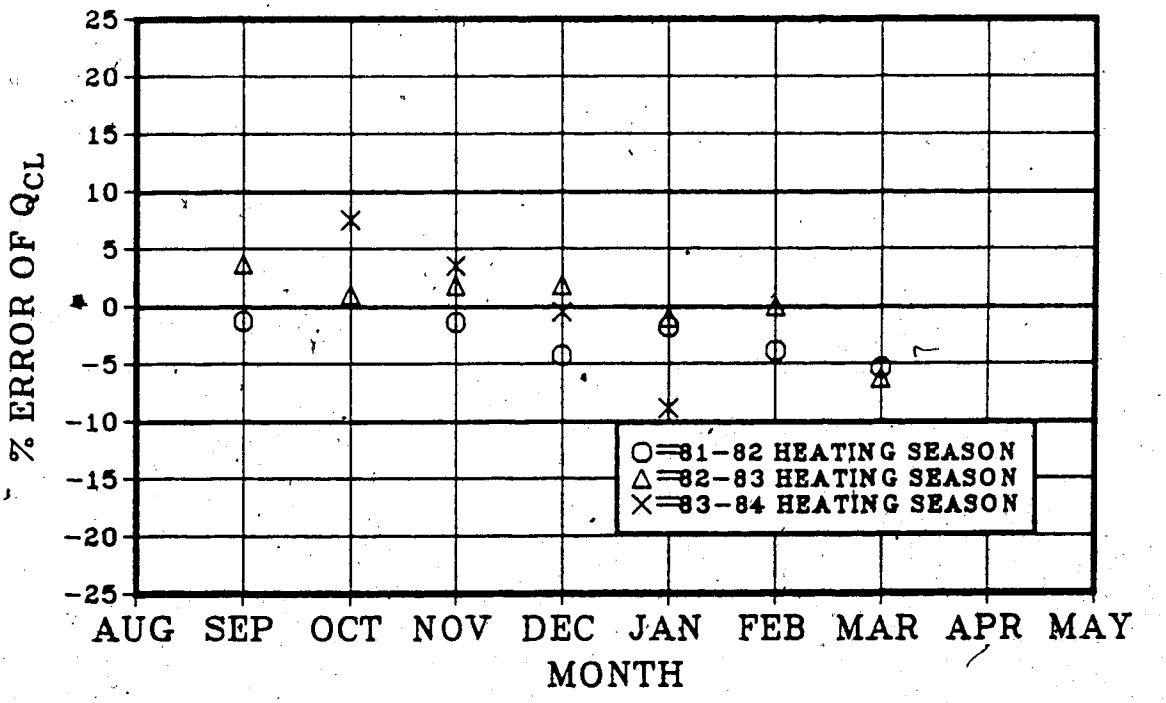

Figure 6.20 Percent Error of Collector Loss

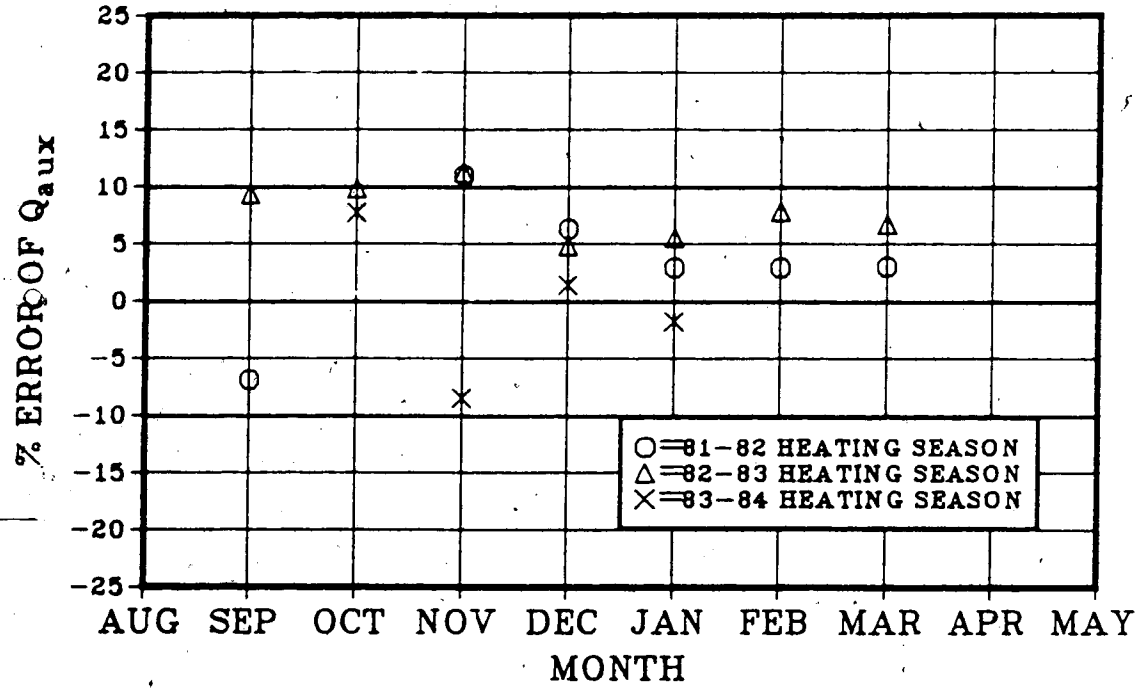

Figure 6.21 Percent Error of Auxiliary Energy

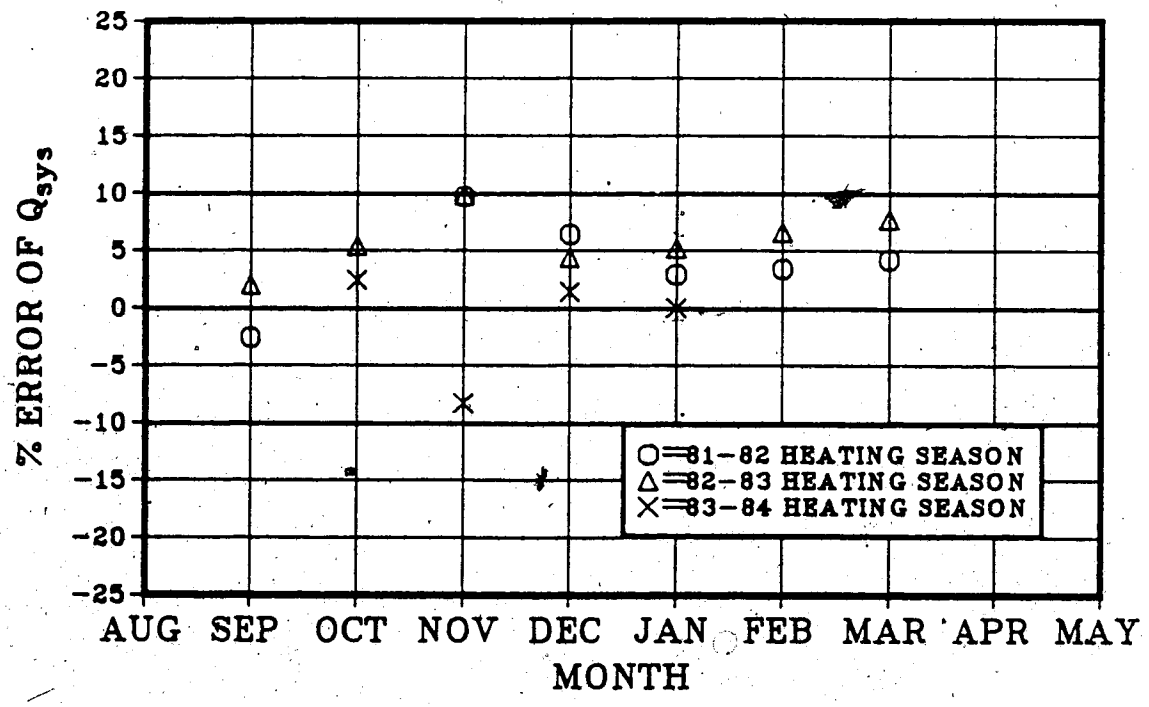

Figure 6.22 Percent Error of Total System Energy Supply

closely to those measured with the errors mainly lie within ±10%. The Simulated value of Q_c for January 1984 is 21.4% over-predicted. This discrepancy may be because:

1. the adjusted measured quantity may be different from the actual measurement.
2. collector tilt angle was changed from 68°, the optimum angle, to 88° in December 1983. Using the efficiency curve of a collector tilted at optimum angle to estimate the solar energy collected by a collector tilted at 88°, a discrepancy is expected. The effect of collector tilt angle will be discussed in next section.

Since actual monthly measurements of energy quantities are unknown, the accuracy of the adjusted measured quantities is unable to be determined. However, it is believed the errors created by missing data can be more or less eliminated if the average monthly quantities'' of the three heating seasons are used, instead, for comparisons. The average monthly values of the energy quantities from both experiments and simulations are shown in Table 6.17 and their percent errors are plotted in Figure 6.23. In this case, the errors are within ±5% for more than 80% of the items. The average Q_{aux} and Q_{sys} are over-predicted for every month although the discrepancies are small. This

'' For example: the average January value of the measured Q_c is [0.72+1.05+0.84]/3 = 0.87 GJ from Tables 6.5 to 6.7.

Table 6.17 Averages of Monthly Energy Quantities

	Experiment				Simulation			
	Q_c (GJ)	Q_{cL} (GJ)	Q_{aux} (GJ)	Q_{sys} (GJ)	Q_c (GJ)	Q_{cL} (GJ)	Q_{aux} (GJ)	Q_{sys} (GJ)
Sep	2.07	2.96	2.08	4.15	2.03	3.00	2.12	4.15
Oct	2.17	2.63	3.85	6.02	2.07	2.73	4.18	6.25
Nov	0.89	1.42	7.78	8.67	0.88	1.43	8.08	8.96
Dec	0.70	1.51	11.25	11.95	0.72	1.49	11.69	12.41
Jan	0.87	1.89	11.37	12.24	0.94	1.82	11.63	12.57
Feb	1.43	2.39	8.79	10.22	1.48	2.34	9.24	10.72
Mar	1.96	3.18	7.20	9.16	2.14	3.00	7.55	9.69
Total	10.09	15.98	52.32	62.41	10.26	15.81	54.49	64.75

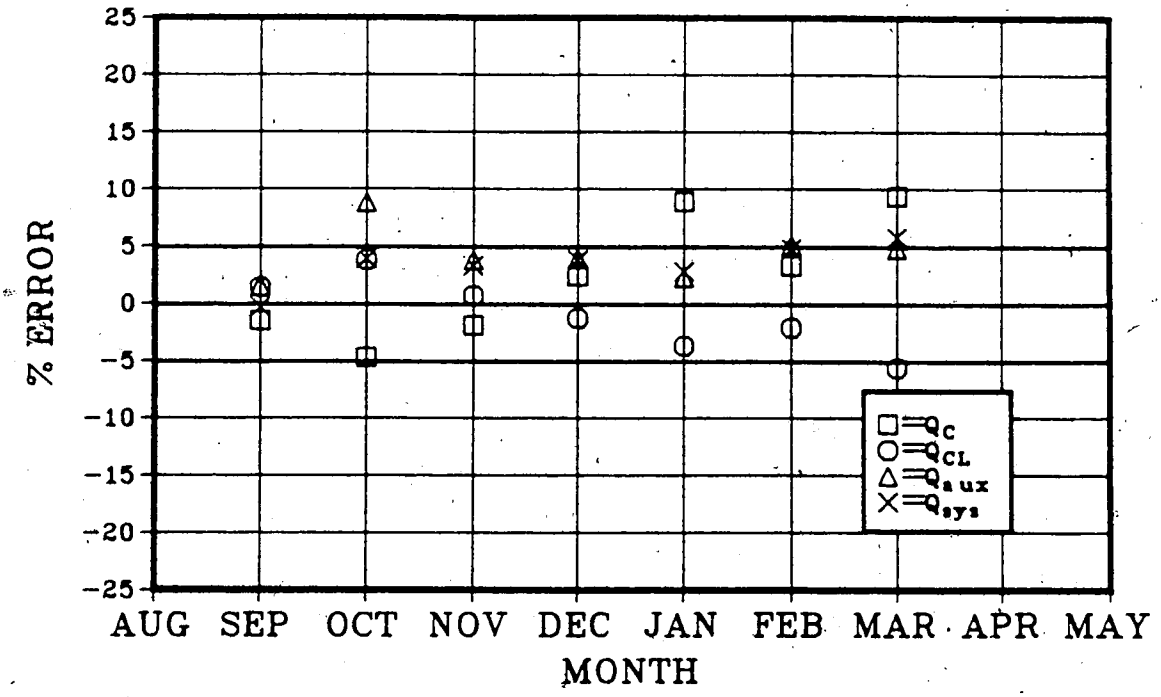

Figure 6.23 Percent Error of The Average Monthly Quantities

implies that a slightly lower value of the module UA factor than 140 W/°C would give even better judgement of the load. Appendix E-1 indicates that the value of 140 W/°C is the round off value of 137.9 W/°C. Therefore, the more appropriate value for the module UA factor should be 137 or 138 W/°C.

6.3 Parametric Study

In preceding sections, the performance of the solar heating system was analyzed based on a fixed design. Simulations, on the other hand, provide the opportunity to determine the effects of changes of design parameters. Of all the physical parameters, only few are considered to be significant[12]. Since the collector and storage facility are regarded as the principal components, and the overall performance of a solar heating system is generally the result of the thermal performance of the collector and storage unit, investigation of the effects of changes in their parameters is essential. In this section, simulations are used to show how the collector area and the storage size affect the solar contribution. The effect of collector tilt angle also will be discussed. The selected period of study is the 82-83 heating season (ie., from September 1982 to March 1983). The area of the collector is increased by assuming that identical arrays are added in series. The rockbed is sized as a ratio to the collector area. Simulations were done at storage sizes of 0.01, 0.05, 0.18 and 0.50 m^3/m^2 for collector areas of 11.1, 33.3 and 99.9 m^2.

Figure 6.24a shows the seasonal solar heating contribution as a funtion of the collector area for the four ratios of storage capacity (ie., the ratios of storage volume to collector area in m^3/m^2). Figure 6.24b gives

---

[12]Mentioned by Duffie et al.(1980), p.365.

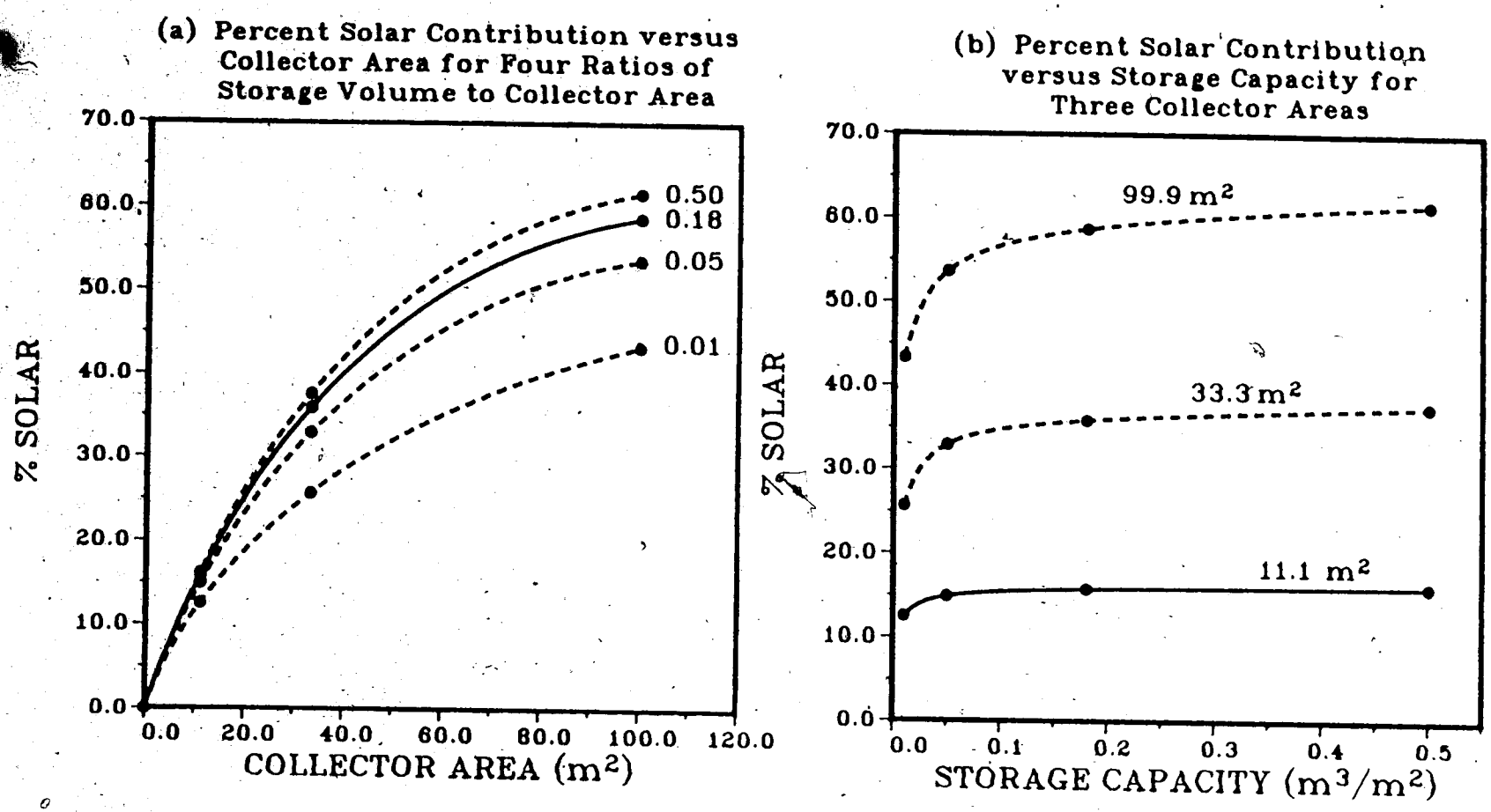

Figure 6.24 Effects of Changes of Collector Area and Storage Capacity for 82-83 Heating Season

essentially the same information, but is in terms of the storage capacity. The solid curves in the figures represent the design values of the collector area and storage capacity for the system. As seen from Figure 6.24a, the percent solar contribution increases faster at small collector areas than at large areas. Thus an increment in collector area produces more useful energy for small collector areas than for large collector areas. This indicates that a larger collector is oversized for longer period of the heating season than is a small collector. Figure 6.24 shows that change of storage size for small collectors has small effect on solar contribution. Within the test range for the heating season, the storage effect is relatively insignificant for the 11.1 m^2 collector. As the collector area increases, the effect of decreasing storage size become more pronounced since the bottom of the bed is at a higher average temperature than the room temperature, resulting in an increase in air temperature to the collector. Generally, the solar contribution is relatively insensitive to storage volume once a critical storage capacity is exceeded. The performance of the solar heating system is much more sensitive to collector area than to storage volume.

September 1982 and December 1982 are the two extreme months in the 82-83 heating season: one has the highest percent solar contribution (September) and the other has the lowest percentage (December) as shown in Table 6.6. The effects of the collector area for the storage size of

0.18 m^3/m^2 for these two months and the whole heating season are compared in Figure 6.25. It is clear that the curve for the whole heating season lies between the two extreme monthly curves. The variation of the shape of the monthly curves depends on the relative magnitudes of the heating load and the insolation. As in December 1982, a month with limited incident radiation, the solar contribution can only increase gradually as collector area is added. However in September 1982, the relatively high radiation level coupled with the low magnitude of heating load lead to a sharp increase in the solar contribution at small collector areas until approximately 30 m^2 is reached. After this point, the improvement in solar contribution to space heating is not as pronounced, due to the fact that the collector is oversized for a great part of the month.

Figure 6.26 compares the effects of the storage size for the 11.1 m^2 collector for the same two months and the heating season. For the cold climate in Edmonton, storage effect seems to be insignificant for this system during the heating season, as most of the energy from the collector will be used immediately for space heating in HFC, with only little energy stored in the rockbed. Therefore, even if there was no storage, the 11.1 m^2 collector would still supply approximately 10% of the load over the heating season. For December 1982, change of storage appears to have no effect at all on the solar contribution as it remains constant within the test range. Towards the summer,

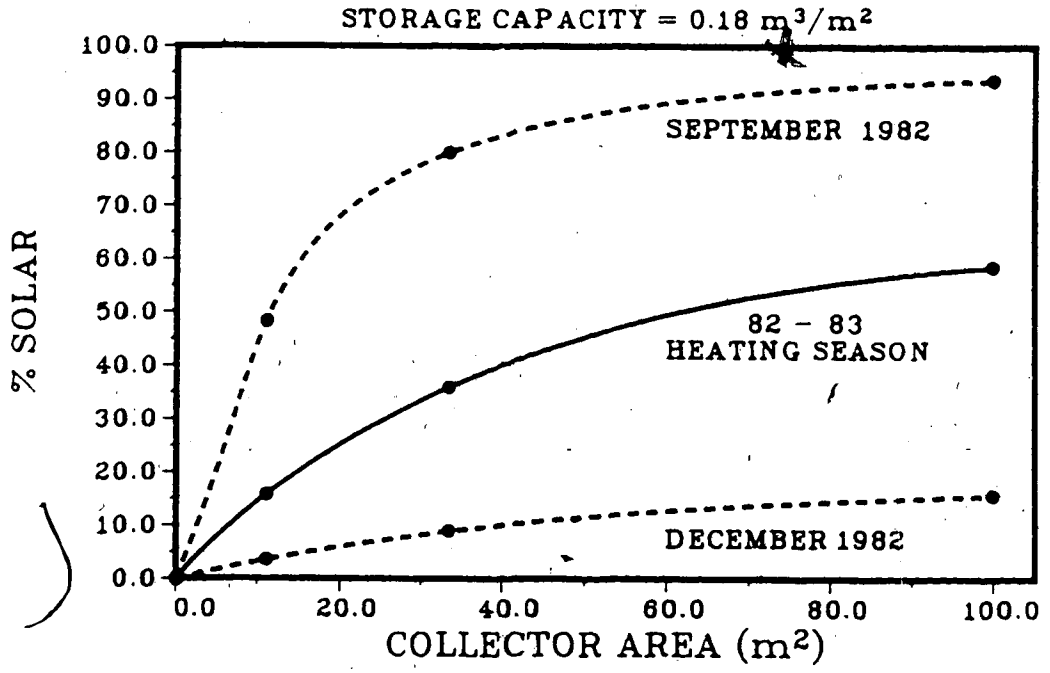

Figure 6.25 Comparison of The Effect of Collector Area for September 1982, December 1982 and 82-83 Heating Season

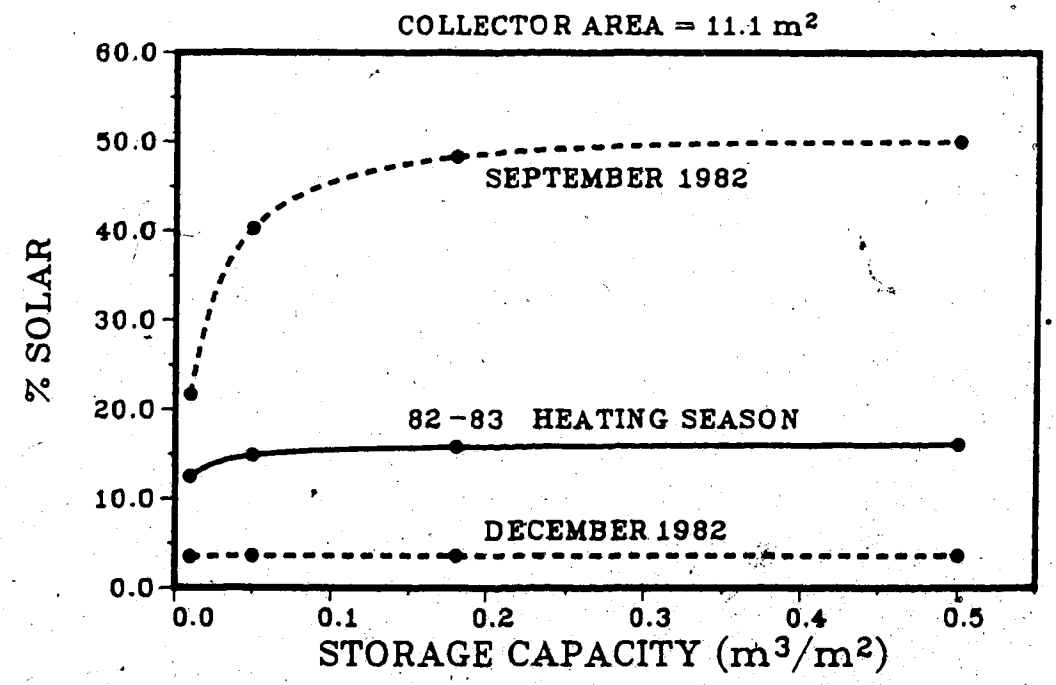

Figure 6.26 Comparison of The Effect of Storage Capacity for September 1982, December 1982 and 82-83 Heating Season

the significance of storage increases since more energy will be stored. As indicated, the decrease in percent solar contribution from normal storage (0.18 m^3/m^2) to no storage reaches about 30% of the load in September 1982. The critical storage capacity decreases from approximately 0.15 m^3/m^2 in September to almost zero in December and is about 0.05 m^3/m^2 for the whole season. Therefore, the existing storage capacity of 0.18 m^3/m^2 is adequate for this system for the period of a heating season.

The energy quantities for the above studies are summarized in Tables 6.18 and 6.19. The addition of the solar heating system increased the heating load. As shown, the load is to some degree a function of system size, since operation of larger systems keep the module at slightly higher mean temperatures. In December 1982, space heating was mainly supplied by the electric heater rather than the solar heating system, thus no significant change in the load due to change of system size is observed for that month.

The collector component was modelled by using a collector efficiency curve which was calculated based on an optimum tilt angle at 68°. Collector performance at other tilt angles is therefore unable to be determined by the model. However, by means of the results of Balcomb et al.(1975)[13], the effect of collector tilt on percent solar contribution can be approximated indirectly from Figure 6.24. The results of Balcomb et al. are given

[13]Provided by the manufacturer for the Solaron series 2000 flat plate air type collector.

Table 6.18 Summary of Energy Quantities for Different Collector Areas and Storage Volumes for 82-83 Heating Season

Collector Area (m^2)	Storage Volume (m^3)	Q_c (GJ)	Q_{sys} (GJ)	% Solar
11.1	0.11	7.91	63.10	12.5
	0.56	9.38	62.99	14.9
	2.00	9.95	62.99	15.8
	5.55	10.11	62.90	16.1
33.3	0.33	16.31	63.49	25.7
	1.67	20.92	63.64	32.9
	6.00	22.99	63.97	35.9
	16.65	24.15	64.28	37.6
99.9	1.00	27.81	64.09	43.4
	5.00	34.95	65.24	53.6
	18.00	39.41	67.15	58.7
	50.00	42.51	68.86	61.7

Table 6.19 Energy Quantities for Different Collector Areas and Storage Volumes for September and December 1982

Month	Collector Area (m^2)	Storage Volume (m^3)	Q_c (GJ)	Q_{sys} (GJ)	% Solar
Sep 82	11.1	0.11	1.00	4.61	21.7
		0.56	1.84	4.56	40.3
		2.00	2.19	4.53	48.3
		5.55	2.27	4.54	50.0
	33.3	6.00	4.38	5.48	79.9
	99.9	18.00	7.71	8.23	93.7
Dec 82	11.1	0.11	0.39	11.02	3.5
		0.56	0.40	11.02	3.6
		2.00	0.40	11.00	3.6
		5.55	0.40	11.03	3.6
	33.3	6.00	0.98	11.05	8.9
	99.9	18.00	1.74	11.10	15.7

in Figure 6.27 which shows the relative collector area required to provide the same annual fuel savings as a system at optimum collector tilt for those at other tilt angles. As indicated, the optimum collector tilt for space heating is equal to the latitude plus 5° to 15°. For Edmonton at 53.6° N latitude, the optimum collector tilt would be 58.6° to 68.6°. If a collector was tilted at 88°, the relative collector area required would be 1.07 of the area of the collector at optimum tilt angle. In other words, if a collector of 11.1 m^2 was tilted at 88°, the equivalent area for the collector tilted at 68° would be 11.1/1.07 = 10.4 m^2. The corresponding percent solar contributions for 11.1 m^2 and 10.4 m^2 in Figure 6.24a for normal storage are about 15.8% and 14.8% respectively (a difference in approximately 1%). The percent difference in the amount of solar energy collected by the collectors is thus (15.8-14.8)/15.8 x 100% = 6.3%. Therefore the change in collector tilt angle from 68° to 88° results in a decrease of about 6.3% in collected solar energy and approximately 1% in solar contribution for a heating season.

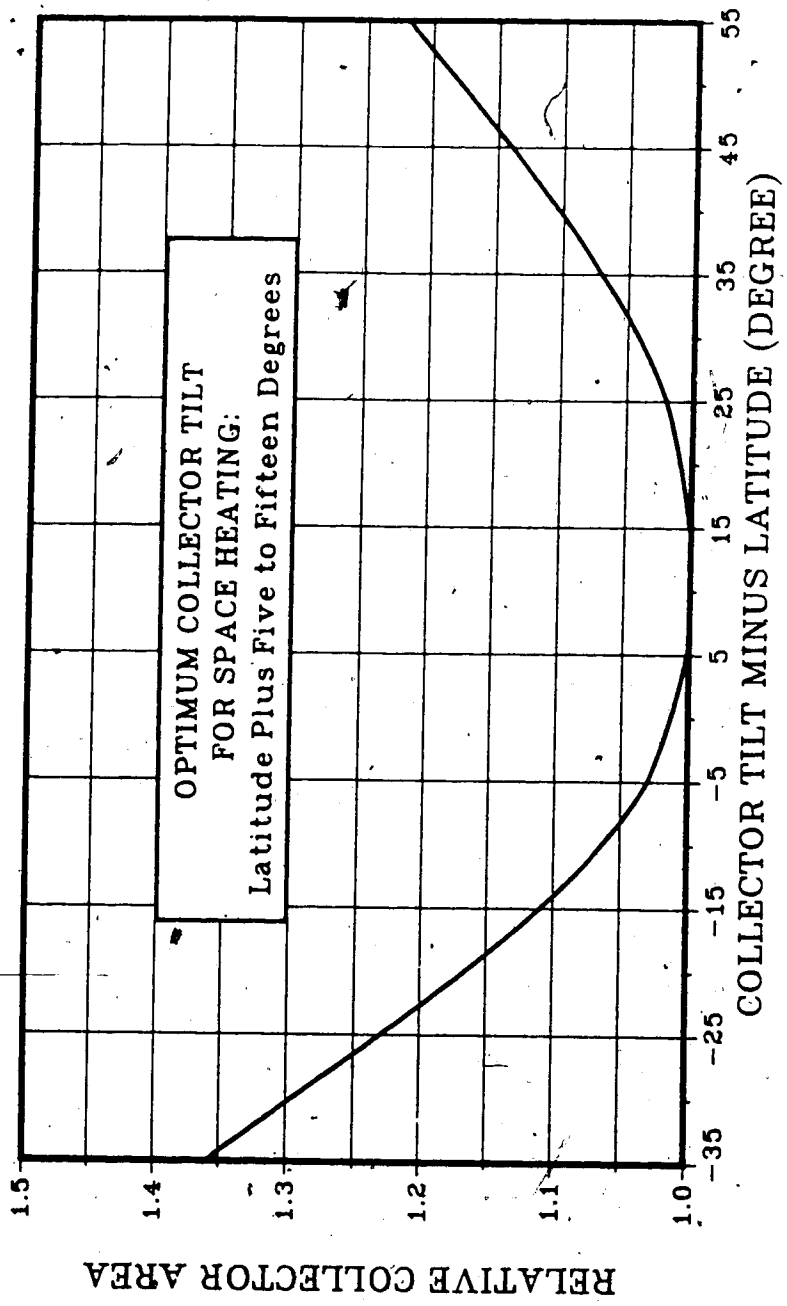

Figure 6.27 Corrections for Non-optimum Collector Tilt for A Typical Installation at 35 Degree North Latitude (Balcomb et al. 1975)

7. CONCLUSIONS AND RECOMMENDATIONS

7.1 Conclusions

A model has been developed by using the TRNSYS program to simulate the solar heating system at the Alberta Home Heating Research Facility. The model has been tested and applied to the analysis of the performance of the system. Available measurements also have been presented to compare the simulations. The results lead to the following conclusions.

7.1.1 Modelling

The model is able to provide detailed information on energy flows and temperature profiles at different locations of the solar heating system for a wide range of performance studies. The model is flexible enough to examine system modification such as changes of the physical parameters for collector, storage, and other components, so that determination of the parameter effects, which are essentially impossible to get by other means, can be obtained from simulations. The model has the potential for very detailed analysis. Application to detailed analysis requires further justification of component parameters and detailed comparisons to experiments to ensure that all of the information obtained from simulations are reasonably accurate. With the available experimental information provided, the model was proven to be able to obtain

agreements that are comparable to the accuracy of the measurements of the collector performance and heating load on the physical system. However, the prediction of the percentage of energy storage in the rockbed was usually less than those measured.

With or without the effect of non-normal solar incidence, the standard test curve of the collector efficiency predicts low collected solar energy. Hourly collector efficiency curve requires consideration of incidence angle modification to improve accuracy. The monthly curve is more representative of the overall collector performance and includes the incidence angle effect.

7.1.2 Analysis

Conclusions drawn from the analysis of the solar heating system can be summarized as follows.

1. The collector parameters $F_r(\tau\alpha)$ and $F_r U_L$ from the standard test curve did not represent the physical properties of the assembled collector.
2. Improper operation of dampers occurred in the system during storage bed operation mode so that air leaked from the module to the collector. The percentage of damper leakage was found to range from 2 to 15% over the years. The energy lost due to damper leakage reached from about 1 to 13% of the net energy required by the system for 2 and 15% leakage

respectively. For a constant normal damper leakage of 4%, the average loss over a period of a heating season was about 3.5%.

3. The overall performance of the system for each heating season is essentially the same. From the total incidence energy on the collector, only 37 to 40% was collected by the collector so that the major loss occurred at the collector array. From the collected energy, approximately 8% was lost through the ducts located outside the module; 35 to 55% was sent to storage; and the rest was delivered directly to space heating. Approximately 94% of the stored energy was drawn from the rockbed by the load and 5 to 6% was lost mainly to the heated space. The average of the total incidence energy on the collector for the period from September to March was about 26 GJ.

   The solar contribution evaluated by the maximum contribution method discussed in Chapter 5 ranged from about 4 to 5% in December or January to about 50% in September, and the maximum possible contribution of solar energy for a whole heating season was approximately 15%. In other words, a minimum of about 85% of the heating load was met by electric energy. The average sum of the solar and electric energy supplied to the system for the period was around 62 to 64 GJ.

4. The effect of change of collector area on solar contribution is more pronounced at small collector areas, as a larger collector would be oversized for a longer period of time especially in summer. The solar contribution is relatively insensitive to storage volume once a critical storage capacity is exceeded. This critical storage capacity is larger in summer than in winter. Within a heating season, the existing storage capacity of 0.18 m^3/m^2 is adequate for the 11.1 m^2 collector. The increase in collector tilt angle from 68 to 88° resulted in a decrease of about 1% in solar contribution and 6% in collected solar energy. The performance of the solar heating system is much more sensitive to collector area than to storage volume and collector slope.

5. Energy saving of at least 4% of electricity consumption over a heating season could be achieved by fixing the leakage dampers and reducing the length of the ductwork connecting the collector to the module. The energy recovered from duct loss during collector on period by attaching the collector to the south wall is slightly more than the loss due to the increase in collector slope.

7.2 Recommendations

The following points are recommended for further studies, improving simulations and system performance.

1. More thermocouples are needed at different levels of the bin to study the rockbed behavior in more detail.
2. Periodic measurements of air flow to the collector, storage unit and the room are necessary to determine the leakages , if any, to the components.
3. Energy lost from the ducts located outside the module can be determined experimentally by installing thermocouples at the entries and exits of the duct sections.
4. Experimental determination of damper leakage loss, duct loss and bin loss are required to justify those obtained from simulations.
5. System performance for the summer period, and the effects of changes of collector area and storage capacity on annual performance of the system should be studied.
6. It is recommended that the solar collector be attached to the south wall of the module to minimize the energy losses from the ducts.
7. The module UA factor should be changed from 140 to 137 W/°C for better representative of the overall heat loss from the module for long term simulations.
8. Mode 3 of the TYPE 1 flat plate solar collector component is a theoretical steady state model which

includes consideration of the effects of collector slope and windspeed on $F_r(\tau\alpha)$ and $F_r U_L$. The model facilitates the estimate of collector performance under different conditions for the collectors with different numbers of glass covers. If all of the PARAMETERS required by this model were known, it would be worth using this model to predict the collector performance.

9. If a record of total radiation on collector surface is available and non-normal incidence effect is not considered, the two solar processors, UNIT 9 and 10, can be omitted for reducing computational effort.

REFERENCES

ASHRAE, 1981: *Handbook of Fundamentals.* American Society of Heating, Refrigeration, and Air Conditioning Engineers, Altanta, Chapter 23.

ASHRAE Standard 93-77, 1977: *Methods of Testing to Determine the Thermal Performance of Solar Collectors.* American Society of Heating, Refrigeration, and Air Conditioning Engineers, New York.

Balcomb, J.D., Hedstrom, J.C., and Rogers, B.T., 1975: *Design Considerations of Air Cooled Collector/Rock-Bin Storage Solar Heating System.* Paper presented at the ISES Los Angeles Meeting, August 1975.

Beckman, W.A., Klein, S.A., and Duffie, J.A., 1977: *Solar Heating Design by the f-Chart Method.* Wiley, New York.

Close, D.J., 1967: A Design Approach for Solar Processes. *Solar Energy*, Vol.11, P.112.

Duffie, J.A. and Beckman, W.A., 1980: *Solar Engineering of Thermal Processes.* Wiley, New York.

Elliott, M.A. and Turner, N.C., 1972: *Estimating the Future Rate of Production of the World's Fossil Fuels.* Paper presented at the American Chemical Society Meeting, Boston, Massachusetts.

Fung P.T., 1983: *A Study of the Performance of a Solar Air Heating Sysytem.* M.Sc. Thesis in Mechanical Engineering, University of Alberta.

Gupta, C.L., 1971: On Generalizing the Dynamic Performance of Solar Energy Systems. *Solar Energy*, Vol.13, P.301.

Halacy, D.S., Jr., 1973: *The Coming Age of Solar Energy.* Harper and Row, Revised Edition, P.29.

Hughes, P.J., Klein, S.A., and Close, D.J., 1976: Packed Bed Thermal Storage Models for Solar Air Heating and Cooling Systems. *Journal of Heat Transfer*, Vol.98, P.336.

Klein, S.A., et al., 1983: *TRNSYS - A Transient System Simulation User's Manual.* University of Wisconsin-Madison, Engineering Experiment Station Report 38-12.

Kreith, F. and Kreider, J.F., 1978: *Principles of Solar Engineering.* McGraw Hill, New York, P.7.

Persons, R.W., Duffie, J.A., and Mitchell, J.W., 1979: Comparison of Measured and Predicted Rock Bed Storage Performance. *Solar Energy*, Vol.24, P.199.

Rapp, D., 1981: *Solar Energy.* Prentice Hall, Englewood Cliffs, P.9.

Robertson, J.A.L., 1981: *Nuclear Energy in Canada: The CANDU System.* Atomic Energy of Canada Limited, Report AECL-6328.

Sadler, G.W. and Leung, E.Y., 1985: *A Summary of Operation Results for the Air Solar Heating System for Module 6 of the Alberta Home Heating Research Facility.* Paper presented at the Joint ASES/ASME Solar Energy Conference, Knoxville, Tennessee, March 25-29.

Schumann, T.E.W., 1929: Heat Transfer: A Liquid Flowing Through a Porous Prism, *Journal of the Franklin Institute*, Vol.208, P.405.

Zaheeruddin, M., 1983: *A Simulation Model for a Direct Gain Passive House and its Experimental Verification.* Ph.D. Thesis in Mechanical Engineering, University of Alberta.

BIBLIOGRAPHY

Ackerman, M.Y., Dale, J.D., Forest, T.W., Sadler, G.W., Wilson, D.J., and Zaheeruddin, M., 1983: *Final Report on the Alberta Home Heating Research Facility: Results of the 1981-82 Heating Season and Part of the 1982-83 Heating Season to January 1983.* University of Alberta, Department of Mechanical Engineering Report No.34.

Eckert, E.R. and Drake, R.M., Jr., 1959: *Heat and Mass Transfer.* McGraw Hill, New York.

Gilpin, R.R., 1980: *Optimum Design for a House Employing Direct Solar Gain: A Computer Simulation Study.* Paper 15.2 presented at the Solar Energy Society of Canada Inc. Annual Meeting, Vancouver, British Columbia.

Gilpin, R.R., Dale, J.D., Forest, T.W., and Ackerman, M.Y., 1980: *Construction of the Alberta Home Heating Research Facility and Results for the 1979-80 Heating Season.* University of Alberta, Department of Mechanical Engineering Report No.23.

Gilpin, R.R., Forest, T.W., Ackerman, M.Y., Wilson, D.J., Sadler, G.W., Dale, J.D., and Zaheeruddin, M., 1981: *Second Annual Report on the Alberta Home Heating Research Facility: Results for the 1980-81 Heating Season.* University of Alberta, Department of Mechanical Engineering Report No.24.

Hollands, K.G., Chinneck, J.W., Chanarasheker, M., 1980: Collector and Storage Efficiencies in Solar Heating System. *Solar Energy*, Vol.23, P.471.

Holman, J.P., 1976: *Heat Transfer.* McGraw Hill, Fourth Edition.

Klein, S.A., Beckman, W.A., Duffie, J.A., 1976: A Design Procedure for Solar Heating System. *Solar Energy*, Vol.18, P.113.

Löf, G.O.G., Duff, W.S., Hancock, C.E., and Swartz, D., 1982: *Performance of Eight Solar Heating and Cooling Systems in CSU Solar House I, 1980-1981.* Colorado State University, Final Report for the Period Feb.1980 to Sept.1981.

Lunde, P.J., 1978: Prediction of the Monthly and Annual Performance of Solar Heating Systems. *Solar Energy*, Vol.20, P.283.

Swanson, S.R. and Boehm, R.F., 1977: Calculation of Long-term Solar Collector Heating System Performance. *Solar Energy*, Vol.19, P.129.

Taylor, S.L., 1981: *Assessment of Air Solar System Performance with Alternate Methods of Analysis.* Proceedings of the ASME Solar Energy Division Third Annual Conference, Reno, Nevada, Solar Engineering 1981, P.277.

APPENDIX A: Parameters of Component Models

TYPE 16 Solar Radiation Processor

1. Radiation Mode	-	4 when I_b and I_d are inputs 5 when I and I_{dn} are inputs
2. Tracking Mode	-	1 for fixed surface
3. n	-	day of year of the start of the simulation
4. ϕ	-	latitude, 53.57° for Edmonton
5. Sc	-	solar constant, 1353 W/m²
6. SHFT	-	shift in solar time hour angle, -8.52° for Edmonton

Type 1 Solar Collector

1. Collector Mode	-	1 for linear efficiency
2. Ns	-	number of collectors in series
3. A_C	-	total collector area, 11.1 m²
4. Cpc	-	specific heat of collector fluid, 1006 J/kg·°C for air
5. Efficiency Mode	-	1 for η vs. $(T_{ci} - T_a)/I_T$
6. Gtest	-	mass flow rate per unit area at test conditions
7. $F_r(\tau a)$	-	intercept efficiency
8. $F_r U_L$	-	negative of the slop of the efficiency curve
9. ϵ	-	effectiveness of the collector loop heat exchanger (if ≤0, then no heat exchanger)

10. Cpf - specific heat of fluid entering the cold side of the heat exchanger, 1006 J/kg·°C

11. Optical Mode - 1 for using incidence modifier constant from ASHRAE 93-77

12. b_o - incidence angle modifier constant from ASHRAE 93-77 test, 0.17

TYPE 31 Duct

1. d - duct inside diameter, 254 mm

2. L - duct length, 2670 mm

3. U - overall loss coefficient based upon inside duct surface area, 1.47 W/m²·°C

4. ρ_f - fluid density, 1.2057 kg/m³

5. Cp - fluid specific heat, 1006 J/kg·°C

6. Tif - initial fluid temperature, 22°C

TYPE 2 Controller

1. NSTK - the number of oscillations of the controller in a timestep after which γ_o ceases to change

2. ΔT_H - upper dead band temperature difference

3. ΔT_L - lower dead band temperature difference

TYPE 3 Fan

1. $\dot{m}_{max}$ - maximum flow rate, 0.263 kg/s

TYPE 11 Damper

1. Mode - 2 for flow diverter
   3 for flow mixer

TYPE 10 Rockbed Thermal Storage

1. Cp - specific heat of air, 1006 J/kg·°C
2. L - length of the rockbed in the flow direction, 1040 mm
3. A - cross-sectional area of rockbed, 1.88 m^2
4. P - perimeter of rockbed wall, 5490 mm
5. Cpr - specific heat of rock, 880 J/kg·°C
6. ρ_r - apparent rockbed density, 1530 kg/m^3
7. U - loss coefficient, 0.443 $W/m^2 \cdot °C$
8. K - effective thermal conductivity in the axial direction, 0.125 W/m·°C

TYPE 12 Load

1. Mode - 4 for floating temperature with no auxiliary
2. UA - overall conductance for heat loss from house, 140 W/°C
3. CAP - lumped thermal capacitance of house, 11000 kJ/°C
4. Tri - initial room temperature, 22°C
5. Cpf - specific heat of heat source fluid, 1006 J/kg·°C

6. eC_{min} - product of the effectiveness and minimun capacitance rate of load heat exchanger, 0

TYPE 36 System Analyzer

1. T_{s1} - set temperature of top storage bed for HFS with 1/2 electric coil on, 24°C
2. T_{s2} - set temperature of top storage bed for HFS with electric coil off, 36°C
3. T_{co_2} - air set temperature at collector outlet for HFC with electric coil off, 33°C
4. P_1 - electric power supply for first stage heating, 3.75 kW
5. P_2 - electric power supply for two stage heating, 7.5 kW
6. P_{min} - minimum power supply to keep the fan on, 0.631 kW

APPENDIX B: Subroutine Program of The System Analyzer

```
C     ************************************************************
C     *                                                          *
C     * THIS ROUTINE IDENTIFIES  THE MODES OF  OPERATION AND     *
C     * AUXILIARY ENERGY FOR FIRST AND SECOND STAGE HEATING.     *
C     * THE ROUTINE ALSO CALCULATES "COLLECTOR ON"  INCIDENT     *
C     * RADIATION,  ENERGY  TO THE  ROCK BED,  TOTAL  ENERGY     *
C     * SUPPLY TO SPACE HEATING, TOTAL ENERGY SUPPLY TO  THE     *
C     * SYSTEM, AND ENERGY LOSSES.                               *
C     *                                                          *
C     ************************************************************
C
C
        SUBROUTINE TYPE36 (TIME,XIN,OUT,T,DTDT,PAR,INFO)
        DIMENSION XIN(20),OUT(20),PAR(10),INFO(10)
        COMMON /LUNITS/LUR,LUW,IFORM
        IF(INFO(7).GE.0) GO TO 100
C     FIRST CALL OF SIMULATION
        INFO(6)=9
        INFO(9)=0
        CALL TYPECK(1,INFO,9,6,0)
100     CF=XIN(1)
        CF1=XIN(2)
        CF2=XIN(3)
        TCO=XIN(4)
        TST=XIN(5)
        QLOSS=XIN(6)
        QC=XIN(7)
        QS=XIN(8)
        RAD=XIN(9)
        QAUX=PAR(6)
        RADC=0.
        QDLL=0.
        QOMDL=0.
        QT=0.
        QSTORE=0.
        IF(CF1.EQ.1.0.OR.CF2.EQ.1.0) GO TO 200
        WRITE(LUW,1000) INFO(1),INFO(2)
1000    FORMAT(//2X,24H***** WARNING ***** UNIT,I3,5H TYPE,
       .  I3/4X,39HDETECTED INCORRECT POSITIONS OF DAMPERS)
        RMODE=-5.
        GO TO 300
200     IF(CF1.EQ.1.0.AND.CF2.EQ.1.0) GO TO 1
        IF(CF1.EQ.1.0.AND.CF2.LT.1.0) GO TO 2
        IF(CF.EQ.0.) GO TO 3
C     STORAGE
        RMODE=4.
        RADC=RAD
        QSTORE=QC-QLOSS
        GO TO 300
C     SYSTEM OFF
```

```
3       RMODE=5.
        QAUX=0.
        GO TO 300
2       IF(TST.LT.PAR(1)) GO TO 5
        IF(TST.GT.PAR(2)) GO TO 6
C     HEAT FROM STORAGE (1/2 COIL ON)
        RMODE=2.0
        QAUX=PAR(4)
        GO TO 9
C     HEAT FROM STORAGE (COIL OFF)
6       RMODE=2.1
        GO TO 9
C     ELECTRIC HEATING (FULL COIL ON)
5       RMODE=3.
        QAUX=PAR(5)
9       QT=QS
        GO TO 10
1       IF(TCO.GT.PAR(3)) GO TO 8
C     HEAT FROM COLLECTOR (1/2 COIL ON)
        RMODE=1.
        QAUX=PAR(4)
        GO TO 11
C     HEAT FROM COLLECTOR (COIL OFF)
8       RMODE=1.1
11      QT=QC-QLOSS
        RADC=RAD
10      IF(CF.EQ.0.) WRITE(LUW,2000) INFO(1),INFO(2)
2000    FORMAT(//2X,24H***** WARNING ***** UNIT,I3,5H TYPE,
     .    I3/4X,28HDETECTED INCORRECT FLOW RATE)
300     QH=QAUX+QT
        IF(CF2.LT.1.) QDLL=QLOSS-QC
        IF(CF2.EQ.1.) QOMDL=QLOSS
        IF(CF2.LT.1.) QC=0.
        QSYS=QAUX+QC
        OUT(1)=QC
        OUT(2)=QSTORE
        OUT(3)=QAUX
        OUT(4)=QH
        OUT(5)=QSYS
        OUT(6)=QOMDL
        OUT(7)=QDLL
        OUT(8)=RADC
        OUT(9)=RMODE
        RETURN
        END
```

Appendix C: Recommended System of Units for TRNSYS Simulation

It is recommended to use a modified metric system for TRNSYS simulation of hour by hour dynamic thermal behavior of a solar heating system. The modified metric system is shown in the following table which uses the SI conventions except that the hour (hr) is the standard unit of time instead of the second (s).

DIMENSION	RECOMMENDED UNITS
time	hr
length	m
area	m^2
volume	m^3
mass	kg
temperature	°C
energy	kJ
energy flow	kJ/hr
energy flux	$kJ/m^2 \cdot hr$
mass flow rate	kg/hr
specific heat	$kJ/kg \cdot °C$
heat transfer coefficient	$kJ/hr \cdot m^2 \cdot °C$
thermal conductivity	$kJ/hr \cdot m \cdot °C$
angle	degrees

Appendix D: Sample of Simulation Control Program with Results

A simulation control program with results for the study of the solar heating system performance for the two clear days, February 20th and 21st, 1982 are shown as follows. The recommended unit system was used in the following simulation.

```
          TRNSYS - A TRANSIENT SIMULATION PROGRAM
    FROM THE SOLAR ENERGY LAB AT THE UNIVERSITY OF WISCONSIN
                    VERSION  12.1  11/1/83


 SIMULATION      0.0            4.800E+01     1.000E-01

 TOLERANCES     -1.000E-01     -1.000E-01

 WIDTH     72

 LIMITS    20     4

 UNIT  1      TYPE  9      DATA READER (FORMATTED)
   PARAMETERS  28
   9.000E+00   1.000E+00 -1.000E+00  1.000E+00  0.0
  -2.000E+00   1.000E+00  0.0        -3.000E+00  1.000E+00
   0.0        -4.000E+00  1.000E+00  0.0        -6.000E+00
   3.600E+00   0.0        -7.000E+00  3.600E+00  0.0
  -8.000E+00   3.600E+00  0.0        -9.000E+00  3.600E+00
   0.0         0.0         1.000E+00
    (F3.0,2F2.0,F7.0,5F8.1)
********************  SYSTEM CONTROLLER  ********************

 UNIT 16      TYPE  2      CONTROLLER NO.1
   PARAMETERS    3
   5.000E+00   1.500E+00   0.0
   INPUTS  3
    0, 0        5, 4       16, 1
   2.150E+01   2.200E+01   0.0

 UNIT 21      TYPE  2      CONTROLLER NO.2
   PARAMETERS    3
   5.000E+00   1.000E+01  -1.000E+00
   INPUTS  3
    2, 1        4, 3       21, 1
   2.200E+01   2.200E+01   0.0

 UNIT 23      TYPE  2      CONTROLLER NO.3
   PARAMETERS    3
   5.000E+00   7.000E+00   0.0
   INPUTS  3
    2, 1        0, 0       23, 1
   2.200E+01   2.200E+01   0.0

 UNIT 17      TYPE 15      NOT GATE
   PARAMETERS    1
   1.000E+01
   INPUTS  1
   16, 1
   0.0
```

```
UNIT 18      TYPE 15      DAMPERS CONTROLLER
  PARAMETERS    8
  0.0          0.0          1.200E+01 -4.000E+00   0.0
  0.0          1.200E+01 -4.000E+00
  INPUTS  4
  21, 1        16, 1        17, 1        23, 1
  0.0          0.0          1.000E+00   0.0

UNIT 19      TYPE 15      NOT GATE
  PARAMETERS    1
  1.000E+01
  INPUTS  1
  18, 2
  1.000E+00

UNIT 24      TYPE 15      DAMPER LEAKAGE
  PARAMETERS    5
  0.0          0.0          1.000E+00   0.0          1.200E+01
  INPUTS  3
   0, 0        19, 1        18, 2
  4.000E-02   0.0          1.000E+00

UNIT 20      TYPE 15      FLOW ADJUSTMENT
  PARAMETERS    8
  0.0          0.0          1.000E+00 -4.000E+00   0.0
  0.0          1.100E+01 -4.000E+00
  INPUTS  4
  18, 1         0, 0        19, 1        16, 1
  0.0          5.600E-01   0.0          0.0

UNIT 22      TYPE 15      FAN CONTROLLER
  PARAMETERS    1
  1.200E+01
  INPUTS  2
  20, 1          20, 2
  0.0            0.0
************************************************************

UNIT  6      TYPE 36      SYSTEM ANALYSER
  PARAMETERS    6
  2.400E+01   3.600E+01   3.300E+01   1.350E+04   2.700E+04
  2.272E+03
  INPUTS  9
  22, 1        16, 1        24, 1         2, 1         4, 3
   8, 1         2, 3         4, 6         1, 6
  0.0          0.0          1.000E+00   2.200E+01   2.200E+01
  0.0          0.0          0.0          0.0

UNIT 12      TYPE  3      MAIN FAN
  PARAMETERS    1
  9.455E+02
  INPUTS  3
  11, 1        11, 2        22, 1
```

```
   2.200E+01  0.0          0.0

 UNIT 11      TYPE 11      DAMPER NO.1
   PARAMETERS    1
   3.000E+00
   INPUTS  5
    4, 1         4, 2         5, 4         5, 2         16, 1
   2.200E+01  0.0          2.200E+01  0.0          0.0

 UNIT 13      TYPE 11      DAMPER NO.2
   PARAMETERS    1
   2.000E+00
   INPUTS  3
   12, 1        12, 2        24, 1
   2.200E+01  0.0          1.000E+00
************  COMPONENTS OUTSIDE THE MODULE  ************

 UNIT  7      TYPE 31      DUCT TO COLLECTOR
   PARAMETERS    6
   2.540E-01  2.670E+00  5.300E+00  1.206E+00  1.006E+00
   2.200E+01
   INPUTS  3
   13, 3        13, 4         1, 5
   2.200E+01  0.0         -2.300E+00

 UNIT  2      TYPE  1      AIR COLLECTOR
   PARAMETERS   11
   1.000E+00  1.000E+00  1.110E+01  1.006E+00  1.000E+00
   4.770E+01  5.600E-01  9.382E+00 -1.000E+00  1.006E+00
   0.0
   INPUTS  5
    7, 1         7, 2         7, 2         1, 5         1, 6
   2.200E+01  0.0          0.0         -2.300E+00  0.0

 UNIT  3      TYPE 31      DUCT FROM COLLECTOR
   PARAMETERS    6
   2.540E-01  2.670E+00  5.300E+00  1.206E+00  1.006E+00
   2.200E+01
   INPUTS  3
    2, 1         2, 2         1, 5
   2.200E+01  0.0         -2.300E+00

 UNIT  8      TYPE 15      ADDER
   PARAMETERS    1
   3.000E+00
   INPUTS  2
    3, 4         7, 4
   0.0          0.0
**************************************************************

 UNIT 14      TYPE 11      DAMPER NO.3
   PARAMETERS    1
   2.000E+00
   INPUTS  3
```

```
   3, 1        3, 2        16, 1
  2.200E+01   0.0          0.0

UNIT 15      TYPE 11       DAMPER NO.4
  PARAMETERS    1
  3.000E+00
  INPUTS  5
   4, 3        4, 4        14, 3        14, 4        24, 1
  2.200E+01   0.0          2.200E+01   0.0          1.000E+00

UNIT  4      TYPE 10       ROCK BED
  PARAMETERS    8
  1.006E+00   1.041E+00   1.880E+00   5.486E+00   8.800E-01
  1.527E+03   1.590E+00   4.500E-01
  INPUTS  5
  14, 1       14, 2       13, 1       13, 2        5, 4
  2.200E+01   0.0         2.200E+01   0.0         2.200E+01
  DERIVATIVES  5
  2.200E+01   2.200E+01   2.200E+01   2.200E+01   2.200E+01

UNIT  5      TYPE 12       LOAD
  PARAMETERS    6
  4.000E+00   5.000E+02   1.100E+04   2.200E+01   1.006E+00
  0.0
  INPUTS  6
  15, 1       15, 2        1, 5        0, 0        6, 4
   0, 0
  2.200E+01   0.0         -2.300E+00   0.0         0.0
  0.0
********************  OUTPUT DEVICES  ********************

UNIT 31      TYPE 24       QUANTITY INTEGRATOR
  INPUTS  2
   1, 6        6, 8
  0.0         0.0

UNIT 30      TYPE 25       PRINTER NO.4
  PARAMETERS    1
  1.000E+00
  INPUTS  6
   1, 3        1, 1        1, 2        1, 4        31, 1
  31, 2
  YEAR        MONTH       DATE        HOUR        IT
  ITC

UNIT 28      TYPE 25       PRINTER NO.1
  PARAMETERS    1
  1.000E+00
  INPUTS  10
   6, 9        1, 6        1, 5        5, 4        2, 1
   7, 1        4, 3        4, 1       13, 4       13, 2
  MODE        It          Ta          Tr          Tco
  Tci         Tst         Tsb         mc          mb
```

```
UNIT 29     TYPE 25     PRINTER NO.2
  PARAMETERS   1
  1.000E+00
  INPUTS 10
   2, 3        8, 1        6, 2        4, 5        4, 6
   4, 7        6, 3        6, 4        6, 5        5, 3
  Qu          Qloss       Qstore      DU          Qs
  Qe          Qaux        Qh          Qsys        Ql

UNIT 26     TYPE 24     QUANTITY INTEGRATOR
  INPUTS 10
   6, 1        6, 6        6, 2        4, 6        6, 7
   4, 7        6, 3        6, 4        6, 5        5, 3
  0.0         0.0         0.0         0.0         0.0
  0.0         0.0         0.0         0.0         0.0

UNIT 27     TYPE 25     PRINTER NO.3
* PRINT AT BEGINNING AND END OF SIMULATION
  INPUTS 10
  26, 1       26, 2       26, 3       26, 4       26, 5
  26, 6       26, 7       26, 8       26, 9       26,10
  QC          QOMDL       QSTORE      QS          QDLL
  QE          QAUX        QH          QSYS        QL

UNIT 25     TYPE 26     PLOTTER
  PARAMETERS   4
  1.000E+00  0.0         4.800E+01   6.000E+01
  INPUTS  5
   2, 1        7, 1        4, 3        4, 1        1, 5
  Tco         Tci         Tst         Tsb         Ta
*****************************************************************

END


TRANSIENT SIMULATION     STARTING AT TIME =  0.0
                         STOPPING AT TIME =  4.800E+01
                                TIMESTEP =  1/10
   DIFFERENTIAL EQUATION ERROR TOLERANCE = -1.000E-01
         ALGEBRAIC CONVERGENCE TOLERANCE = -1.000E-01
```

TIME = 0.0

YEAR	MONTH	DATE	HOUR	IT
8.200E+01	2.000E+00	2.000E+01	0.0	0.0
ITC	MODE	It	Ta	Tr
0.0	5.000E+00	0.0	-2.210E+00	2.200E+01
Tco	Tci	Tst	Tsb	mc
-2.210E+00	2.200E+01	2.200E+01	2.200E+01	0.0
mb	Qu	Qloss	Qstore	DU
0.0	0.0	0.0	0.0	0.0
Qs	Qe	Qaux	Qh	Qsys
0.0	0.0	0.0	0.0	0.0
Ql	QC	QOMDL	QSTORE	QS
1.210E+04	0.0	0.0	0.0	0.0
QDLL	QE	QAUX	QH	QSYS
0.0	0.0	0.0	0.0	0.0
QL				
0.0				

TIME = 1.0000

YEAR	MONTH	DATE	HOUR	IT
8.200E+01	2.000E+00	2.000E+01	1.000E+00	0.0
ITC	MODE	It	Ta	Tr
0.0	5.000E+00	0.0	-4.010E+00	2.094E+01
Tco	Tci	Tst	Tsb	mc
-4.010E+00	-3.984E+00	2.200E+01	2.200E+01	0.0
mb	Qu	Qloss	Qstore	DU
0.0	0.0	0.0	0.0	-5.255E+00
Qs	Qe	Qaux	Qh	Qsys
0.0	9.643E+00	0.0	0.0	0.0
Ql				
1.247E+04				

TIME = 2.0000

YEAR	MONTH	DATE	HOUR	IT
8.200E+01	2.000E+00	2.000E+01	2.000E+00	0.0
ITC	MODE	It	Ta	Tr
0.0	3.000E+00	0.0	-5.145E+00	2.019E+01
Tco	Tci	Tst	Tsb	mc
-4.256E+00	1.357E+01	2.199E+01	2.155E+01	3.782E+01
mb	Qu	Qloss	Qstore	DU
9.077E+02	-6.780E+02	2.546E+02	0.0	-3.771E+02
Qs	Qe	Qaux	Qh	Qsys
1.785E+03	1.541E+01	2.700E+04	2.878E+04	2.700E+04
Ql				
1.267E+04				

TIME = 3.0000

YEAR	MONTH	DATE	HOUR	IT
8.200E+01	2.000E+00	2.000E+01	3.000E+00	0.0
ITC	MODE	It	Ta	Tr
0.0	5.000E+00	0.0	-6.150E+00	2.141E+01
Tco	Tci	Tst	Tsb	mc
-6.150E+00	-2.700E+00	2.191E+01	2.111E+01	0.0

mb	Qu	Qloss	Qstore	DU
0.0	0.0	0.0	0.0	-1.275E+03
Qs	Qe	Qaux	Qh	Qsys
0.0	9.741E-01	0.0	0.0	0.0
Ql				
1.378E+04				

TIME = 4.0000

YEAR	MONTH	DATE	HOUR	IT
8.200E+01	2.000E+00	2.000E+01	4.000E+00	0.0
ITC	MODE	It	Ta	Tr
0.0	5.000E+00	0.0	-6.485E+00	2.017E+01
Tco	Tci	Tst	Tsb	mc
-6.455E+00	-6.481E+00	2.191E+01	2.111E+01	0.0
mb	Qu	Qloss	Qstore	DU
0.0	0.0	0.0	0.0	-1.282E+03
Qs	Qe	Qaux	Qh	Qsys
0.0	1.215E+01	0.0	0.0	0.0
Ql				
1.333E+04				

TIME = 5.0000

YEAR	MONTH	DATE	HOUR	IT
8.200E+01	2.000E+00	2.000E+01	5.000E+00	0.0
ITC	MODE	It	Ta	Tr
0.0	3.000E+00	0.0	-6.690E+00	2.112E+01
Tco	Tci	Tst	Tsb	mc
-5.693E+00	1.397E+01	2.162E+01	2.080E+01	3.782E+01
mb	Qu	Qloss	Qstore	DU
9.077E+02	-7.446E+02	2.815E+02	0.0	-2.247E+03
Qs	Qe	Qaux	Qh	Qsys
4.571E+02	3.488E-01	2.700E+04	2.746E+04	2.700E+04
Ql				
1.390E+04				

TIME = 6.0000

YEAR	MONTH	DATE	HOUR	IT
8.200E+01	2.000E+00	2.000E+01	6.000E+00	0.0
ITC	MODE	It	Ta	Tr
0.0	5.000E+00	0.0	-6.890E+00	2.071E+01
Tco	Tci	Tst	Tsb	mc
-6.890E+00	-6.887E+00	2.147E+01	2.105E+01	0.0
mb	Qu	Qloss	Qstore	DU
0.0	0.0	0.0	0.0	-2.294E+03
Qs	Qe	Qaux	Qh	Qsys
0.0	3.804E+00	0.0	0.0	0.0
Ql				
1.380E+04				

TIME = 7.0000

YEAR	MONTH	DATE	HOUR	IT
8.200E+01	2.000E+00	2.000E+01	7.000E+00	0.0
ITC	MODE	It	Ta	Tr
0.0	3.000E+00	0.0	-5.285E+00	2.065E+01

Tco	Tci	Tst	Tsb	mc
-4.374E+00	1.398E+01	2.129E+01	2.069E+01	3.782E+01
mb	Qu	Qloss	Qstore	DU
9.077E+02	-6.946E+02	2.627E+02	0.0	-2.751E+03
Qs	Qe	Qaux	Qh	Qsys
5.831E+02	2.875E+00	2.700E+04	2.758E+04	2.700E+04
Ql				
1.297E+04				

TIME = 8.0000

YEAR	MONTH	DATE	HOUR	IT
8.200E+01	2.000E+00	2.000E+01	8.000E+00	7.200E+01
ITC	MODE	It	Ta	Tr
0.0	5.000E+00	7.200E+01	-3.965E+00	2.108E+01
Tco	Tci	Tst	Tsb	mc
3.326E-01	-3.984E+00	2.109E+01	2.100E+01	0.0
mb	Qu	Qloss	Qstore	DU
0.0	0.0	0.0	0.0	-2.788E+03
Qs	Qe	Qaux	Qh	Qsys
0.0	-1.258E+00	0.0	0.0	0.0
Ql				
1.252E+04				

TIME = 9.0000

YEAR	MONTH	DATE	HOUR	IT
8.200E+01	2.000E+00	2.000E+01	9.000E+00	6.336E+02
ITC	MODE	It	Ta	Tr
1.685E+02	4.000E+00	5.616E+02	-1.810E+00	2.006E+01
Tco	Tci	Tst	Tsb	mc
2.270E+01	2.051E+01	2.130E+01	2.096E+01	5.295E+02
mb	Qu	Qloss	Qstore	DU
0.0	1.167E+03	5.287E+02	6.380E+02	-2.616E+03
Qs	Qe	Qaux	Qh	Qsys
0.0	8.442E+00	2.272E+03	2.272E+03	3.439E+03
Ql				
1.094E+04				

TIME = 10.0000

YEAR	MONTH	DATE	HOUR	IT
8.200E+01	2.000E+00	2.000E+01	1.000E+01	2.520E+03
ITC	MODE	It	Ta	Tr
2.055E+03	1.100E+00	1.886E+03	-4.650E-01	2.000E+01
Tco	Tci	Tst	Tsb	mc
3.763E+01	1.952E+01	2.286E+01	2.094E+01	5.295E+02
mb	Qu	Qloss	Qstore	DU
0.0	9.645E+03	6.538E+02	0.0	-1.757E+03
Qs	Qe	Qaux	Qh	Qsys
0.0	1.209E+01	2.272E+03	1.126E+04	1.192E+04
Ql				
1.023E+04				

TIME = 11.0000

YEAR	MONTH	DATE	HOUR	IT
8.200E+01	2.000E+00	2.000E+01	1.100E+01	5.479E+03

ITC	MODE	It	Ta	Tr
5.014E+03	1.100E+00	2.959E+03	-3.050E-01	2.065E+01
Tco	Tci	Tst	Tsb	mc
5.074E+01	2.021E+01	2.284E+01	2.093E+01	5.295E+02
mb	Qu	Qloss	Qstore	DU
0.0	1.626E+04	8.048E+02	0.0	-1.766E+03
Qs	Qe	Qaux	Qh	Qsys
0.0	6.193E+00	2.272E+03	1.773E+04	1.853E+04
Ql				
1.048E+04				

TIME = 12.0000

YEAR	MONTH	DATE	HOUR	IT
8.200E+01	2.000E+00	2.000E+01	1.200E+01	8.845E+03
ITC	MODE	It	Ta	Tr
8.380E+03	1.100E+00	3.366E+03	5.550E-01	2.152E+01
Tco	Tci	Tst	Tsb	mc
5.636E+01	2.108E+01	2.282E+01	2.093E+01	5.295E+02
mb	Qu	Qloss	Qstore	DU
0.0	1.879E+04	8.583E+02	0.0	-1.768E+03
Qs	Qe	Qaux	Qh	Qsys
0.0	-1.734E+00	2.272E+03	2.020E+04	2.106E+04
Ql				
1.048E+04				

TIME = 13.0000

YEAR	MONTH	DATE	HOUR	IT
8.200E+01	2.000E+00	2.000E+01	1.300E+01	1.262E+04
ITC	MODE	It	Ta	Tr
1.215E+04	4.000E+00	3.773E+03	2.500E+00	2.091E+01
Tco	Tci	Tst	Tsb	mc
6.105E+01	2.054E+01	4.545E+01	2.106E+01	5.295E+02
mb	Qu	Qloss	Qstore	DU
0.0	2.157E+04	8.603E+02	2.071E+04	1.877E+04
Qs	Qe	Qaux	Qh	Qsys
0.0	7.124E+01	2.272E+03	2.272E+03	2.384E+04
Ql				
9.205E+03				

TIME = 14.0000

YEAR	MONTH	DATE	HOUR	IT
8.200E+01	2.000E+00	2.000E+01	1.400E+01	1.615E+04
ITC	MODE	It	Ta	Tr
1.568E+04	4.000E+00	3.528E+03	4.025E+00	2.033E+01
Tco	Tci	Tst	Tsb	mc
6.021E+01	2.267E+01	5.340E+01	2.307E+01	5.295E+02
mb	Qu	Qloss	Qstore	DU
0.0	1.999E+04	8.416E+02	1.915E+04	3.786E+04
Qs	Qe	Qaux	Qh	Qsys
0.0	1.427E+02	2.272E+03	2.272E+03	2.226E+04
Ql				
8.151E+03				

TIME = 15.0000

YEAR	MONTH	DATE	HOUR	IT
8.200E+01	2.000E+00	2.000E+01	1.500E+01	1.922E+04
ITC	MODE	It	Ta	Tr
1.876E+04	1.100E+00	3.074E+03	3.625E+00	2.018E+01
Tco	Tci	Tst	Tsb	mc
5.247E+01	1.973E+01	5.439E+01	2.669E+01	5.295E+02
mb	Qu	Qloss	Qstore	DU
0.0	1.743E+04	7.297E+02	0.0	4.899E+04
Qs	Qe	Qaux	Qh	Qsys
0.0	1.858E+02	2.272E+03	1.898E+04	1.970E+04
Ql				
8.275E+03				

TIME = 16.0000

YEAR	MONTH	DATE	HOUR	IT
8.200E+01	2.000E+00	2.000E+01	1.600E+01	2.163E+04
ITC	MODE	It	Ta	Tr
2.116E+04	1.100E+00	2.405E+03	3.030E+00	2.076E+01
Tco	Tci	Tst	Tsb	mc
4.507E+01	2.039E+01	5.423E+01	2.671E+01	5.295E+02
mb	Qu	Qloss	Qstore	DU
0.0	1.314E+04	6.670E+02	0.0	4.881E+04
Qs	Qe	Qaux	Qh	Qsys
0.0	1.799E+02	2.272E+03	1.475E+04	1.541E+04
Ql				
8.866E+03				

TIME = 17.0000

YEAR	MONTH	DATE	HOUR	IT
8.200E+01	2.000E+00	2.000E+01	1.700E+01	2.294E+04
ITC	MODE	It	Ta	Tr
2.248E+04	4.000E+00	1.318E+03	1.575E+00	2.155E+01
Tco	Tci	Tst	Tsb	mc
3.699E+01	2.648E+01	5.320E+01	2.703E+01	5.295E+02
mb	Qu	Qloss	Qstore	DU
0.0	5.596E+03	6.961E+02	4.900E+03	4.913E+04
Qs	Qe	Qaux	Qh	Qsys
0.0	1.729E+02	2.272E+03	2.272E+03	7.868E+03
Ql				
9.990E+03				

TIME = 18.0000

YEAR	MONTH	DATE	HOUR	IT
8.200E+01	2.000E+00	2.000E+01	1.800E+01	2.323E+04
ITC	MODE	It	Ta	Tr
2.248E+04	5.000E+00	2.916E+02	-6.850E-01	2.063E+01
Tco	Tci	Tst	Tsb	mc
1.672E+01	-6.516E-01	5.223E+01	2.735E+01	0.0
mb	Qu	Qloss	Qstore	DU
0.0	0.0	0.0	0.0	4.895E+04
Qs	Qe	Qaux	Qh	Qsys
0.0	1.816E+02	0.0	0.0	0.0
Ql				
1.066E+04				

TIME = 19.0000

YEAR	MONTH	DATE	HOUR	IT
8.200E+01	2.000E+00	2.000E+01	1.900E+01	2.323E+04
ITC	MODE	It	Ta	Tr
2.248E+04	2.100E+00	0.0	-2.795E+00	2.058E+01
Tco	Tci	Tst	Tsb	mc
-1.969E+00	1.458E+01	4.945E+01	2.417E+01	3.782E+01
mb	Qu	Qloss	Qstore	DU
9.077E+02	-6.294E+02	2.363E+02	0.0	3.769E+04
Qs	Qe	Qaux	Qh	Qsys
2.635E+04	1.475E+02	2.272E+03	2.862E+04	2.272E+03
Ql				
1.169E+04				

TIME = 20.0000

YEAR	MONTH	DATE	HOUR	IT
8.200E+01	2.000E+00	2.000E+01	2.000E+01	2.323E+04
ITC	MODE	It	Ta	Tr
2.248E+04	5.000E+00	0.0	-4.800E+00	2.149E+01
Tco	Tci	Tst	Tsb	mc
-4.800E+00	-1.503E+00	3.927E+01	2.182E+01	0.0
mb	Qu	Qloss	Qstore	DU
0.0	0.0	0.0	0.0	1.866E+04
Qs	Qe	Qaux	Qh	Qsys
0.0	6.911E+01	0.0	0.0	0.0
Ql				
1.314E+04				

TIME = 21.0000

YEAR	MONTH	DATE	HOUR	IT
8.200E+01	2.000E+00	2.000E+01	2.100E+01	2.323E+04
ITC	MODE	It	Ta	Tr
2.248E+04	5.000E+00	0.0	-4.045E+00	2.033E+01
Tco	Tci	Tst	Tsb	mc
-4.135E+00	-4.058E+00	3.916E+01	2.183E+01	0.0
mb	Qu	Qloss	Qstore	DU
0.0	0.0	0.0	0.0	1.858E+04
Qs	Qe	Qaux	Qh	Qsys
0.0	7.933E+01	0.0	0.0	0.0
Ql				
1.219E+04				

TIME = 22.0000

YEAR	MONTH	DATE	HOUR	IT
8.200E+01	2.000E+00	2.000E+01	2.200E+01	2.323E+04
ITC	MODE	It	Ta	Tr
2.248E+04	2.000E+00	0.0	-4.285E+00	2.056E+01
Tco	Tci	Tst	Tsb	mc
-3.408E+00	1.418E+01	3.279E+01	2.076E+01	3.782E+01
mb	Qu	Qloss	Qstore	DU
9.077E+02	-6.690E+02	2.520E+02	0.0	8.665E+03
Qs	Qe	Qaux	Qh	Qsys
1.116E+04	4.485E+01	1.350E+04	2.466E+04	1.350E+04

Ql
1.242E+04

TIME = 23.0000

YEAR	MONTH	DATE	HOUR	IT
8.200E+01	2.000E+00	2.000E+01	2.300E+01	2.323E+04
ITC	MODE	It	Ta	Tr
2.248E+04	2.000E+00	0.0	-3.635E+00	2.133E+01
Tco	Tci	Tst	Tsb	mc
-2.823E+00	1.488E+01	2.612E+01	2.102E+01	3.782E+01
mb	Qu	Qloss	Qstore	DU
9.077E+02	-6.726E+02	2.515E+02	0.0	1.518E+03
Qs	Qe	Qaux	Qh	Qsys
4.414E+03	1.202E+01	1.350E+04	1.791E+04	1.350E+04
Ql				
1.248E+04				

TIME = 24.0000

YEAR	MONTH	DATE	HOUR	IT
8.200E+01	2.000E+00	2.100E+01	0.0	2.323E+04
ITC	MODE	It	Ta	Tr
2.248E+04	5.000E+00	0.0	-3.030E+00	2.091E+01
Tco	Tci	Tst	Tsb	mc
-3.030E+00	-3.039E+00	2.428E+01	2.120E+01	0.0
mb	Qu	Qloss	Qstore	DU
0.0	0.0	0.0	0.0	1.576E+02
Qs	Qe	Qaux	Qh	Qsys
0.0	1.046E+01	0.0	0.0	0.0
Ql				
1.197E+04				

TIME = 25.0000

YEAR	MONTH	DATE	HOUR	IT
8.200E+01	2.000E+00	2.100E+01	1.000E+00	2.323E+04
ITC	MODE	It	Ta	Tr
2.248E+04	3.000E+00	0.0	-3.855E+00	2.012E+01
Tco	Tci	Tst	Tsb	mc
-3.013E+00	1.387E+01	2.379E+01	2.092E+01	3.782E+01
mb	Qu	Qloss	Qstore	DU
9.077E+02	-6.421E+02	2.411E+02	0.0	-5.776E+02
Qs	Qe	Qaux	Qh	Qsys
3.460E+03	1.619E+01	2.700E+04	3.046E+04	2.700E+04
Ql				
1.199E+04				

TIME = 26.0000

YEAR	MONTH	DATE	HOUR	IT
8.200E+01	2.000E+00	2.100E+01	2.000E+00	2.323E+04
ITC	MODE	It	Ta	Tr
2.248E+04	5.000E+00	0.0	-4.280E+00	2.147E+01
Tco	Tci	Tst	Tsb	mc
-4.280E+00	-1.059E+00	2.196E+01	2.101E+01	0.0
mb	Qu	Qloss	Qstore	DU
0.0	0.0	0.0	0.0	-2.055E+03

Qs	Qe	Qaux	Qh	Qsys
0.0	-2.267E+00	0.0	0.0	0.0

Ql
1.287E+04

TIME = 27.0000

YEAR	MONTH	DATE	HOUR	IT
8.200E+01	2.000E+00	2.100E+01	3.000E+00	2.323E+04
ITC	MODE	It	Ta	Tr
2.248E+04	5.000E+00	0.0	-4.395E+00	2.032E+01
Tco	Tci	Tst	Tsb	mc
-4.305E+00	-4.394E+00	2.195E+01	2.101E+01	0.0
mb	Qu	Qloss	Qstore	DU
0.0	0.0	0.0	0.0	-2.058E+03
Qs	Qe	Qaux	Qh	Qsys
0.0	8.140E+00	0.0	0.0	0.0

Ql
1.236E+04

TIME = 28.0000

YEAR	MONTH	DATE	HOUR	IT
8.200E+01	2.000E+00	2.100E+01	4.000E+00	2.323E+04
ITC	MODE	It	Ta	Tr
2.248E+04	3.000E+00	0.0	-4.970E+00	2.108E+01
Tco	Tci	Tst	Tsb	mc
-3.997E+00	1.439E+01	2.133E+01	2.077E+01	3.782E+01
mb	Qu	Qloss	Qstore	DU
9.077E+02	-6.961E+02	2.641E+02	0.0	-2.775E+03
Qs	Qe	Qaux	Qh	Qsys
2.238E+02	-1.220E+00	2.700E+04	2.722E+04	2.700E+04

Ql
1.303E+04

TIME = 29.0000

YEAR	MONTH	DATE	HOUR	IT
8.200E+01	2.000E+00	2.100E+01	5.000E+00	2.323E+04
ITC	MODE	It	Ta	Tr
2.248E+04	5.000E+00	0.0	-4.810E+00	2.075E+01
Tco	Tci	Tst	Tsb	mc
-4.810E+00	-4.813E+00	2.116E+01	2.102E+01	0.0
mb	Qu	Qloss	Qstore	DU
0.0	0.0	0.0	0.0	-2.743E+03
Qs	Qe	Qaux	Qh	Qsys
0.0	1.846E+00	0.0	0.0	0.0

Ql
1.278E+04

TIME = 30.0000

YEAR	MONTH	DATE	HOUR	IT
8.200E+01	2.000E+00	2.100E+01	6.000E+00	2.323E+04
ITC	MODE	It	Ta	Tr
2.248E+04	3.000E+00	0.0	-4.705E+00	2.050E+01
Tco	Tci	Tst	Tsb	mc
-3.815E+00	1.402E+01	2.104E+01	2.068E+01	3.782E+01

mb	Qu	Qloss	Qstore	DU
9.077E+02	-6.783E+02	2.550E+02	0.0	-3.041E+03
Qs	Qe	Qaux	Qh	Qsys
4.974E+02	3.233E+00	2.700E+04	2.750E+04	2.700E+04
Ql				
1.260E+04				

TIME = 31.0000

YEAR	MONTH	DATE	HOUR	IT
8.200E+01	2.000E+00	2.100E+01	7.000E+00	2.323E+04
ITC	MODE	It	Ta	Tr
2.248E+04	5.000E+00	0.0	-4.700E+00	2.116E+01
Tco	Tci	Tst	Tsb	mc
-4.700E+00	-4.700E+00	2.090E+01	2.098E+01	0.0
mb	Qu	Qloss	Qstore	DU
0.0	0.0	0.0	0.0	-2.999E+03
Qs	Qe	Qaux	Qh	Qsys
0.0	-2.771E+00	0.0	0.0	0.0
Ql				
1.293E+04				

TIME = 32.0000

YEAR	MONTH	DATE	HOUR	IT
8.200E+01	2.000E+00	2.100E+01	8.000E+00	2.324E+04
ITC	MODE	It	Ta	Tr
2.248E+04	5.000E+00	7.200E+00	-4.605E+00	2.002E+01
Tco	Tci	Tst	Tsb	mc
-4.265E+00	-4.606E+00	2.090E+01	2.097E+01	0.0
mb	Qu	Qloss	Qstore	DU
0.0	0.0	0.0	0.0	-3.002E+03
Qs	Qe	Qaux	Qh	Qsys
0.0	7.641E+00	0.0	0.0	0.0
Ql				
1.231E+04				

TIME = 33.0000

YEAR	MONTH	DATE	HOUR	IT
8.200E+01	2.000E+00	2.100E+01	9.000E+00	2.341E+04
ITC	MODE	It	Ta	Tr
2.248E+04	3.000E+00	1.728E+02	-4.315E+00	2.123E+01
Tco	Tci	Tst	Tsb	mc
6.411E+00	1.466E+01	2.082E+01	2.081E+01	3.782E+01
mb	Qu	Qloss	Qstore	DU
9.077E+02	-3.139E+02	3.543E+02	0.0	-3.197E+03
Qs	Qe	Qaux	Qh	Qsys
-3.754E+02	-4.114E+00	2.700E+04	2.662E+04	2.700E+04
Ql				
1.277E+04				

TIME = 34.0000

YEAR	MONTH	DATE	HOUR	IT
8.200E+01	2.000E+00	2.100E+01	1.000E+01	2.570E+04
ITC	MODE	It	Ta	Tr
2.477E+04	1.100E+00	2.290E+03	-4.965E+00	2.130E+01

Tco	Tci	Tst	Tsb	mc
4.251E+01	2.080E+01	2.082E+01	2.085E+01	5.295E+02
mb	Qu	Qloss	Qstore	DU
0.0	1.156E+04	8.245E+02	0.0	-3.192E+03
Qs	Qe	Qaux	Qh	Qsys
0.0	-4.654E+00	2.272E+03	1.300E+04	1.383E+04
Ql				
1.313E+04				

TIME = 35.0000

YEAR	MONTH	DATE	HOUR	IT
8.200E+01	2.000E+00	2.100E+01	1.100E+01	2.897E+04
ITC	MODE	It	Ta	Tr
2.804E+04	4.000E+00	3.269E+03	-5.380E+00	2.110E+01
Tco	Tci	Tst	Tsb	mc
5.344E+01	2.029E+01	3.229E+01	2.081E+01	5.295E+02
mb	Qu	Qloss	Qstore	DU
0.0	1.765E+04	9.502E+02	1.670E+04	5.168E+03
Qs	Qe	Qaux	Qh	Qsys
0.0	2.315E+01	2.272E+03	2.272E+03	1.992E+04
Ql				
1.324E+04				

TIME = 36.0000

YEAR	MONTH	DATE	HOUR	IT
8.200E+01	2.000E+00	2.100E+01	1.200E+01	3.288E+04
ITC	MODE	It	Ta	Tr
-3.195E+04	4.000E+00	3.910E+03	-4.925E+00	2.014E+01
Tco	Tci	Tst	Tsb	mc
6.141E+01	2.080E+01	4.946E+01	2.135E+01	5.295E+02
mb	Qu	Qloss	Qstore	DU
0.0	2.162E+04	1.035E+03	2.059E+04	2.568E+04
Qs	Qe	Qaux	Qh	Qsys
0.0	1.021E+02	2.272E+03	2.272E+03	2.389E+04
Ql				
1.253E+04				

TIME = 37.0000

YEAR	MONTH	DATE	HOUR	IT
8.200E+01	2.000E+00	2.100E+01	1.300E+01	3.683E+04
ITC	MODE	It	Ta	Tr
3.590E+04	1.100E+00	3.953E+03	-3.950E+00	2.066E+01
Tco	Tci	Tst	Tsb	mc
6.149E+01	2.014E+01	5.176E+01	2.183E+01	5.295E+02
mb	Qu	Qloss	Qstore	DU
0.0	2.207E+04	1.007E+03	0.0	2.973E+04
Qs	Qe	Qaux	Qh	Qsys
0.0	1.149E+02	2.272E+03	2.334E+04	2.434E+04
Ql				
1.230E+04				

TIME = 38.0000

YEAR	MONTH	DATE	HOUR	IT
8.200E+01	2.000E+00	2.100E+01	1.400E+01	4.040E+04

ITC	MODE	It	Ta	Tr
3.946E+04	1.100E+00	3.564E+03	-3.805E+00	2.144E+01
Tco	Tci	Tst	Tsb	mc
5.762E+01	2.084E+01	5.156E+01	2.185E+01	5.295E+02
mb	Qu	Qloss	Qstore	DU
0.0	1.959E+04	9.676E+02	0.0	2.962E+04
Qs	Qe	Qaux	Qh	Qsys
0.0	1.074E+02	2.272E+0	2.089E+04	2.186E+04
Ql				
1.262E+04				

TIME = 39.0000

YEAR	MONTH	DATE	HOUR	IT
8.200E+01	2.000E+00	2.100E+01	1.500E+01	4.367E+04
ITC	MODE	It	Ta	Tr
4.273E+04	4.000E+00	3.269E+03	-3.705E+00	2.075E+01
Tco	Tci	Tst	Tsb	mc
5.708E+01	2.442E+01	5.320E+01	2.502E+01	5.295E+02
mb	Qu	Qloss	Qstore	DU
0.0	1.739E+04	1.002E+03	1.639E+04	4.442E+04
Qs	Qe	Qaux	Qh	Qsys
0.0	1.620E+02	2.272E+03	2.272E+03	1.966E+04
Ql				
1.223E+04				

TIME = 40.0000

YEAR	MONTH	DATE	HOUR	IT
8.200E+01	2.000E+00	2.100E+01	1.600E+01	4.625E+04
ITC	MODE	It	Ta	Tr
4.428E+04	1.100E+00	2.585E+03	-3.890E+00	2.007E+01
Tco	Tci	Tst	Tsb	mc
4.515E+01	1.957E+01	5.196E+01	2.697E+01	5.295E+02
mb	Qu	Qloss	Qstore	DU
0.0	1.362E+04	8.161E+02	0.0	4.783E+04
Qs	Qe	Qaux	Qh	Qsys
0.0	1.828E+02	2.272E+03	1.508E+04	1.590E+04
Ql				
1.198E+04				

TIME = 41.0000

YEAR	MONTH	DATE	HOUR	IT
8.200E+01	2.000E+00	2.100E+01	1.700E+01	4.776E+04
ITC	MODE	It	Ta	Tr
4.579E+04	1.000E+00	1.505E+03	-5.135E+00	2.070E+01
Tco	Tci	Tst	Tsb	mc
3.278E+01	2.016E+01	5.183E+01	2.699E+01	5.295E+02
mb	Qu	Qloss	Qstore	DU
0.0	6.720E+03	7.114E+02	0.0	4.765E+04
Qs	Qe	Qaux	Qh	Qsys
0.0	1.764E+02	1.350E+04	1.951E+04	2.022E+04
Ql				
1.292E+04				

TIME = 42.0000

YEAR	MONTH	DATE	HOUR	IT
8.200E+01	2.000E+00	2.100E+01	1.800E+01	4.811E+04
ITC	MODE	It	Ta	Tr
4.579E+04	5.000E+00	3.564E+02	-8.240E+00	2.105E+01
Tco	Tci	Tst	Tsb	mc
1.303E+01	-8.193E+00	4.646E+01	2.328E+01	0.0
mb	Qu	Qloss	Qstore	DU
0.0	0.0	0.0	0.0	3.207E+04
Qs	Qe	Qaux	Qh	Qsys
0.0	1.194E+02	0.0	0.0	0.0
Ql				
1.465E+04				

TIME = 43.0000

YEAR	MONTH	DATE	HOUR	IT
8.200E+01	2.000E+00	2.100E+01	1.900E+01	4.811E+04
ITC	MODE	It	Ta	Tr
4.579E+04	2.100E+00	0.0	-1.125E+01	2.025E+01
Tco	Tci	Tst	Tsb	mc
-1.014E+01	1.216E+01	4.366E+01	2.218E+01	3.782E+01
mb	Qu	Qloss	Qstore	DU
9.077E+02	-8.480E+02	3.184E+02	0.0	2.521E+04
Qs	Qe	Qaux	Qh	Qsys
2.136E+04	1.066E+02	2.272E+03	2.363E+04	2.272E+03
Ql				
1.575E+04				

TIME = 44.0000

YEAR	MONTH	DATE	HOUR	IT
8.200E+01	2.000E+00	2.100E+01	2.000E+01	4.811E+04
ITC	MODE	It	Ta	Tr
4.579E+04	2.000E+00	0.0	-1.263E+01	2.072E+01
Tco	Tci	Tst	Tsb	mc
-1.146E+01	1.210E+01	3.339E+01	2.080E+01	3.782E+01
mb	Qu	Qloss	Qstore	DU
9.077E+02	-8.960E+02	3.364E+02	0.0	9.280E+03
Qs	Qe	Qaux	Qh	Qsys
1.163E+04	4.559E+01	1.350E+04	2.513E+04	1.350E+04
Ql				
1.668E+04				

TIME = 45.0000

YEAR	MONTH	DATE	HOUR	IT
8.200E+01	2.000E+00	2.100E+01	2.100E+01	4.811E+04
ITC	MODE	It	Ta	Tr
4.579E+04	2.000E+00	0.0	-1.355E+01	2.112E+01
Tco	Tci	Tst	Tsb	mc
-1.225E+01	1.215E+01	2.640E+01	2.095E+01	3.782E+01
mb	Qu	Qloss	Qstore	DU
9.077E+02	-9.290E+02	3.507E+02	0.0	1.707E+03
Qs	Qe	Qaux	Qh	Qsys
-4.892E+03	1.472E+01	1.350E+04	1.839E+04	1.350E+04
Ql				
1.734E+04				

TIME = 46.0000

YEAR	MONTH	DATE	HOUR	IT
8.200E+01	2.000E+00	2.100E+01	2.200E+01	4.811E+04
ITC	MODE	It	Ta	Tr
4.579E+04	3.000E+00	0.0	-1.531E+01	2.155E+01
Tco	Tci	Tst	Tsb	mc
-1.401E+01	1.201E+01	2.293E+01	2.117E+01	3.782E+01
mb	Qu	Qloss	Qstore	DU
9.077E+02	-9.899E+02	3.716E+02	0.0	-1.111E+03
Qs	Qe	Qaux	Qh	Qsys
1.340E+03	4.812E-01	2.700E+04	2.834E+04	2.700E+04
Ql				
1.843E+04				

TIME = 47.0000

YEAR	MONTH	DATE	HOUR	IT
8.200E+01	2.000E+00	2.100E+01	2.300E+01	4.811E+04
ITC	MODE	It	Ta	Tr
4.579E+04	5.000E+00	0.0	-1.616E+01	2.001E+01
Tco	Tci	Tst	Tsb	mc
-1.616E+01	-1.615E+01	2.281E+01	2.119E+01	0.0
mb	Qu	Qloss	Qstore	DU
0.0	0.0	0.0	0.0	-1.119E+03
Qs	Qe	Qaux	Qh	Qsys
0.0	1.418E+01	0.0	0.0	0.0
Ql				
1.809E+04				

TIME = 48.0000

YEAR	MONTH	DATE	HOUR	IT
8.200E+01	2.000E+00	2.200E+01	0.0	4.811E+04
ITC	MODE	It	Ta	Tr
4.579E+04	3.000E+00	0.0	-1.610E+01	2.082E+01
Tco	Tci	Tst	Tsb	mc
-1.480E+01	1.133E+01	2.159E+01	2.061E+01	3.782E+01
mb	Qu	Qloss	Qstore	DU
9.077E+02	-9.940E+02	3.735E+02	0.0	-2.672E+03
Qs	Qe	Qaux	Qh	Qsys
6.970E+02	1.575E+00	2.700E+04	2.770E+04	2.700E+04
Ql	QC	QOMDL	QSTORE	QS
1.846E+04	2.479E+05	1.323E+04	1.043E+05	1.043E+05
QDLL	QE	QAUX	QH	QSYS
1.585E+04	2.565E+03	3.604E+05	5.951E+05	6.083E+05
QL				
6.076E+05				

UNIT	1	WAS CALLED	482 TIMES
	16		772
	21		872
	23		786
	17		30
	18		80
	19		24
	24		24
	20		76
	22		70
	6		708
	12		316
	11		468
	13		269
	7		738
	2		471
	3		602
	8		577
	14		336
	15		379
	4		1181
	5		987
	31		482
	30		49
	28		49
	29		49
	26		482
	27		2
	25		49

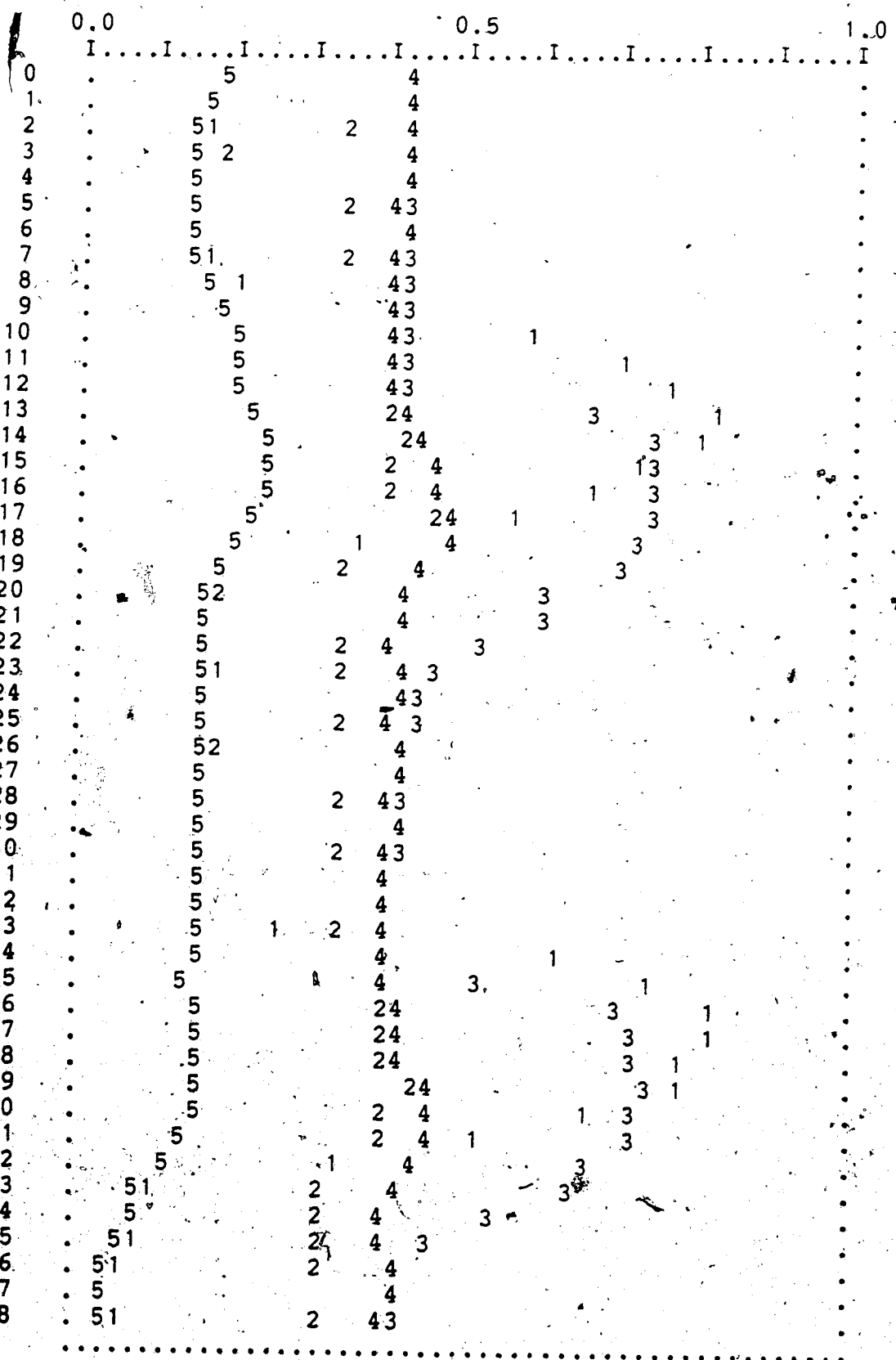
0.0
0.5
1.0

SYMBOL	IDENTIFIER	SCALE FACTOR	ZERO POINT
1	Tco	1.000E+02	-2.000E+01
2	Tci	1.000E+02	-2.000E+01
3	Tst	1.000E+02	-2.000E+01
4	Tsb	1.000E+02	-2.000E+01
5	Ta	1.000E+02	-2.000E+01

Appendix E: Estimations of Component Properties

E-1: Overall Heat Loss Coefficient - Area Product of The Module

The overall heat loss coefficient - area products (UA factor) of Module 5 and 6 for each month of each of the 81-82, 82-83 and 83-84 heating seasons are shown in Table E1.1. The UA factors were calculated by dividing the measurements of the monthly energy consumptions of the modules by the summations of the average hourly differences between the room and the ambient temperatures. Thus the factors represent the monthly heating requirements of the modules for each degree difference between the indoor and outdoor temperatures.

Module 5 and 6 have identical construction except for the 63% increase in ceiling insulation and addition of solar heating system in Module 6. Module 5 was used as a control module to compare the heating load of Module 6. The addition of the solar heating system increases the infiltration rate. As a result, the average UA factors of the two modules over the three heating seasons are almost the same (around 140 W/°C) even though the ceiling of module 6 is better insulated.

Table E1.1: UA Factors of Module 5 and Module 6

	Module 6			Module 5		
	81-82	82-83	83-84	81-82	82-83	83-84
Sep	132.3	123.8	/	/	143.1	/
Oct	/	148.1	142.5	140.9	145.7	141.1
Nov	126.9	131.8	153.5	142.3	132.8	144.3
Dec	131.7	135.8	139.4	134.0	138.0	130.3
Jan	137.0	135.8	147.7	128.4	130.4	148.0
Feb	133.8	140.2	/	134.4	132.1	/
Mar	144.5	140.2	/	134.8	136.7	/
Average		137.9			137.5	

E-2: Lumped Thermal Capacitance of The Module

Consider the energy balance equation for the module, Equation (4.14), it can be expressed as

$$CAP \cdot dT_r/dt + UA \cdot T_r = \dot{Q}_H + UA \cdot T_a \qquad (E2.1)$$

Assume that CAP, UA, $\dot{Q}_H$ and T_a are constants, then the solution of Equation (E2.1) is

$$T_r = a \cdot e^{-\frac{UA}{CAP}t} + b \qquad (E2.2)$$

where

$a = T_{ri} - T_a - \dot{Q}_H/UA$

$b = T_a + \dot{Q}_H/UA$

and T_{ri} = initial room temperature

From Equation (E2.2), the lumped thermal capacitance, CAP, can be obtained as

$$CAP = UA \cdot t/\ln[a/(T_r - b)] \qquad (E2.3)$$

Table E2.1 shows the experimental data of the room and ambient temperatures for a four hour cooling period with a minimum electric power supply of 610 W for keeping the fan on. The ambient temperature is assumed constant by taking its average value, -20.68°C, and the UA factor is given in Appendix E-1. Therefore, CAP evaluated at 3 hrs is

$$CAP = 140 \times 3600 \times 3/\ln\left(\frac{18.8 + 20.68 - 610/140}{14.3 + 20.68 - 610/140}\right) \text{ J/°C}$$

$= 11028 \text{ kJ/°C}$

$\simeq 11000 \text{ kJ/°C}$

For checking purposes, substitute the CAP value of 11000 kJ/°C back into Equation (E2.2). The room temperature determined by using the estimated CAP is shown and compared with the experimental temperature in Table E2.2.

Table E2.1: Experimental Data of Room and Ambient Temperatures for Four Hours on Jan 9, 1982

t (hr)	T_r (°C)	T_a (°C)
0	18.8	-20.8
1	16.6	-20.6
2	15.4	-20.6
3	14.3	-20.7
4	13.4	-20.7

Table E2.2: Comparison of room Temperatures

t (hr)	T_r (°C)	
	Experiment	Cap=11000 kJ/°C
0	18.8	18.8
1	16.6	17.2
2	15.4	15.7
3	14.3	14.3
4	13.4	12.9

E-3: Overall Heat Loss Coefficient and Ntu of The Rockbed

1. Overall Heat Loss Coefficient

The rockbed storage unit consists of a container with interior cross sectional area of 4.5 ft. by 4.5 ft. filled to a depth of 3.4 ft. with gravel, leaving an air space of 2.25 ft. from the top wall panel. The top and side walls have almost identical construction except that each pair of the opposite side panels is fastened by connecting a 0.5 in. threaded metal rod across the rocks from one side to the other side. The rockbed rests on the basement floor with 2 in. of polystyrene insulation between the lower plenum and the basement floor. A section of the wall construction is shown in Figure E3.1

To find the overall heat loss coefficient of the rockbed, the method presented in ASHRAE Handbook, 1981 Fundamentals, Chapter 23, is used. The rock pile is treated as a lumped mass with uniform temperature. The temperature of the lumped mass is considered to be the average temperature of the rocks. Therefore, heat transfers are assumed starting from the lumped mass surface to the wall panels passing through the air spaces between the mass and the walls. Since the vertical walls are in contact with the rocks, the thickness of air spaces the vertical surfaces facing is very small and so ignored. Heat losses through the entry and exit of the storage unit are also neglected. Table E3.1 gives the thermal resistances of each construction layer of the horizontal and vertical walls.

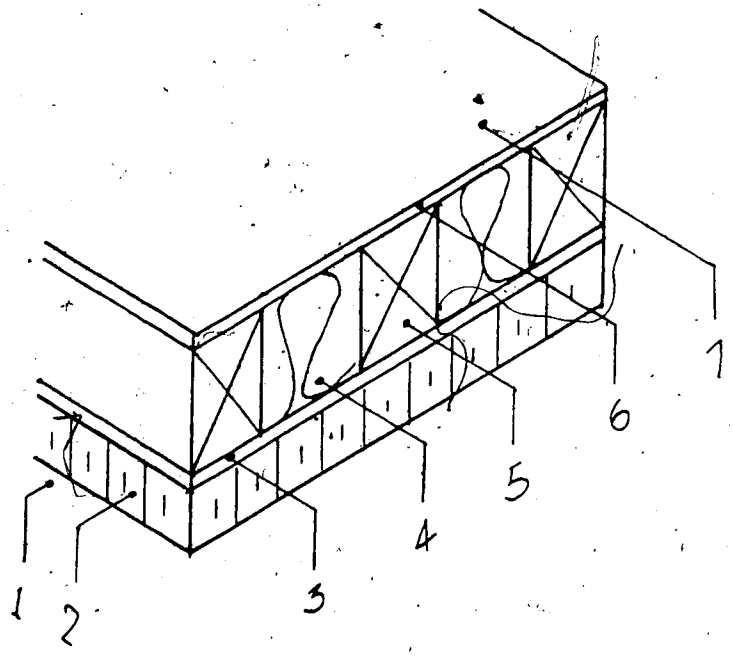

Construction

1. 27" air space from the top wall
   (assume 0 for vertical walls)
2. 2" rigid insulation (polystyrene)
3. 1/4" plywood (1/2" for vertical wall)
4. R-12 fiber glass
5. 2"x4" studs @ 16" o.c.
   (@ 12" o.c. for vertical wall)
6. 1/4" plywood
7. outside surface (still air)

Figure E3.1: Wall Construction of Rockbed

Table E3.1: Thermal Resistances of Each Layer of The Horizontal and Vertical Walls

Construction	Horizontal*		Vertical*	
	Between Framing	AT Framing	Between Framing	At Framing
1. air space	1.72	1.72	/	/
2. polystyrene	10.00	10.00	10.00	10.00
3. plywood	0.31	0.31	0.62	0.62
4. fiber glass	12.00	/	12.00	/
5. studs	/	4.35	/	4.35
6. plywood	0.31	0.31	0.31	0.31
7. outside surface	0.61	0.61	0.68	0.68
Total resistance	24.95	17.30	23.61	15.96

* Resistance expressed in $ft^2 \cdot °F \cdot hr/Btu$ and obtained from ASHRAE Handbook, 1981 Fundamentals, Chapter 23, Table 1 to Table 4K

To calculate the heat loss coefficient, the U-value, of each wall and to correct for the effect of framing members, the following equation from ASHRAE is used

$$U = (S/100)U_s + (1-S/100)U_i \qquad \text{(E3.1)}$$

where

U_i = U-value for area between framing members

U_s = U-value for area backed by framing members

S = percentage of area backed by framing members

Assume 20% framing for horizontal panel and 24% for vertical panels. Thus, the average U-values for the walls, based on the information obtained from Table E3.1, are

1. Horizontal wall

$$U = 0.2/17.3 + 0.8/24.94$$
$$= 0.0436 \text{ Btu/hr}\cdot\text{ft}^2\cdot{}^\circ\text{F} \qquad \text{(E3.2)}$$

2. Vertical wall

$$U = 0.24/15.96 + 0.76/23.61$$
$$= 0.0472 \text{ Btu/hr}\cdot\text{ft}^2\cdot{}^\circ\text{F} \qquad \text{(E3.3)}$$

Since the vertical wall contains steel rod for fastening, the effect of this highly conductive material should be determined. A good approximation can be made by a *Zone Method*. This method defines two zone area: *Zone A*, containing the highly conductive element; *Zone B*, the remaining portion of the total area. The U-value of each

zone is calculated separately and then combined to obtain the overall heat loss coefficient of the wall.

Figure E3.2 shows the section of *Zone A* of a vertical wall. The calculation of the resistance of *Zone A* is given in Table E3.2. The area conductance C·A of each layer is determined by adding the area conductances of its metal and non-metal sections. Area conductances of the layers are converted to area resistances R/A and added to obtain the total resistance of *Zone A*. The reciprocal of the total resistance is the UA factor of the zone.

The U-value of *Zone B* is 0.0472 Btu/hr·ft²·°F from Equation (E3.3). The total area of a vertical wall is considered to be the surface in contact with the rocks. Therefore,

Area of Zone B = width of rockbed x depth of rock pile
- area of Zone A
= 4.5 x 3.4 - 0.785
= 14.52 ft²

Total area = 4.5 x 3.4
=15.3 ft²

Thus, the overall heat loss coefficient of the vertical wall including the effect of the highly conductive material is

$$U = (14.52 \times 0.0472 + 1/14.96)/15.3$$
$$= 0.0492 \text{ Btu/hr·ft}^2\text{·°F}$$

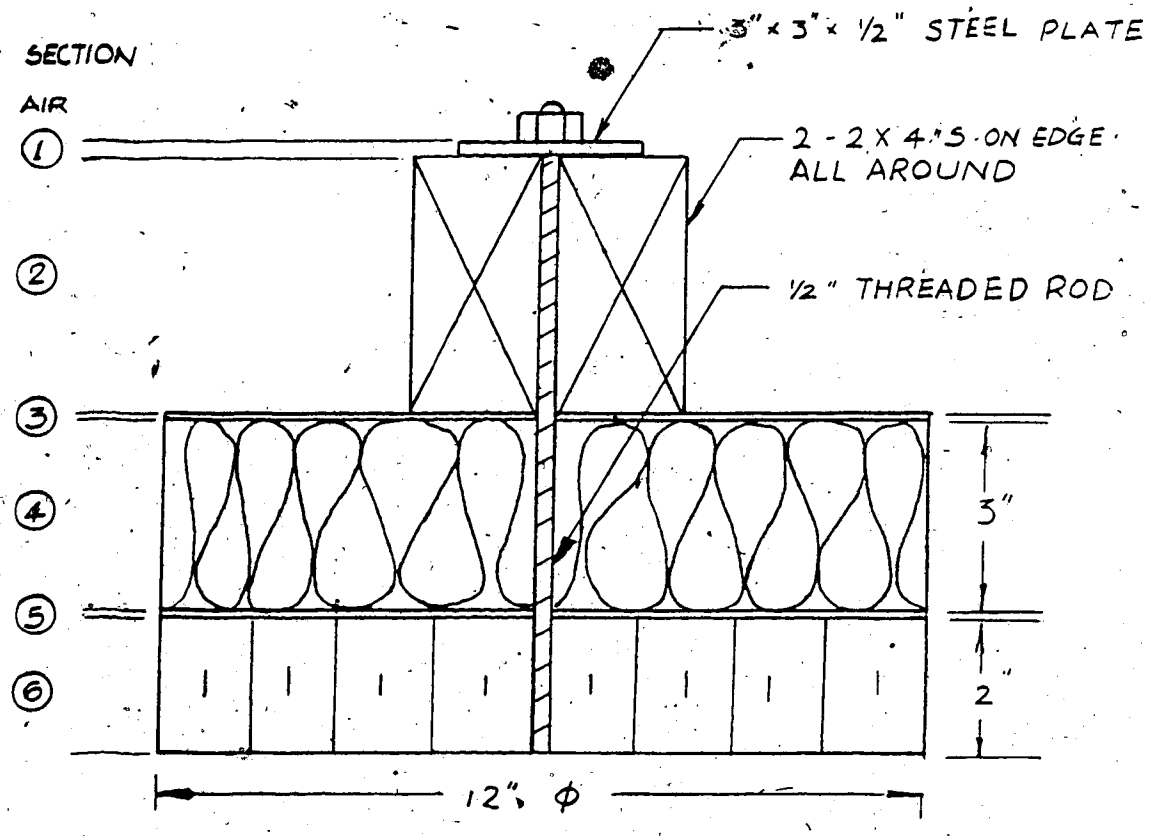

Area of *Zone A* = 0.785 ft²

found by using Equation (7) of ASHRAE, P.23.3

Figure E3.2: A Section of *Zone A* of A Vertical Wall

Table E3.2: Calculations of The Resistance of *Zone A*

Layer	Area x Conductance (ft^2 x Btu/hr·ft^2·°F)	C·A (Btu/hr·°F)	R/A (°F·hr/Btu)
air	0.785x1.46	1.146	0.873
1. steel	0.063x312/0.5	39.300	0.025
2. steel	0.0014x312/4		
wood	0.333x0.230	0.186	5.382
3. steel	0.0014x312/0.25		
wood	0.7836x3.2	4.255	0.235
4. steel	0.0014x312/3		
fiberglass	0.7836x0.0833	0.211	4.742
5. steel	0.0014x312/0.25		
wood	0.7836x1.6	3.00	0.333
6. steel	0.0014x312/2		
insulation	0.7836x0.1	0.297	3.370
		Total R/A	14.960

Now that the U-value of the top and side panels are known, it is necessary to calculate the overall heat loss coefficient, U_o, of the storage unit. Assuming that heat losses through the bottom is the same as that through the top. The coefficient U_o based on the total area of the four vertical walls in contact with the rocks is

$$U_o = \frac{4x15.3x0.0492 + 2x4.5x4.5x0.0436}{4 \times 15.3}$$

$$= 0.078 \text{ Btu/hr} \cdot \text{ft}^2 \cdot {}^\circ\text{F}$$

$$= 0.443 \text{ W/m}^2 \cdot {}^\circ\text{C}$$

2. Ntu

The Ntu of a packed bed storage unit represents the ratio of the heat transfer coefficient between the fluid and solid to the heat removal coefficient by the fluid. If Ntu is infinite, the bed and fluid temperatures are everywhere equal. For a well-designed rockbed, a large Ntu is desirable for promoting thermal stratification and energy exchange between rocks and fluid. The Ntu is defined as

$$\text{Ntu} = h_v AL/\dot{m}C_f \qquad \text{(E3.4)}$$

where h_v is the volumetric heat transfer coefficient (i.e., the usual heat transfer coefficient times the bed particulate surface area per unit bed volume) which can be estimated from the Löf and Hawley equation. That is

$$h_v = 650(G/D)^{0.7} \quad W/m^3 \cdot °C \qquad (E3.5)$$

where G is the mass velocity in $kg/s \cdot m^2$ and D is the particle diameter in meters.

The rockbed has the following characteristics:

L = length in flow direction = 1040 mm

A = cross sectional area = 1.88 m^2

D = equivalent diameter of pebbles = 16 mm

Air flowrate = 0.122 m^3/s for charging

= 0.218 m^3/s for discharging

To calculate the Ntu value to justify whether the infinite Ntu model can be used to predict the performance of the storage unit, a high flow rate (0.218 m^3/s) and a low temperature (eg. 21°C) to evaluate the air properties are selected so that the Ntu criterion will be more severe. Therefore

C_f = 1006 $J/kg \cdot °C$

$\dot{m}$ = 0.218 x 1.205 kg/s

Then

$h_v = 650(0.218 \times 1.205/1.88/0.016)^{0.7}$ $W/m^3 \cdot °C$

= 2963 $W/m^3 \cdot °C$

Ntu = (2963x1.88x1.04)/(0.218x1.205x1006)

= 22

Thus Ntu is larger than 10 and the infinite Ntu model is appropriate.

E-4: Overall Heat Loss Coefficient of The Duct Outside The Module

Figure E4.1 shows the cross section of the 10 in. plastic duct located outside of the module with 1 in. insulation of fiber glass, so that

$$r_1 \simeq r_2 = 5 \text{ in} = 127 \text{ mm}$$

$$r_3 = 6 \text{ in} = 152 \text{ mm}$$

The conductivity of the fiber glass, k_F, is approximately 0.0421 W/m·°C.

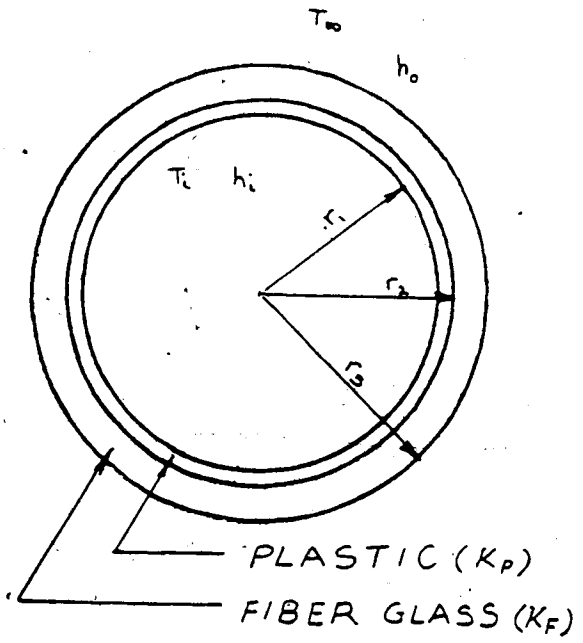

Figure E4.1: A Cross Section of The Insulated Duct Outside The Module

The overall heat loss coefficient of the duct based upon inside surface area can be calculated using the following equation

$$U_i = \frac{1}{\frac{1}{h_i} + \frac{r_1 \ln(r_2/r_1)}{k_P} + \frac{r_1 \ln(r_3/r_2)}{k_F} + \frac{r_1}{r_3 h_o}} \qquad \text{(E4.1)}$$

Since $r_1 \simeq r_2$ and the conductivity of the plastic k_P is much greater than that of the fiber glass, the second term in the denominator of Equation (E4.1) can be neglected when compared with the third term. Thus,

$$U_i = \frac{1}{\frac{1}{h_i} + \frac{r_1 \ln(r_3/r_2)}{k_F} + \frac{r_1}{r_3 h_o}} \qquad \text{(E4.2)}$$

To find the inside surface conductance, h_i, the nature of the flow should be determined first by checking the Reynold number, Re which is equal to

$$Re = u_m d/\nu \qquad \text{(E4.3)}$$

The volumetric flow rate passing through the ducts to and from the collector is 0.122 m^3/s, so that the mean velocity of the flow is

$$u_m = 0.122/0.127^2\pi \text{ m/s}$$

$$= 2.41 \text{ m/s}$$

at $T = 350°K$, $\nu = 20.76 \times 10^{-6}\ m^2/s$

$$Re = (2.41 \times 2 \times 0.127)/(20.76 \times 10^{-6})$$

$$= 29486 > 10000$$

Therefore, the flow is turbulent. Actually, the air temperature inside the duct is less than 350°K. The Reynold number should be larger because of smaller value of ν, the kinematic viscosity, at lower temperature. The flow is certainly turbulent.

Assuming that the flow and temperature conditions are fully developed and the duct is smooth, so that the internal surface conductance can be assumed constant along the duct and determined by using Prandtl analogy which is

$$\frac{St}{Cf} = \frac{0.5}{1 + 1.99\ Re^{-0.125}(Pr-1)} \qquad (E4.4)$$

for $3 \times 10^3 < Re < 10^5$

where

St = Stanton number = $Nu/Pr \cdot Re$

Cf = drag coefficient = $0.0791\ Re^{-0.25}$

Nu = Nusselt number = $h_i d/k$

Pr = Prandtl number

k = thermal conductivity

d = diameter of duct

Assuming the average air temperature is 300°K inside the duct

$\therefore \nu = 15.68 \times 10^{-6}$ m²/s

$k = 0.02624$ W/m·°C

$Pr = 0.708$

$Re = 2.41 \times 2 \times 0.127 / 15.68 \times 10^{-6}$

$= 39040$

$Cf = 0.0791 \times (39040)^{-0.25}$

$= 5.6273 \times 10^{-3}$

Substitute the above properties into Equation (E4.4) to obtain

$St = 3.33 \times 10^{-3}$

$Nu = 92.034$

$\therefore h_i = 9.51$ W/m²·°C

For the outside surface conductance, h_o, it is assumed equal to 6 Btu/hr·ft²·°F (34.07 W/m²·°C) at 15 mph wind speed from P.23.12, Table 1, ASHRAE Handbook, 1981 Fundamentals.

Now substitute h_i, k_F, and h_o into Equation (E4.2), the overall heat loss coefficient based upon inside duct surface area is

$U_i = 1/(0.105 + 0.55 + 0.024)$ W/m²·°C

$= 1.47$ W/m²·°C